

THESIS ON MECHANICAL ENGINEERING E113

Steel Selection Considerations for Hot-Dip Galvanizing

SIRLI SEPPER



TALLINN UNIVERSITY OF TECHNOLOGY
School of Engineering
Department of Mechanical and Industrial Engineering

Dissertation was accepted for the defence of the degree of Doctor of Philosophy in Engineering on 9.11.2017

Supervisors: Sen. Res. Priidu Peetsalu, Department of Mechanical and Industrial Engineering, Tallinn University of Technology, Tallinn, Estonia

Sen. Res., Prof. emeritus Priit Kulu, Department of Mechanical and Industrial Engineering, Tallinn University of Technology, Tallinn, Estonia

Consultant: Jussi Ustal, AS Paldiski Tsingipada, Paldiski, Estonia

Opponents: Assoc. Prof. Audrius Žunda, Institute of Power and Transport Machinery Engineering, Aleksandras Stulginskis University, Kaunas, Lithuania

Assoc. Prof. Alexander Ryabchikov, Institute of Forestry and Rural Engineering, Estonian University of Life Sciences, Tartu, Estonia

Defence of the thesis: 21.12.2017, Tallinn

Declaration:

Hereby I declare that this doctoral thesis, my original investigation and achievement, submitted for the doctoral degree at Tallinn University of Technology, has not been submitted for any academic degree.

/Sirli Sepper/



Euroopa Liit
Euroopa
Regionaalarengu Fond



Eesti tuleviku heaks



DoRa
ESF PROGRAMM



Eesti hariduse ja teaduse heaks
ARCHIMEDES

Copyright: Sirli Sepper, 2017

ISSN 1406-4758

ISBN 978-9949-83-193-7 (publication)

ISBN 978-9949-83-194-4 (PDF)

MEHHAOTEHNIKA E113

Terase valiku mõjurid kuumtsinkimiseks

SIRLI SEPPER

Contents

LIST OF PUBLICATIONS.....	7
INTRODUCTION.....	8
ABBREVIATIONS AND SYMBOLS	11
1. THEORETICAL BACKGROUND	12
1.1 Hot-dip galvanizing process.....	12
1.2 Influence of properties of steel on coating formation.....	14
1.2.1 Impact of chemical composition of steel.....	14
1.2.2 Role of surface roughness of steel.....	16
1.2.3 Influence of microstructure of steel.....	17
1.2.4 Galvanizing of high strength steels	18
1.3 Objectives of the study	22
2. MATERIALS AND METHODS	24
2.1 Galvanizing process description.....	24
2.2 Microstructural analysis of steel and zinc coating.....	24
2.3 Substrate preparation.....	24
2.3.2 Study of hydrogen embrittlement during acid pre-treatment	25
2.3.3 Study of the HDG effect on the mechanical properties of high strength steels.....	26
2.3.4 Study of the impact of silicon content.....	27
3 RESULTS AND DISCUSSIONS	29
3.1 Impact of the microstructure of steel on coating formation	29
3.1.1 Effect of ferrite grain size.....	29
3.1.2 Analysis of ferrite grain elongation and recrystallization	30
3.1.3 Impact of the size and shape of carbide grains.....	31
3.2 Influence of pretreatment on hydrogen embrittlement.....	34
3.3 Effect of HDG on the mechanical properties of steel.....	37
3.4 Impact of silicon content	41

4	CONCLUSIONS	49
	REFERENCES.....	51
	ACKNOWLEDGEMENTS	59
	ABSTRACT	60
	KOKKUVÕTE.....	62
	APPENDICES.....	65
	Curriculum vitae.....	67
	Elulookirjeldus	69

LIST OF PUBLICATIONS

The present doctoral dissertation is based on the following peer reviewed publications, referred to in the text Paper I - Paper V:

- Paper I **Sepper, S.**, Peetsalu, P., Saarna, M. Methods to evaluate the appearance of hot dip galvanized coatings. *Agronomy Research*, 9(S1), 2011, 229 - 236.
- Paper II **Sepper, S.**, Peetsalu, P., Mikli, V., Saarna, M. The effect of substrate microstructure on morphology of zinc coatings. *Proceedings of the 8th International Conference of DAAAM Baltic Industrial Engineering*, 2012, 717 - 722.
- Paper III **Sepper, S.**, Peetsalu, P., Saarna, M., Kirs, V., Mikli, V. High strength steel behaviour during hot dip galvanizing. *Proceedings 20th International Federation for Heat Treatment and Surface Engineering (IFHTSE) Congress*, 2012, 525 - 529.
- Paper IV **Sepper, S.**, Peetsalu, P., Saarna, M., Mikli, V., Kulu, P. Effect of hot dip galvanizing on the mechanical properties of high strength steels. *Key Engineering Materials*, 2014, 12 - 15.
- Paper V **Sepper, S.**, Peetsalu, P., Kulu, P., Saarna, M., Mikli, V. The role of silicon in the hot dip galvanizing process. *Proceedings of the Estonian Academy of Sciences*, 2016, 65, 2, 159–165.

Copies of these articles are included in the Appendices.

INTRODUCTION

The DoRa programme activity 3, “Research cooperation between universities and businesses” supports studies of doctoral students whose research is conducted in close cooperation between the university and a company in Estonia. The objective of the activity is to contribute to the increase of the number of highly-skilled specialists in priority fields. Driven by this programme, I have been provided a unique opportunity to carry out scientific research along with industrial applications. The research was conducted under the cooperation of three parties – the author, Tallinn University of Technology and AS Paldiski Tsingipada (Zincpot). The author is employed as a technologist at the company.

AS Paldiski Tsingipada is a hot-dip galvanizing plant established in 2006. In its relatively young age, it is characteristic of the company to learn continuously and embed updated knowledge in the processes in order to thrive and grow in increasingly competitive environments. This research project was an ideal opportunity for the company to become a knowledge-based industry where research and development are the foundation of production.

Hot-dip galvanizing is one of a family of metal-coating processes used to protect substrate metal surfaces from corrosion by the barrier protection and galvanic protection. In the barrier protection, the zinc coating, which separates the steel from the corrosion environment, will first corrode before the corrosive environment reaches the steel. In the galvanic protection, zinc is less noble or anodic to iron at ambient conditions, and will sacrificially corrode to protect the substrate steel (Marder, 2000).

During hot-dip galvanizing, steel or cast iron is immersed in a bath of molten zinc after careful cleaning and preparation (Hornsby, 1995). One key factor in providing high quality zinc coating is proper steel selection. The chemistry of the steel influences the appearance, thickness, smoothness and adhesion of the coating. Reactive elements in the steel such as silicon and phosphorus affect the galvanizing process. An appropriate selection of composition can therefore give more consistent quality of a coating (Steels suitable for galvanizing, 2016).

Besides chemical composition of the steel, the microstructure and the mechanical properties of the steel are important properties of structural steel. In recent years, high strength steels have attracted much interest because they make it possible to lighten the structures while maintaining load carrying capabilities. New steel

grades (Weldox, Hardox, etc.) with fine grain size and quenched and tempered condition have been developed as a result of customer demands. However, in order to use thinner gauges and meet customer's durability expectations, corrosion protection, and hence hot-dip galvanizing, appears crucial.

New steel grades are a challenge to the galvanizers to produce a quality coating. Galvanizers and the customers must be aware of how steel selection might affect the final result: how the chemical composition and the microstructure of steel affect the coating formation and how zinc bath temperature might affect the mechanical properties of steel.

Scientific novelty

In the context of the new steel grades and their microstructures, one aim of the present thesis was to study the effect of the substrate microstructure (ferrite grain size, ferrite grain shape, carbide grain size, carbide grain shape) on the batch hot-dip galvanized coatings. In the literature, several studies report the effect of new steel grades microstructures only in a continuous hot-dip galvanizing line. Regarding to the batch hot-dip galvanizing, several authors have only studied the effect of welding HAZ on the coating formation; however, the effect of carbide grains and ferrite grains has not been characterized in this extent in the studies published.

Concerning the mechanical properties, many studies have analyzed the mechanical properties of different steels (also high strength steels) after hot-dip galvanizing. Our industrial field tests confirmed the findings of other researchers reporting that hot-dip galvanizing has a relatively minor effect on the mechanical properties of investigated steels. However, our methods for testing the change in the mechanical properties include the heat effect of the galvanizing temperature and that of a zinc coating separately. To eliminate the effect of the chemical reaction between the iron and zinc and the coating properties, tests were made with dipping the tensile test specimens into the molten salt. The effect of heat was studied.

Fundamental understanding of the phenomenon how silicon influences the coating formation is still lacking. To fill that gap, the focus of my study is on the role of silicon in the galvanizing process. Most experiments from the literature use samples that contain many elements. Our industrial field tests used electrolytic iron and an added amount of silicon, which were melted in the vacuum induction furnace and casted into a copper mould. The same method was presented by

Uchiyama (Uchiyama *et al.*, 1983) and Liberski (Liberski *et al.*, 2014), but galvanizing was performed in a pure zinc bath. In our experiments, galvanizing was performed in an industrial zinc bath with 99.3% Zn, containing also Al, Bi, Fe, Ni, Sn, and Pb. The temperature inside the specimen was measured. It was detected that coating formation probably takes place in solid state. In addition, the Fe-Zn layer formation was found.

The results of the PhD thesis research have been published in the form of 5 scientific papers in international journals and conference proceedings. The publications directly connected to the research topic are given at the end of the thesis. The results of the PhD thesis research have been reported at 7 international conferences (Intergalva, DAAAM Baltic, BALTMATTRIB, etc.).

ABBREVIATIONS AND SYMBOLS

Abbreviations:

HAZ – Heat Affected Zone

HDG – Hot-Dip Galvanizing

HSLA – High Strength Low Alloy

LME – Liquid Metal Embrittlement

OAC – Oxy Acetylene Cutting

Symbols:

A_g – percentage non-proportional elongation at maximum force (F_m)

A_{80} – Ultimate elongation of non-proportional test pieces, %

AS – aspect ratio (ratio of maximum diameter to minimum diameter)

D – diffusion coefficient

G – grain size index

R_m – tensile strength

R_p – proof strength

$R_{p\ 0.2}$ – proof strength at 0.2% plastic extension

$R_{p\ 0.05}$ – proof strength at 0.05% plastic extension

Δ – change in dimensions

t – time

1. THEORETICAL BACKGROUND

1.1 Hot-dip galvanizing process

Hot-dip galvanizing is a process of immersing iron or steel in a bath of liquid zinc to produce a corrosion resistant, multi-layered coating of zinc-iron alloy and zinc metal (Inspection course, 2016). The corrosion protection is dependent on the coating thickness and environmental conditions (ASM Handbook, 1994). Rapid chemical attack of the component surface by zinc produces a layer of zinc/iron (Zn-Fe) phases which form a strong chemical bond with a component surface (Hornsby, 1995). The three main steps in the hot-dip galvanizing process are surface preparation, galvanizing, and post-treatment (Fig. 1.1).

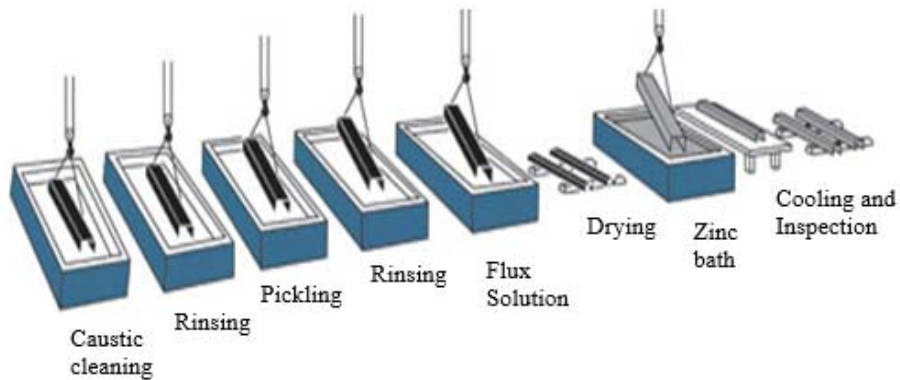


Figure 1.1 Model of the hot-dip galvanizing process (Inspection course, 2016)

According to the Fe-Zn phase diagram (Fig. 1.2), during hot-dip galvanizing at 450 °C, an intermetallic layer is formed composed of Γ -Fe₅Zn₂₁, δ -FeZn₁₀, ζ -FeZn₁₃, and η layer. The enthalpies of the formation of all intermetallic compounds are very close to each other and therefore an unstable behavior of the system might occur with small additions of silicon and phosphorus in steel (Guttman, 1994).

Starting from the base steel, each layer contains a higher proportion of zinc until the outer layer, which is relatively pure zinc. Table 1.1 below gives the properties of these layers. The intermetallic compounds vary not only in composition and morphology of the crystals, but also significantly in hardness and resistance to compressive load (Pokorny *et al.*, 2016 a).

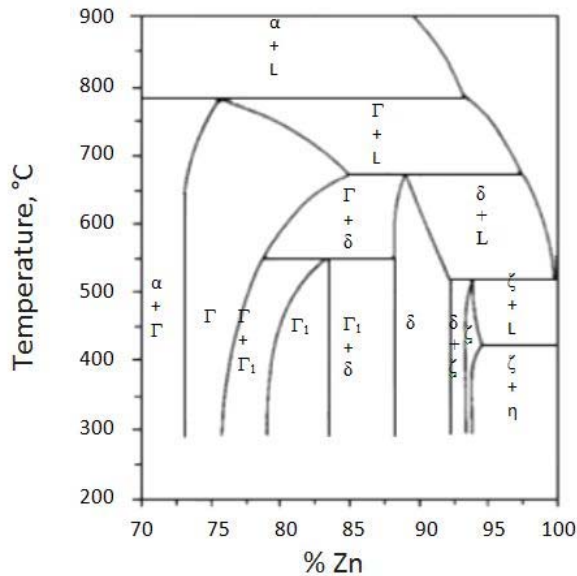


Figure 1.2 Binary Fe-Zn phase diagram (Guttman, 1994)

Table 1.1 Properties of alloy layers of hot-dipped galvanized steels (Galvanizing, 2016)

Layer	Iron %	Melting Point °C	Crystal Structure	Vickers hardness
Eta (η)	0.03	419	Hexagonal	70-72
Zeta (ζ)	5.7-6.3	530	Monoclinic	175-185
Delta (δ)	7-11	530-670	Hexagonal	240-300
Gamma (Γ)	20-27	670-780	Cubic	-----
Steel Base	99+	1510	Cubic	150-175

Hot-dip galvanized coating formation can be described as a diffusion process. Zinc diffuses into steel and Fe diffuses into zinc. As the diffusion coefficient of zinc is higher than that of steel ($D_{Zn} > D_{Fe}$), it is believed that zinc readily diffuses into steel and forms intermetallic compounds (Xu *et al.*, 2007). On the other hand, it is known that when solid iron is immersed into liquid zinc, loss of iron weight takes place. Part of the iron dissolved diffuses into the bath where it contributes to the formation of intermetallic particles about twenty microns in diameter, known as dross (Giorgi *et al.*, 2004). So the Fe-Zn reaction diffusion takes place in both direction, but the main diffusion process is that of zinc moving through the intermetallic phases towards the steel interface (Allen *et al.*, 1962, 1963). It is believed that the Γ layer will grow towards the iron, the ζ layer towards the zinc and δ layer in both directions but mainly towards zinc (Hortsmann *et al.*, 1970). On the other hand, some reports in the literature (Rowland, 1947) claim that the

rate of Fe diffusion in the alloy layer is greater than that of Zn. The layers therefore tend to grow outward from the steel to form the alloy layers.

1.2 Influence of properties of steel on coating formation

1.2.1 Impact of chemical composition of steel

Coating appearance and zinc consumption mainly depend on the zinc–steel reactivity and on the drainage of zinc from workpieces during their withdrawal (Fratesi *et al.*, 2002). The zinc–steel reactivity is mostly influenced by silicon and phosphorus content in the steel, but also carbon in excess of about 0.2% and manganese in excess of about 1.3% increase in the Zn-Fe layer formation (Hornsby, 1995).

A small amount of Si exists in structural steels because Si is used as a de-oxidant in the steel making process. Si is also a low-cost and very effective strengthening alloying element for steels (Tang, 2008). Silicon concentration of steel plays a major role in the hot-dip galvanizing process. It influences the thickness, uniformity, nature of the structure, and the mutual position of phases within a coating (Paramonov *et al.*, 2011). The effect of silicon was first studied in the early 1940s by Sandelin (Sandelin, 1940 a; 1940 b). He found that ~0.1 % Si in steels could lead to an accelerated growth of the alloy layers, providing thick, gray appearance and brittle coating.

Rapid growth of the zinc coating occurs at two silicon concentration ranges: 0.03-0.14% (Sandelin area) and above 0.3%. Steels containing little silicon (<0.03%) and very low content of phosphorus have compact and continuous zinc coating (galvanizing temperature 450 °C), which are composed of a Γ , δ , ζ and η layer (Pokorny *et al.*, 2016 a; Che *et al.*, 2009; Che *et al.*, 2005; Horstmann, 1975). Steels containing 0.15–0.25% Si also produce a compact and coherent coating (Sebisty effect) (Sebisty *et al.*, 1967; Che *et al.*, 2009; Che *et al.*, 2005).

Many studies have described the influence of silicon on the coating formation, but a fundamental understanding of the phenomenon is still lacking. Most researchers agree that the low solubility of silicon in the ζ layer is important. It leads silicon segregation to the grain boundaries and formation of areas of liquid Zn between the ζ crystals. The loose layer of ζ fails to shield δ from the liquid Zn, allowing a direct contact between these two thermodynamically incompatible phases, resulting in excessive Fe loss and “ejection” of layer ζ deep into the bath (Che *et*

al., 2009; Mackowiak *et al.*, 1979; Peng *et al.*, 2005; Liberski *et al.*, 2014). However, some theories state that ferrosilicon particles in the coating can act as nucleation sites for the nucleation of the ζ phase (Porter, 1991). These theories seem questionable because as a result of studies of many researchers, no Si particles have been found in the coating (including experiments in the current study at Tallinn University of Technology). Furthermore, the resolution of the particles in these studies was poor and no precise analyses of the composition of the particles have been reported (Notowidjojo, 1990).

Other investigations (Proskurin *et al.*, 1988) claim that the reason for this unfavorable effect of silicon on hot-dip galvanizing is a significant reduction in the wetting capacity of the metal surface. Recent investigations claim that Si content in steel has no direct influence on the galvanizing process but affects it indirectly by influencing the effusion of hydrogen (Schulz *et al.*, 2003; Thiele *et al.*, 2006). According to this theory, hydrogen can affect the coating formation during the hot-dip galvanizing process. When steel is heated to the galvanizing temperature, hydrogen is expelled from the surface of the steel, which could affect the galvanizing behavior. More research is needed to develop a holistic theory of layer formation.

Most of the studies that describe the effect of silicon during galvanizing use samples which contain many elements. So silicon is not the only variable in their experiments. For example, Kopyciński studied four different steel grades (Si > 0.20%) and two ductile irons (Kopyciński, 2010). Galvanizing was performed in the Zn-Ni bath at 450 °C at the dipping time up to 10 min. The growth rates for the δ and ζ phases indicated a leading role of the ζ phase and a slow growth rate of the δ phase (Kopyciński, 2010).

Zeinab *et al.* investigated the effect of the Si content of a steel substrate on the performance of the hot-dip galvanized layer (Zeinab, 2017). The steels they used contained different amounts of C, Mn, P, Si. The results illustrate that the steel containing 1.46% Si has a greater reactivity between zinc and iron. Gamma layer is formed with steel containing 0.56 and 1.46% Si, but it will not be formed with steel containing 0.08% Si. Neither will the delta (δ) layer be formed with steel at 0.56% Si.

Uchiyama *et al.* melted electrolytic iron and a given amount of silicon to analyze silicon reactivity in galvanizing. Galvanizing was performed in the temperature range of 440 °C to 600 °C for 600 s in a pure zinc bath. They presented an

existence area map of different coating layers depending on silicon concentration and the immersion temperature (Uchiyama *et al.*, 1983).

As silicon reactivity is connected with the development of an excessive ζ phase, the high temperature galvanizing >530 °C is a solution to the problem; however, it is not economical. According to the phase diagram, at this temperature, the ζ phase transforms to the δ phase, which is less sensitive to the silicon content of steel (Notowidjojo, 1990).

In the case of phosphorus content, it is strictly controlled in steels because it causes cold brittleness of steels, or the tendency to be quite brittle while in a cold state (Liu *et al.*, 2016). It is generally accepted that phosphorus like silicon promotes formation of a thicker Fe–Zn intermetallic layer with the phase zeta (ζ) dominating in the structure (Pokorny *et al.*, 2016; Pelerin *et al.*, 1981; Gladman *et al.*, 1973; Chen *et al.*, 2014). On the other hand, it has been found that phosphorous in steel acts as an inhibitor for the growth of gamma phase (Jordan *et al.*, 1997 b; Allegra *et al.*, 1983).

In the present thesis, only the effect of silicon on coating formation was studied. The reason is that in practice, phosphorus content in construction steels that are hot-dip galvanized today in batch line is generally low and at such level it does not affect the galvanizing process.

1.2.2 Role of surface roughness of steel

The roughness of the steel surface influences the thickness and structure of the coatings. Shot or grit blasting is widely used to clean castings of sand, to remove welding slag, fire burn, heavy rust or paint, or to roughen the surface of the work (A guide to good galvanizing, 1972). A rough steel surface obtained by grit blasting and course grinding has a higher surface area and thus generates thicker galvanized coatings. Studies have shown (Steels suitable for galvanizing, 2016) that sand blasting leads to a large increase in coating thickness on most steels (80–100%). According to other studies (A guide to good galvanizing, 1972), grit or shot blasting of mild or low alloy steels enables one to obtain coatings of up to more than twice the normal thickness without changing the galvanizing technique. For example, the thickness of the coating increased by sand blasting before galvanizing in a pure zinc bath from 50 μm to 100 μm in the steel with 0.003% Si (Ahmadi *et al.*, 2009).

Oktay *et al.* suggested that intermediate roughness and sharp asperities generated with abrasive particles having sizes in the range of 100-270 μm can produce

suitable galvanizing coatings on the steels having silicon contents in the Sandelin range (Oktay *et al.*, 2016).

In the present thesis the role of steel surface roughness is not studied, but during the substrate preparation it was recognized that surface roughness influences the structure and thickness of the coating. Therefore, the surface roughness was held constant during the experiments.

1.2.3 Influence of microstructure of steel

Ferrite grain growth in the HAZ is the dominant microstructural feature of the material's welding and thermal cutting processes with fine grain low carbon steel. Bayraktar *et al.* have studied the grain growth mechanism during the welding of interstitial free steels (Bayraktar *et al.*, 2007). Observations in the welded joints indicated the presence of very large grains near the fusion line that were oriented along the directions of the heat flow.

Also, different strengthening mechanisms (thermomechanical rolling, quenching and tempering, continuous annealing) are used to develop new steel grades. The steels with high yield strength have been achieved by using microalloying technology and the strengthening mechanisms (Mao *et al.*, 2010). Change in the grain size takes place during strengthening by grain size reduction and during strain hardening (Chandrasekaran, 2003).

Numerous reviews and books describe the microstructure change as a result of the thermal cutting and welding process and the strengthening mechanisms. However, no detailed information describing the influence of steel microstructure of the zinc coating is available.

According to ISO 14713-2:2009, thermal cutting changes the steel composition and structure in the zone and around the cut surface, so that the minimum coating thickness may be more difficult to obtain (ISO 14713-2, 2009).

Hisamatsu postulated that finer grain size of interstitial-free steel is more reactive (Hisamatsu, 1989). More grain boundary area is available for reaction and more rapid Fe-Zn phase growth results. Recent investigations have shown that the substrate grain size has no significant effect on the kinetics of phase growth in a galvanizing bath containing less than 0.001% Al. Galvanizing bath containing 0.20% Al led to outburst formation with finer substrate grain size (Jordan *et al.*, 1997 a).

Kuklik studied the effect of oxygen cutting on zinc coating thickness and morphology (Kuklik, 2011). He concluded that chemical composition in the HAZ differs from that in the substrate (as a result of depletion of some impurity elements). The coating of silicon killed steels in HAZ (Si 0.2%) acted like common unkilld steel grades.

Wegrzynkiewicz *et al.* described the influence of the way of cutting of steel on the structure and the growth kinetics of the Zn layer (Wegrzynkiewicz *et al.* 2014 a). They concluded that the cutting methods tested influence essentially the growth kinetics of Zn layer. But insufficient cleaning after OAC and laser cutting (remaining oxide layers) might have been created by the barrier hindering the diffusion process. In another work (Wegrzynkiewicz *et al.*, 2014 b), additional processing was used after OAC cutting: softening annealing, grinding and electropolishing. They concluded that the best way to reduce the Zn coating reduction is the application of an additional heat treatment – softening annealing that removes the HAZ created after thermal cut. They also concluded that additional grinding or electropolishing does not significantly reduce the diversification of the Zn coating thickness observed on the cut surface as compared to that of rolled. Material in the initial stage (steel S355JR) showed the ferritic-pearlitic structure. As a result of the heat treatment caused by cutting in the surface steel layer, the HAZ with lower bainite and martensite was observed.

1.2.4 Galvanizing of high strength steels

High strength steels have attracted much interest in recent years because increased strength makes it possible to reduce wall thicknesses and the weight of the structure while maintaining load carrying capabilities (Ritakallio, 2012). However, in order to use thinner gauges and meet customer's durability expectations, corrosion protection, and hence hot-dip galvanizing, becomes crucial (Petit *et al.*, 2012; Khondker *et al.*, 2007).

The first issue that involves high strength steel behavior during the hot-dip galvanizing process is a phenomenon called hydrogen embrittlement, which can lead to the premature failure of the structure. ASTM F2329 warns of the risk of internal hydrogen embrittlement when parts with a specified hardness of 33 HRC and higher are acid pickled prior to galvanizing (ASTM F2329, 2011). In general, the higher the strength levels of the steel, the greater the risk of hydrogen embrittlement (Eliaz *et al.*, 2002). Also, failures of welded structures fabricated from structural steel grade S355 have been reported. Local stresses, high hardness (in the heat affected zone) and diffusible hydrogen are the main factors responsible for failures of zinc coated products in general (Mraz *et al.*, 2009).

Three conditions must be met to cause hydrogen embrittlement failure: (1) steel that is susceptible to hydrogen damage, (2) stress (typically as an applied load), and (3) atomic hydrogen. If all three of these elements are present in sufficient quantities, and given time, hydrogen damage results in crack initiation and growth until the occurrence of fracture (Brahimi, 2014).

The more hydrogen amounts present in steel products, the more the risk of hydrogen embrittlement, which increases the risk of failure (Mabhoa *et al.*, 2010). Hydrogen diffuses into the steel only in atomic form (Gabe, 1997). The atomic hydrogen absorbed in steel is located in two positions in the microstructure: interstitial lattice positions (diffusible hydrogen) or crystalline defects (trapped hydrogen) (Shirband *et al.*, 2011). Atomic hydrogen can combine within the steel to form molecular hydrogen, which is trapped in the region of dislocations. An internal gas pressure can become so high that it might promote plastic deformation of the microstructure and cracking mechanism (Timmins, 1996).

Atomic hydrogen can be absorbed by the steel during the surface preparations steps such as pickling and fluxing process (Carpio *et al.*, 2009; Shirband *et al.*, 2011). During pickling, two major reactions can occur:

- chemical dissolution of the scale $\text{FeO} + 2\text{HCl} \rightarrow \text{FeCl}_2 + \text{H}_2\text{O}$ (1.1)
- chemical dissolution of the iron $\text{Fe} + 2\text{HCl} \rightarrow \text{FeCl}_2 + \text{H}_2$ (1.2)

The removal of scale (more commonly Fe_3O_4) is the desired result in the pickling process. The chemical dissolution of the iron is usually unwanted, and inhibitors are used to eliminate or decrease it (Chappell *et al.*, 1930).

Carpio *et al.* measured the hydrogen content after each operation in the galvanizing process (Carpio *et al.*, 2009). They stated that during fluxing the hydrogen content increases; this phenomenon does not occur during pickling due to the inhibitor presence, which does not allow reactions between acids and ferrum. The hydrogen absorption is affected by the composition of the steel surface. Phosphorous is reported to enhance the H absorption (Grabke *et al.*, 2010). Silicon lowers the solubility of hydrogen and thus causes a decrease in hydrogen permeation (Pressouyre, 1983).

Another issue of concern in galvanizing high strength steels is the zinc bath temperature, which might affect the mechanical properties of high strength steels. At the galvanizing temperature – usually around 450 °C – the steel being processed will lose approximately 50% of its room temperature yield strength,

regaining it on cooling after galvanizing (Industrial Galvanizers Specifiers Manual, 2016).

The possibility of effects of galvanizing on the mechanical properties was first reported already in 1975 (BNF Metals Technology Centre, 1975). The mechanical properties of 19 structural steels were investigated before and after galvanizing. The published report (BNF Metals Technology Centre, 1975) ‘Galvanizing of structural steels and their weldments’ concludes that hot-dip galvanizing does not affect tensile strength, proof strength, bend, or impact properties of structural steels. Changes in some mechanical properties (tensile elongation of 40% cold rolled steel tended to be increased by galvanizing) were detected only when the steel had been cold worked prior to galvanizing. Susceptibility to hydrogen embrittlement after pickling occurred also only with cold rolled steels with tensile strength >800 MPa but this was largely alleviated by the zinc immersion cycle even for the highest strength steel considered (930 MPa tensile strength). The work hence indicated that the galvanizing process had no detrimental effects on the mechanical properties of structural steels in use at that time (EGGA Engineering Summary, 2009).

In recent years, other studies have focused on the influence of hot-dip galvanizing on the mechanical properties of modern grades of structural steels (Langill, 2009; Dimatteo *et al.*, 2011; Aden-Ali *et al.*, 2009; Černý *et al.*, 2006; Hemmilä, 2016; EGGA Engineering Summary, 2009; Guertsman *et al.*, 2008).

Langill investigated mechanical properties of different steels (A36, A572 Grade 50, A572 Grade 65) after hot-dip galvanizing (Langill, 2009). Cold work processes and welding procedures were performed on these steels before the hot-dip galvanizing process. He concluded that hot-dip galvanizing has a relatively minor effect on the mechanical properties of investigated steels.

Dimatteo *et al.* studied hot rolled steel microalloyed with Ti and Nb (Dimatteo *et al.*, 2011). The results of tensile tests showed that the global mechanical properties change a little after galvanization. Comparison with bare steel shows an increase of 10% for the yield strength and the extension of the Lüders bands. Elongation has about the same values for galvanized and non-galvanized specimens. Moreover, coating process has been demonstrated to influence fatigue properties of the microalloyed steel (lower fatigue limit with galvanized specimens).

Aden-Ali *et al.* studied the mechanical properties of silicon-rich TRIP800 steel after hot-dip galvanizing (Aden-Ali *et al.*, 2009). They concluded that after hot-dip galvanization, steel ductility, expressed by elongation ratio and yield strength, increase (by 15% and 8 %, respectively), while tensile strength is reduced by 9%. The influence of hot-dip galvanization on fatigue properties is significant. In fact, under a stress range of 525 MPa, the endurance drops by a factor of ten in comparison with uncoated steel. Hot-dip galvanized and heat-treated steels show similar Lüders plateaus at the yield. These plateaus evidence heterogeneous yielding and localized plastic deformations (Lüders bands).

Černý studied the behavior of four types of structural steel (S235 with two different Si content, Q380TM and Q460TM) in individual technological steps (after hot rolling, after pickling, after degreasing, after fluxing, after hot-dip galvanizing) on the mechanical properties of steels (Černý *et al.*, 2006). On the basis of their experimental works, they stated that hot-dip galvanizing technology has no influence on mechanical, fracture and microstructure properties of hot-dip galvanized steels.

Hemmilä from Rautaruukki Oy considered the effect of pickling and hot-dip galvanizing on the mechanical and impact toughness properties of Optim 900 QC (ultra-high strength steel, yield strength over 900 MPa) (Hemmilä, 2016). The heat of the galvanizing process reduced the tensile strength slightly and increased the yield strength slightly, with negligible effect on ductility. No influence of the pickling process on the tensile or bend properties was observed.

The work performed under IZA ZC-21 project “Effect of Galvanizing on High Performance Steels and their Weldments” (EGGA Engineering Summary, 2009) used steel grades S275, S355, P460, A36, A572 Grade 50 and A572 Grade 65 steels. A number of steel conditions, ranging across various permutations of as-rolled, V-notch welded, 10% and 40% cold rolled, and galvanized, were considered. For all six grades of steel, proof and tensile strengths were slightly decreased (0.5%). HDG was found to have minor effect on the impact energy which is variable, depending on the steel metallurgy and condition. In all cases, the mechanical properties of the as-received plate exceeded the specification requirements by a significant margin, in either the galvanized or ungalvanized conditions.

Nordic Galvanizers Association claims that for high strength steels with yield strength (R_{eH}) > 650 Mpa, the fatigue strength is reduced during galvanizing (Steels suitable for galvanizing, 2016). The reduction may in some cases be as

high as 35%. For steels with lower yield strength than 650 Mpa, the reduction in fatigue strength is very low. It should be noted that steels without or with only poor corrosion protection may very quickly develop local corrosion attack (for example, pitting corrosion), which lowers the fatigue strength dramatically. This means that the fatigue resistance of the galvanized steel is usually superior in the long term.

The data from literature indicate that the HDG process generally produces a slight decrease in tensile strength, a slight increase in yield strength and slight but variable changes in ductility/elongation, which can either decrease or increase. Small decreases in Charpy impact energy have sometimes been observed after hot-dip galvanizing, but the recorded values of absorbed energy remained well above the values specified for the steel (EGGA Engineering Summary, 2009).

Another issue in galvanizing is liquid metal embrittlement (LME). LME is the reduction in the elongation to the failure ratio (Nicholas *et al.*, 1979). It can occur if a sensitive material under stress gets in contact with a liquid metal (Rädecker, 1973). The liquid metal reduces the deformation properties of the solid metal through penetration along the grain boundaries and causes a brittle fracture (Luithle *et al.*, 2015). It is stated that the higher the strength of the wetted material, the higher is the sensitivity to LME (Rostoker *et al.*, 1960). Embrittlement due to zinc has been reported to occur most frequently after hot-dip galvanizing oxy-fuel cut, welded or sharply cold formed parts (Okafor *et al.*, 2013).

1.3 Objectives of the study

The literature review revealed that there is lack of studies focused on the effect of modern high strength steel on the coating formation and quality during the batch HDG process. In addition, the theory of silicon effect is not sufficient to explain many processes during galvanizing. Therefore, it is necessary to study the role of silicon on the coating formation.

It is important to improve knowledge of how high strength steel properties affect the quality of hot-dip galvanized coatings to establish the quality that would satisfy the costumers` demands on 1) zinc coating appearance and corrosion resistance (coating thickness); 2) reliability (steel mechanical properties) of hot-dip galvanized steel structures. The main objectives of this thesis are to study the effect of steel composition and the galvanizing process on the coating formation and steel properties and to propose criteria for steel selection for HDG.

Resulting from the main objectives of the study, the following activities were planned:

1. To study the influence of substrate microstructure (ferrite grain size, ferrite grain shape, carbide grain size, carbide grain shape) on the HDG
2. To analyze hydrogen embrittlement of high strength steel during the pre-treatment process
3. To investigate the effect of zinc bath temperature on the mechanical properties of galvanized steel
4. To study the effect of the chemical composition (silicon content) of steel on the zinc coating formation that is the basis for appearance and corrosion resistance of the coating.

2. MATERIALS AND METHODS

2.1 Galvanizing process description

General galvanizing. A batch-type HDG process was used. According to common practice of the HDG process, which includes degreasing, pickling in HCl, rinsing, and fluxing, the samples were subjected to pre-treatment. The steel sheets were degreased in an acid degreasing agent (KeboClean VZS) and then pickled in HCl (10%) solution containing an inhibitor for the protection of metal surfaces. Next, the sheets were rinsed in water and then dipped in a flux bath. The fluxed sheets were dried for 15 min at 120 °C in a drying oven (in [Paper V] drying oven was not used). Then the sheets were dipped in the zinc bath at the temperature 450 °C. The zinc bath consisted of zinc (99.3% Zn) containing also Al, Bi, Fe, Ni, Sn, and Pb.

Centrifuge galvanizing. The same pre-treatment process was applied like in a general galvanizing line (except there was no drying oven after fluxing). The galvanizing bath temperature was 550 °C. The zinc bath consisted of zinc (99.7% Zn) containing also Al, Bi, Fe, Ni, Sn, and Pb.

2.2 Microstructural analysis of steel and zinc coating

For the examination of the microstructure, hot-dip galvanized specimens were cross sectioned, hot mounted, ground and polished. A nital etchant (nitric acid: 3 %) was used to reveal the microstructures of the specimens and observations were made with optical microscope Zeiss Axiovert 25 and scanning electron microscopy EVO MA-15 (Carl Zeiss). The thickness of coatings was determined by electromagnetic thickness gauge (Dualscope MP0). The chemical composition of the substrate material was measured using Spectrolab M. The Rockwell hardness was measured with a Zwick Roell hardness testing machine. The Vickers hardness was measured with a Micromet 2001 microhardness tester. Vickers hardness at the load of 9.8 N was measured at the polished cross-section of a specimen after the galvanizing process. Tensile strength was measured with an Instron 8800 servo-hydraulic testing machine. Ferrite grain size (G) was determined according to the reference images of the standard DIN 50601.

2.3 Substrate preparation

Four steel grades (hot rolled S355JR, thermomechanically rolled S700MC, cold rolled and annealed C45E and C60E) with different silicon equivalents were used

in the experiment. The chemical compositions of the steels are presented in Table 2.1. The substrate materials were 3 mm thick.

Table 2.1 Chemical composition of the substrate steels, %

Steel	C	Si	P	Mn	Cr
S355JR	0.10	0.01	0.015	0.42	0.02
S700MC	0.05	0.45	0.016	1.85	0.35
C45E	0.44	0.21	0.007	0.66	0.21
C60E	0.62	0.06	0.005	0.67	0.24

To achieve different microstructures, laboratory heat treatment was used. Heat treatment parameters were chosen to imitate the heat affected zone in the welding and thermal cutting processes.

1) Changing the ferrite grain size – S355JR, S700MC and C45E steels were austenitized at the temperature 900 °C, 1000 °C and 1200 °C for 2 h, followed by water quenching and tempering at the temperature of 600 °C for 1 h. High austenitization temperature will induce austenite grain coarsening while carbon held in a solid solution until tempering at 600 °C produces equal carbide grain size.

2) Changing the size of carbide grains (affecting also ferrite grain size and shape) – C45E and C60E steels were austenitized at the temperature 900 °C for 30 min, quenched in water and tempered at 200 °C, 300 °C, 400 °C, 500 °C, 600 °C, and 700 °C for 1 h. Tempering results in the precipitation of carbides and at higher temperatures, in carbide coarsening. Quenching to the martensite, followed by the HDG at 450 °C and 550 °C, resulted in the tempering of the martensite and carbide precipitation.

To guarantee the same chemical composition and surface roughness of the specimens, the decarburized layer was removed by mechanical grinding before the HDG process.

2.3.2 Study of hydrogen embrittlement during acid pre-treatment

To evaluate the hydrogen embrittlement during the HDG surface preparation steps, specimens (substrate steel C35, which was under stress) were used (Fig. 2.1). The chemical composition of the steel is presented in Table 2.2. Hydrogen embrittlement was studied with different strain levels and different substrate heat treatments. As a result of hydrogen embrittlement, a crack occurred where the

maximum stress was applied (Fig. 2.1). Strain level was adjusted with a screw, the change in dimensions (Δ) was measured. The higher the value of Δ , the higher the stress level. To have different strains, the dimension reduction $\Delta=2$ mm and $\Delta=3$ mm was used.

Different mechanical properties of the substrates were achieved with laboratory heat treatments. Steel C35 was austenitized at the temperature 860 °C for 20 min, quenched in water and tempered at 200 and 300 °C for 1 h. The Rockwell hardness after heat treatment was measured (see Table 2.3).

Table 2.2 Chemical composition of the substrate steel, %

Steel grade	C	Si	P	Mn	Cr
C35	0.40	0.19	0.009	0.62	0.33

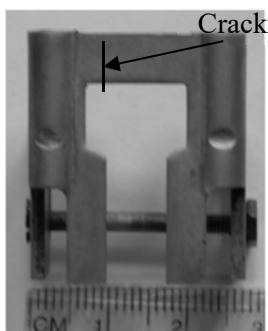


Figure 2.1 Specimen for the evaluation of hydrogen embrittlement

Table 2.3 The Rockwell hardness of C35 after different heat treatments

Heat treatment	HRC
Quenched	55.0
Quenched + tempered 200 °C	48.6
Quenched + tempered 300 °C	46.3

2.3.3 Study of the HDG effect on the mechanical properties of high strength steels

Three steel grades (hot rolled structural steel S355J2, Ruuki optim 650 MC with thermo-mechanical treatment, cold rolled soft annealed C60E) were used in the experiment. The chemical compositions of the steels are presented in Table 2.4. The substrate materials were 3 mm thick.

Table 2.4 Chemical composition of the substrate steels, %

Steel grade	C	Si	P	Mn	Cr
S355J2	0.06	0.02	0.006	0.74	0.05
Ruuki optim 650 MC	0.05	0.16	0.008	1.71	0.03
C60E	0.58	0.05	0.001	0.69	0.24

C60E was austenitized at the temperature 900 °C for 30 min, quenched in water and tempered at 200 °C, 300 °C, 450 °C, and 650 °C for 45 min to evaluate how the zinc bath temperature affects the mechanical properties of the quenched and tempered steel.

2.3.4 Study of the impact of silicon content

To investigate the influence of silicon on the reaction between steel and liquid zinc in [Paper V], centrifugal casting was used to prepare specimens with different silicon content. Steel powder (ATOMET 1001) and calculated amount of Fe–Si powder (Si 46.10%) were melted in a vacuum induction furnace and cast into a copper mould. The chemical composition of the FeSi powder is shown in Table 2.5.

Table 2.5 Chemical composition of the FeSi powder, (%)

Fe	C	Si	Mn	P	S	Al
53.45	0.01	46.10	0.27	0.02	0.001	0.15

The diameter of the cast samples was 35 mm at the thickness of 3 mm. The chemical composition of each specimen was measured using Spectrolab M. The results are presented in Table 2.6. The specimens were annealed at 730 °C for 1 hour and then air cooled. The oxidation layer was removed by mechanical grinding (80 grit). A small hole was drilled near the edge of each sample to help hang the specimens during the galvanizing process.

The dipping time in the liquid zinc was 4, 7, 12, 25, 195, and 1200 s. After galvanizing, the specimens were quenched in water to prevent further diffusion reaction during air cooling.

Table 2.6 Chemical composition of the specimens, %

Sample	C	Si	Mn	P	Fe
1*	<0.01	<0.01	0.04	0.005	99.72
2	<0.01	0.06	0.04	0.007	99.66
3	<0.01	0.11	0.05	0.006	99.60
4	<0.01	0.17	0.05	0.006	99.54
5	<0.01	0.30	0.05	0.007	99.40

* Steel powder ATOMET 1001 without Fe–Si powder addition.

To study temperature changes in the wall of a specimen during dipping in the molten zinc, a Vernier Software thermocouple was used. Figure 2.2 shows the heating curve of the specimens during dipping in the molten zinc at 450 °C. It took approximately 20 s to establish the melting temperature of zinc (419.5 °C) with the investigated specimens.

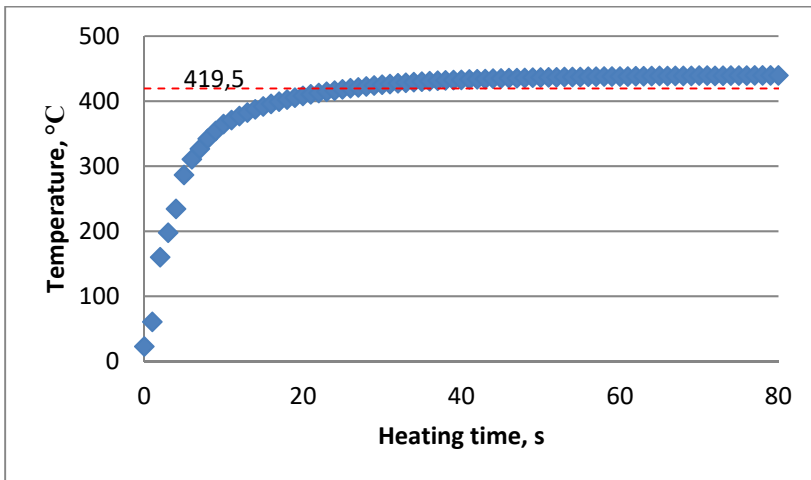


Figure 2.2 Temperature change inside the specimens

3 RESULTS AND DISCUSSIONS

3.1 Impact of the microstructure of steel on coating formation

Experiments were carried out to investigate the effects of substrate microstructure on Fe-Zn reaction kinetics and phase formation during a low and a high temperature HDG process. Laboratory heat treatment was used to imitate the microstructures of new steel grades (with fine ferrite grain size and quenched and tempered microstructures) and to imitate the formation of heat affected zone in the welding and cutting process.

The effect of ferrite and carbide grain size at the galvanizing temperature 450 °C is described in *Paper II*. Additionally, galvanizing experiments at the temperature 550 °C to study the effect of ferrite and carbide grain shape on the coating process were added in this thesis research. Results have also been published in Intergalva 2012 proceedings (Sepper *et al.*, 2012).

3.1.1 Effect of ferrite grain size

To examine the effect of the ferrite grain growth on the zinc layer formation, two structural steels (S355JR; Si 0.01 % and S700MC; Si 0.45 %) and one carbon steel (C45E; Si 0.21 %) were used in this study. The effect of ferrite grain size on the formation of a hot-dip galvanized coating is presented in Table 3.1. Figure 3.1 shows the coating microstructure of steel S355JR with ferrite grain size G12 and G4. The coating has a typical microstructure of non-reactive steel. According to the Fe-Zn phase diagram at the galvanizing temperature 450 °C, Γ , δ , ζ , and η phase were formed (Figs. 3.1, 1a and 1b). At the galvanizing temperature 550 °C, the ζ phase does not form and the coating primarily consists of δ phase (Figs. 3.1, 2a and 2b).

The total Fe-Zn layer growth and coating microstructure for each steel grade showed the same behavior despite the ferrite grain size and the galvanizing temperature. The results showed that the coating structure and thickness are not connected with the grain size of the substrate ferrite of the investigated materials and the galvanizing conditions.

Table 3.1 Effect of ferrite grain size on coating thickness

Heat treatment*	S355JR (Si 0.01 %)			S700MC (Si 0.45 %)			C45E (Si 0.21 %)		
	Grain size G	Coating thickness, μm		Grain size G	Coating thickness, μm		Grain size G	Coating thickness, μm	
		450 °C	550 °C		450 °C	550 °C		450 °C	550 °C
1	12	64	74	14	135	74	12	124	83
2	8	64	83	10	147	81	8	105	82
3	6	57	75	8	149	81	6	100	79
4	4	66	65	4	140	75	3	106	89

* 1 – as received; 2 – austenitized at 900 °C, quenched in water and tempered at 600 °C; 3 – austenitized at 1000 °C, quenched in water and tempered at 600 °C; 4 – austenitized at 1200 °C, quenched in water and tempered at 600 °C

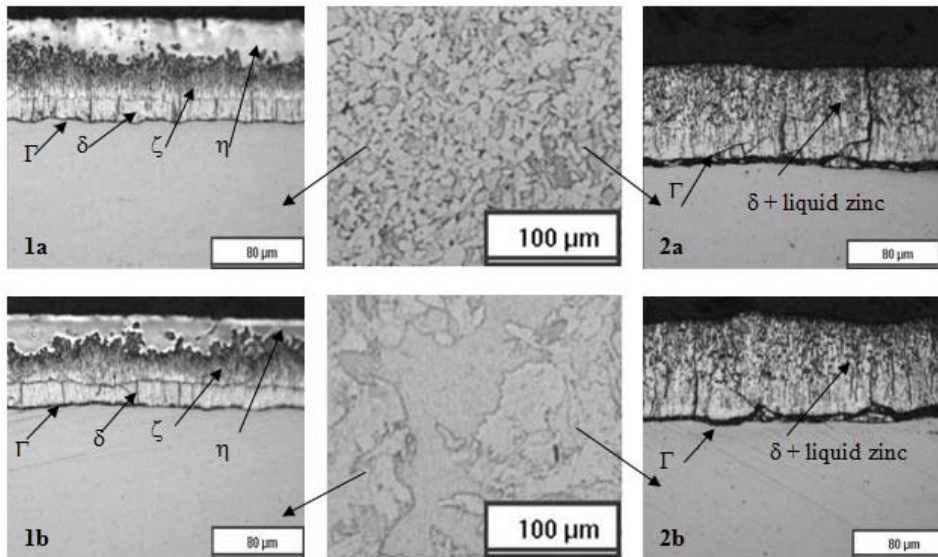


Figure 3.1 Micrographs of the cross-sections of the coatings: a – S355JR (Si 0.01 %) with ferrite grain size G12; b – S355JR with ferrite grain size G4. Galvanizing temperatures: 1 – 450 °C; 2 – 550 °C

3.1.2 Analysis of ferrite grain elongation and recrystallization

Thermomechanically hot rolled microalloyed steel S700MC (high silicon content; Si 0.45%) had elongated ferrite grains as received condition. During the laboratory heat treatment, elongated grains are recrystallized. Figure 3.2 shows the zinc coating microstructure with substrate steel with elongated grains and with

substrate steel with recrystallized grains (heat treatment: austenitized at 900 °C, followed by quenching in water and tempering at 600 °C). The coating thickness is not influenced by ferrite grain shape in both galvanizing temperatures. Ferrite grain shape has an effect on the coating microstructure at the galvanizing temperature 450 °C. Steel S700MC with elongated ferrite grains has a tendency to grow the ζ phase. When the steel has recrystallized grains, the $\delta + \zeta$ phase dominates in the coating microstructure. At the galvanizing temperature 550 °C, the coating morphology is not affected by ferrite grain elongation and recrystallization.

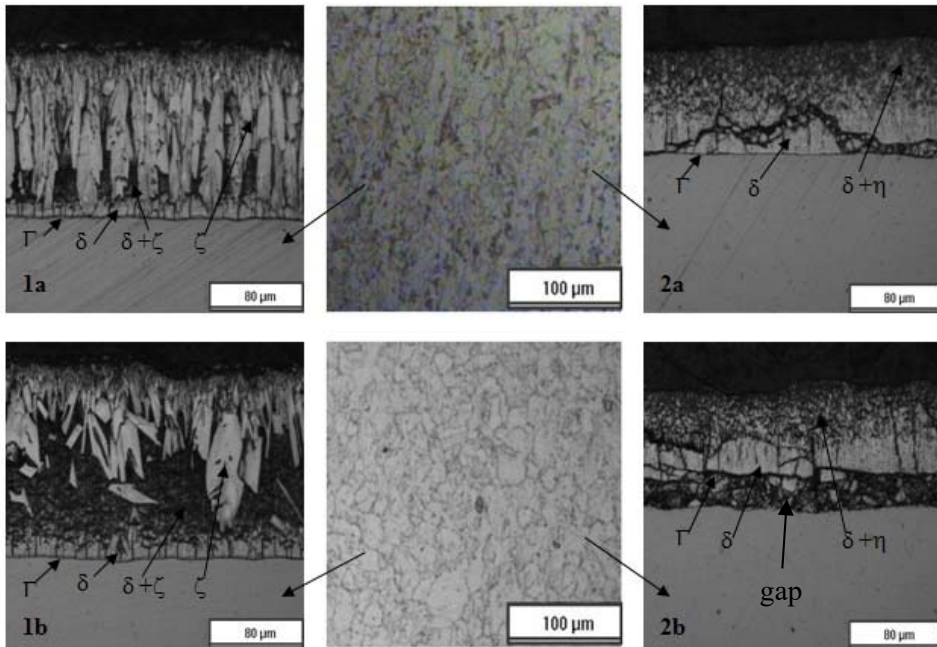


Figure 3.2 Effect of grain elongation and recrystallization on the coating formation: a – S700MC (Si 0.45%) with elongated grains; b – S700MC with recrystallized microstructure. Galvanizing temperatures: 1 – 450 °C; 2 – 550 °C

3.1.3 Impact of the size and shape of carbide grains

Size of the carbide grains

Carbon is the main element in steels influencing strength and hardness at different heat treatment conditions in steel production. In the present study, carbon steels with different carbon content were heat treated in laboratory to achieve differences in the microstructure.

To study the effect of carbides in different heat treatment conditions, two substrate materials were used (C45 with Si content 0.21% and C60 with Si content 0.06%) with several heat treatment conditions (austenitized at the temperature 900 °C, quenched in water and tempered at the temperature 200 – 700 °C with a step of 100 °C).

Differences in the size of carbides that influence the coating formation were observed only at the galvanizing temperature 450 °C (Figs. 3.3, 3.4). At the high temperature galvanizing process (550 °C), the carbides do not affect the coating formation (Figs. 3.4, 1b*, 2b* and 3b*). It was considered that the substrate hardness increases with the decrease of the carbide size.

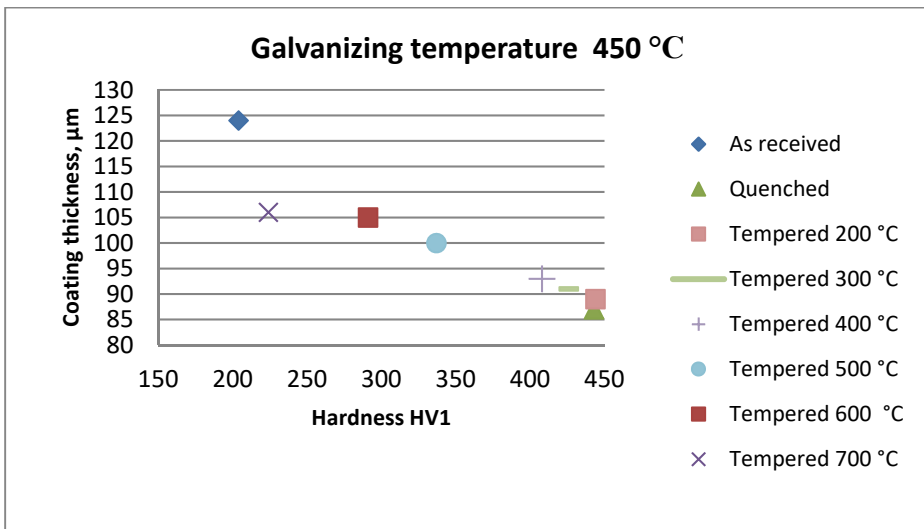


Figure 3.3 Relationship between the coating thickness and substrate (C45E) hardness at 450 °C

At the galvanizing temperature 450 °C, a thinner coating was formed in the case of smaller carbides (Figs. 3.3, 3.4). Reduction in the coating thickness was remarkable with steel C60E (Fig. 3.4, a). The silicon content of the substrate belongs to the Sandelin range and during the galvanizing process, a rapid growth of the ζ layer occurred, producing a coating with excessive thickness. As a result of hardening, carbide size decreased and a continuous compact zinc coating formed, which was composed of the Γ , δ , ζ , and η layer.

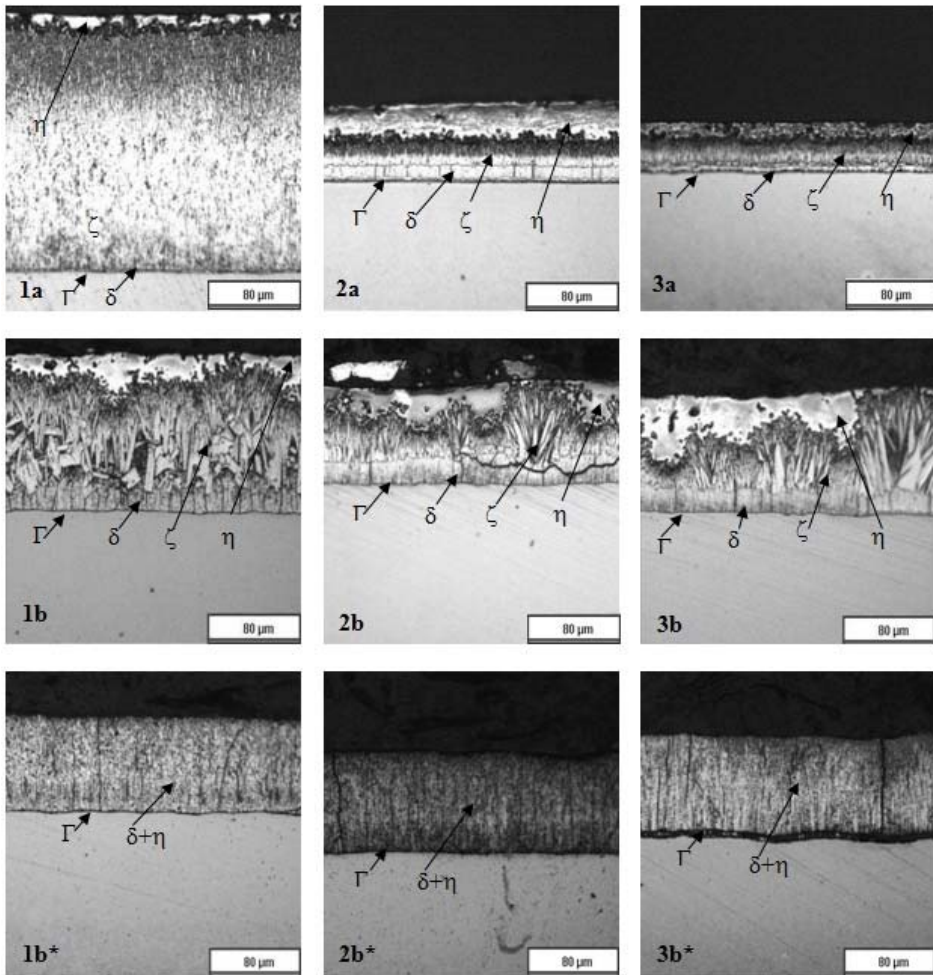


Figure 3.4 Effect of the carbide grain of the steel on the formation of hot-dip galvanized coatings: a – C60E (Si 0.06 %); b – C45E (Si 0.21 %). Heat treatments: 1 – as received (soft annealed); 2 – austenitized 900 °C, tempered 300 °C; 3 – quenched in water.

* - galvanizing temperature 550 °C

The results show that carbide grain size influences the coating formation only at lower galvanizing temperatures (450 °C). With smaller carbide grains, a thinner coating was formed. The reduction of coating thickness mainly resulted from the decrease in the ζ phase thickness. A marked reduction of thickness occurred with Sandelin steel.

Shape of carbide grain

To study the effect of the shape of the carbide grains on the zinc coating formation, carbon steel C45E (Si 0.21%) was used. Heat treatment changes the shape of carbides (spheroidal after tempering and elongated after normalizing). The variation of aspect ratios AS (ratio of maximum diameter to minimum diameter) of the carbides and the influence on the coating thickness is shown in Fig. 3.5. In the current study, the effect of the shape of carbide grain on the coating formation was not observed at the galvanizing temperature 450 °C and 550 °C.

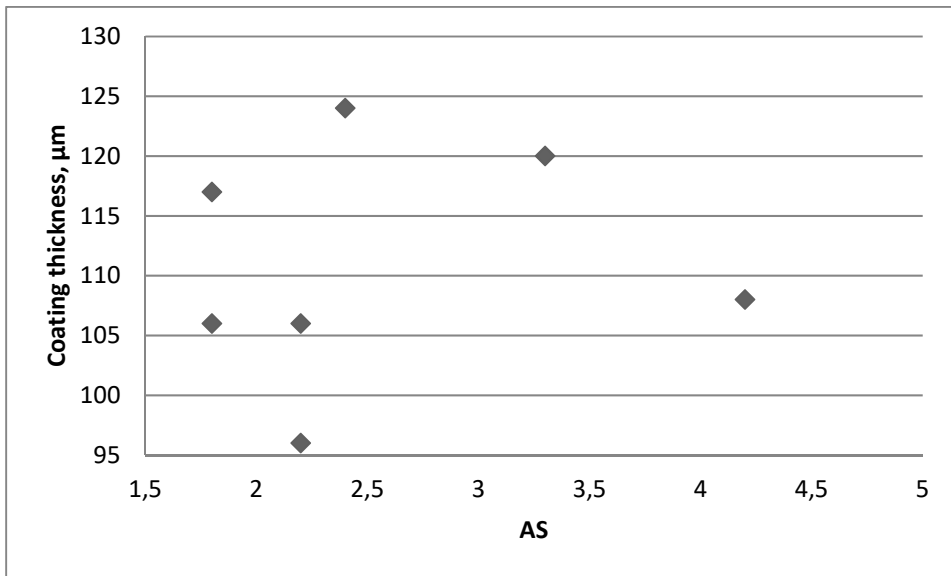


Figure 3.5 Effect of the aspect ratio (AS) of carbides on the coating thickness at 450 °C

3.2 Influence of pretreatment on hydrogen embrittlement

The objective of the experiments was to investigate hydrogen diffusion during the HDG pretreatment processes. This leads to understanding the causes of hydrogen embrittlement of high strength steels during the galvanizing process and thus helps to evaluate the reliability of steel structures. The results are described in *Paper III*.

During the HDG, surface preparation (degreasing, pickling and fluxing) is used which can induce hydrogen into the substrate material and enhance the hydrogen embrittlement. To study the effect of hydrogen during the hot-dip galvanization, it is necessary to have specimens with different hardness at the different tensions. Specimens have to indicate the high hydrogen diffusion rate and sensitivity to

failure during the HDG process. Therefore, C35 steel was used with different heat treatments and deformations. Strain level was adjusted with a screw, the change in dimensions (Δ) was measured (Fig. 3.6). Mechanical properties of the studied specimens describe the properties of the quenched and tempered part or those of the heat affected zone (HAZ) in welding.

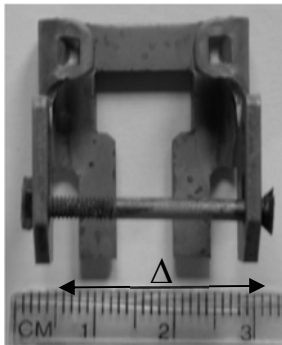


Figure 3.6 Change in the dimensions (Δ) measurement

Specimens were immersed in the surface preparation chemicals used during the HDG process. Different deformation Δ was taken as an indicator of applied stresses. The specimens were dipped in the pretreatment chemicals until hydrogen embrittlement occurred. The highest risk of hydrogen embrittlement was found at maximum hardness values and at maximum deformation.

The first step in the HDG is the degreasing process to remove grease and oil from the surface of the steel. Acid degreasing is a new cost saving development because no water rinsing before the acid pickle and no heating is required. Acid degreaser contains acids which might cause hydrogen embrittlement. The usual degreasing time in the galvanizing process was 30 min.

Quenched specimens (HRC 55) with deformation $\Delta=3$ mm were dipped in the acid degreasing solution (contains inhibitors). No hydrogen embrittlement occurred with the dipping time of 3 h. No hydrogen embrittlement was observed during the degreasing process under the investigated conditions.

The next pretreatment step is pickling to remove rust and scale from the steel surface. The relationship between the Rockwell hardness, applied stresses and hydrogen embrittlement is shown in Fig. 3.7. No hydrogen embrittlement occurred with the substrate Rockwell hardness of 46.3 HRC at the investigated

strain levels. The higher the substrate hardness and the applied strain, the more rapidly hydrogen embrittlement occurred.

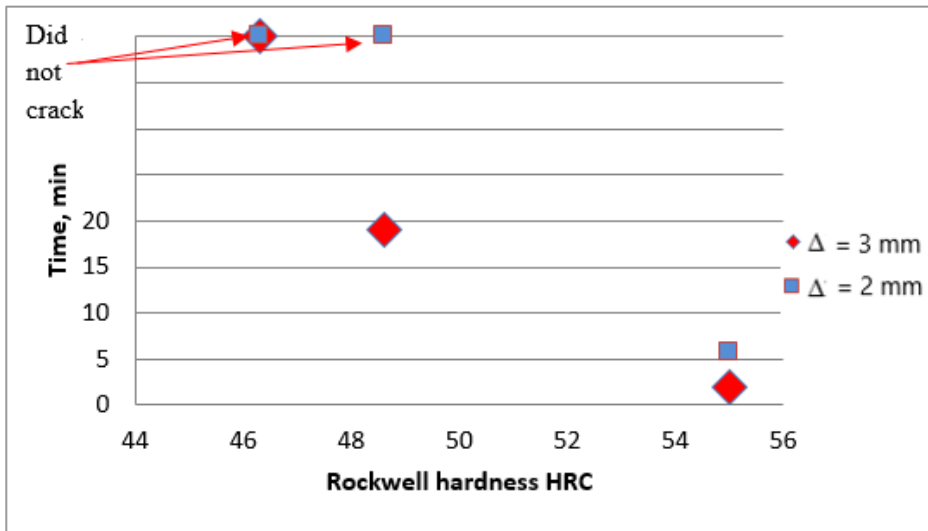


Figure 3.7 Hydrogen embrittlement formation with different substrate hardnesses in the pickling solution

The final pretreatment chemical was flux (zinc ammonium chloride) to assist the molten zinc to react with the steel surface to form the galvanized coating. The regular dipping time was 0.5 – 1 min. The crack formation occurred with quenched specimens with deformation $\Delta=3$ mm in 27 min. Quenched specimens with deformation $\Delta=2$ mm did not suffer from hydrogen embrittlement after dipping for 24 h.

In this study, the hydrogen-entry occurred in the pickling and fluxing solutions (no hydrogen embrittlement in the degreasing solution was observed). But the main process that caused hydrogen embrittlement was the pickling process, although pickling solution contained an inhibitor. Hydrogen embrittlement occurred when the substrate hardness was higher than 48.6 HRC (tensile strength $R_m \geq 1550$ MPa). Usually steels with so high tensile strength are not hot-dip galvanized. The risk of hydrogen embrittlement is higher with higher applied stress values.

Quenched and tempered parts that are hot-dip galvanized should have hardness less than 48.6 HRC to avoid the hydrogen induced failure. The HAZ in welding should have hardness less than 480 HV, which is not allowed according to the

quality requirements of welding. Failures occurring with lower hardness are related to the complex failure mode where hydrogen is not the only reason of the failure.

3.3 Effect of HDG on the mechanical properties of steel

As new steel grades with higher yield and tensile strength have come to the market, it is necessary to learn how they are affected by the galvanizing process. The objective of the experiments was to investigate the effect of zinc bath temperature on the mechanical properties of high strength steels that help to consider the reliability of hot-dip galvanized structures. The results are described in *Paper III* and *Paper IV*.

The effect of zinc bath temperature was studied in two cases: the aging of the thermo-mechanically rolled low carbon steel or tempering the quenched and tempered steel. In engineering, it is required to take into account both of the cases because construction properties are affected by short time heating during dipping in the molten zinc. Additional studies addressed the pickling effect, the heat effect of the galvanizing temperature, and the effect of zinc coating on the results of tensile strength.

The influence of HDG on the properties of quenched and tempered parts was studied in *Paper III* and the results are shown in Fig. 3.8. Specimens were made from C60E and laboratory heat treatment was used before HDG. Hardness will decrease less in tempering at shorter time than in longer time (ASM Handbook, 1991). The results show that during short dipping (4 min) at the temperature 450 °C, hardness decreases to 42–43 HRC (Fig. 3.8). Heating during dipping will decrease hardness of the quenched and tempered steel parts the tempering temperature of which is lower than 450 °C. Higher temperature tempered steel parts have no loss in hardness. The same phenomena occur at the galvanizing temperature 550 °C and it can be predicted that hardness will be 30 HRC.

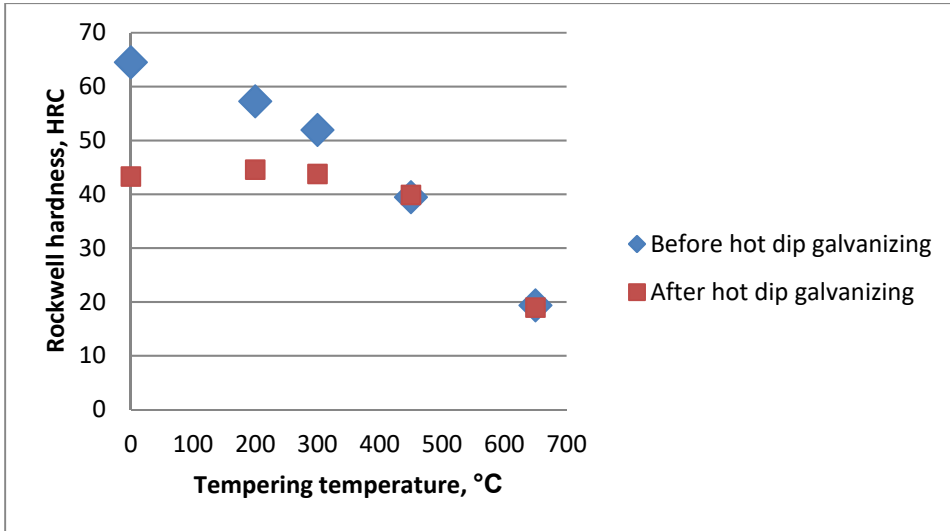


Figure 3.8 HDG heat effect on the quenched and tempered parts (galvanizing temperature 450 °C)

During the HDG, surface preparation steps (degreasing, pickling and fluxing) are used that can induce hydrogen into the substrate material and enhance the hydrogen embrittlement. According to the experiments, the main process that caused hydrogen embrittlement was pickling, although pickling solution contained an inhibitor. To find out if the pickling process can affect the mechanical properties of the steel, the tensile test specimens were pickled for 2 h in 10% HCl acid containing inhibitor. The tensile test was carried out immediately after pickling. The results of the study showed that the pickling process did not affect the mechanical properties of structural steel S355J2 and high strength steel S650MC (Tables 3.2 and 3.3).

To study the effect of the galvanizing temperature on the mechanical properties of high strength steels, in our experiments, two temperatures were applied: 450 °C (normal galvanizing) and 550 °C (high temperature galvanizing). To eliminate the effect of chemical reaction between the iron and zinc, tests were made with dipping the tensile test specimens into the molten salt (450 °C and 550 °C). Mechanical properties of steels are shown in Tables 3.2 and 3.3 and stress-strain curves are presented in Fig. 3.9.

Table 3.2 Tensile test results of S650MC steel

Sample	$R_{p0.05}$ [MPa]	$R_{p0.2}$ [MPa]	R_m [MPa]	A_g [%]	A_{80} [%]
1	727 ± 17.9	782 ± 2.1	826 ± 9.0	8.9 ± 0.5	14.9 ± 0.1
2	721 ± 13.6	774 ± 4.6	827 ± 0.4	8.6 ± 0.7	14.8 ± 1.1
3	794 ± 16.9	772 ± 8.5	819 ± 8.2	9.0 ± 0.7	15.6 ± 0.2
4	806 ± 23	784 ± 2.1	825 ± 3.5	8.6 ± 0.6	14.4 ± 1.1

1 - as received condition, 2 - after pickling, 3 - after dipping in the salt 450 °C, 4 - after dipping in the salt 550 °C

Table 3.3 Tensile test results of S355J2 steel

Sample	$R_{p0.2}$ [MPa]	R_m [MPa]	A_g [%]	A_{80} [%]
1	424 ± 3.5	489 ± 3.2	15.7 ± 0.2	26.9 ± 0.5
2	428 ± 2.0	493 ± 1.3	15.2 ± 0.1	26.2 ± 0.3
3	481 ± 13.5	495 ± 4.0	14.9 ± 0.2	25.9 ± 0.7
4	470 ± 7.6	496 ± 2.0	15.2 ± 0.4	25.4 ± 0.5

1 - as received condition, 2 - after pickling, 3 - after dipping in the salt 450 °C, 4 - after dipping in the salt 550 °C

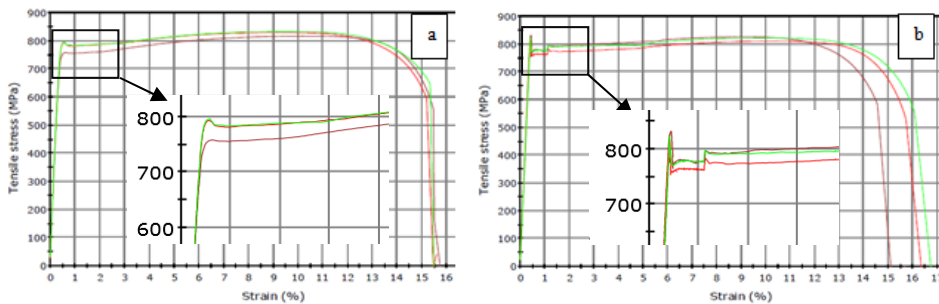


Figure 3.9 Stress-strain curves: a – S650MC as received; b – S650MC after dipping in salt 450 °C

After heating steels S650MC and S355J2 in the molten salt an increase in $R_{p0.05}$ (in the case of S650MC) and $R_{p0.2}$ (in the case of S355J2) was observed, but A_{80} , R_m and A_g had virtually minor changes. The greatest change is visible in the stress-strain curves (S650MC and S355J2), where Lüders strain (elongation) appears after heating. This behavior is characterized by an initially high yield stress, followed immediately by a sudden fall in stress. With continued straining, the stress stays approximately unchangeable for several strain percentage before

normal strain hardening behavior begins (Meier *et al.*, 2015). This effect is also the reason of the increase in the strength properties $R_{p0.05}$ (and $R_{p0.2}$).

The tensile test results of hot-dip galvanized S355J2 and S650MC are presented in Tables 3.4 and 3.5. As hot-dip galvanized specimens include zinc coating thickness, these results are not comparable with “as received” results. When discounting the coating thickness and calculating the yield and tensile strength using only the base steel thickness, an extra load resistance during the tensile test is expected. Load at R_m in both investigated steels is higher with zinc coating because zinc coating increases the strength of the specimen.

Table 3.4 Tensile test results (S650MC) after HDG

Sample	$R_{p0.05}$ [MPa]	$R_{p0.2}$ [MPa]	R_m [MPa]	A_g [%]	A_{80} [%]	Load at R_m [kN]	Thickness [mm]
1	766 ± 11.7	738 ± 8.1	775 ± 8.7	9.2 ± 0.2	15 ± 1.8	50.2 ± 0.7	3.16
2	822 ± 17.7	785 ± 3.7	826 ± 1.5	9.3 ± 0.2	16.1 ± 0.5	48.4 ± 1.7	2.98
3	779 ± 10.8	752 ± 5.5	790 ± 4.8	9.3 ± 0.4	15.9 ± 0.7	50.3 ± 0.2	3.10
4	798 ± 5.2	784 ± 1.6	823 ± 2.4	9.7 ± 0.1	16.4 ± 0.4	49.6 ± 0.4	2.98

1 – hot-dip galvanized (450 °C) with zinc layer, 2 – hot-dip galvanized (450 °C) without zinc layer, 3 – hot-dip galvanized (550 °C) with zinc layer, 4 – hot-dip galvanized (550 °C) without zinc layer

Table 3.5 Tensile test results (S355J2) after HDG

Sample	$R_{p0.2}$ [MPa]	R_m [MPa]	A_g [%]	A_{80} [%]	Load at R_m [kN]	Thickness [mm]
1	465 ± 5.8	477 ± 2.7	13.8 ± 0.1	24.9 ± 0.7	30.8 ± 0.3	3.14
2	488 ± 2.9	496 ± 1.3	14.3 ± 0.2	23.9 ± 1.2	29.7 ± 0.4	3.00
3	470 ± 11.7	476 ± 5.9	14.2 ± 0.1	23.6 ± 0.5	30.2 ± 0.8	3.12
4	475 ± 8.3	489 ± 3.6	15.5 ± 0.5	25.9 ± 1.0	29.4 ± 0.8	2.98

1 – hot-dip galvanized (450 °C) with zinc layer, 2 – hot-dip galvanized (450 °C) without zinc layer, 3 – hot-dip galvanized (550 °C) with zinc layer, 4 – hot-dip galvanized (550 °C) without zinc layer

After zinc layer removal in 10% HCl, similar to as received specimens, the tendency of increase in $R_{p0.05}$ value (and in the case of S355J2 increase in the $R_{p0.2}$ value) occurs. Lüders strain appears in the stress-strain curves after the HDG (in both steels investigated – S650MC and S355J2) as a result of the heating and aging effect.

Aging is the mechanism that increases the strength properties while elongation is decreased (Rashid, 1976). Aging can vary with the same steel grade as it can be

produced using different chemistry and thermo-mechanical rolling or even cold rolling. Aging can be explained by carbon and nitrogen atoms diffusion to the dislocations and locking them. Additional stress over that normally required for the movement of the dislocations is needed in order to tear some of the dislocations away from their restraining impurity atoms. This results in the increase in stress, which sets some dislocations in motion, and corresponds to the upper yield point stress. When the dislocation line is pulled free from the influence of the soluted atoms, it can slip at a lower yield point stress (Cottrell's theory).

It is concluded in *Paper IV* that short heating of low carbon steel at the HDG temperature (usual dipping time in molten zinc is 4 – 8 min) does not cause ferrite grain growth. The grain size was measured after heating at different temperatures (450 °C, 550 °C, and 650 °C for 30 min).

High strength low alloy steels are subjected to the aging process during immersion to the zinc bath even with a relatively short heating time. Tests made with carbon steel C35 showed that hydrogen diffuses from the pickling process to the steel even in the case of acid with an inhibitor. Hydrogen leads parts to the failure when hardness is over 48.6 HRC, which responds to the tensile strength 1550 MPa. The tensile strength and hardness of HSLA steels is under 48.6 HRC and therefore hydrogen induced failure alone cannot be the reason of the failure during HDG even after aging. Hydrogen can make material more brittle and stresses in construction with welding defects can lead to the failure during the HDG.

3.4 Impact of silicon content

The coating thickness in addition to coating appearance is important because it is related to the service life of the hot-dip galvanized steel. Conscious customers' demand to the galvanizers is to provide specific coating thickness in accordance with environmental class requirements. It is important to consider the chemical composition of steel (especially silicon content) during selecting the steel because the appearance and the thickness of the coating are directly related to it. The galvanizers can choose the dipping time in molten zinc based on the silicon content to establish thickness demands.

Paper V describes the coating formation with different substrate silicon content at 450 °C, which is the common galvanizing temperature. Galvanizing time for coating formation was 4, 7, 12, and 25 s and for coating growth 195 and 1200 s after longer incubation time.

Coating growth with dipping time up to 25 s

Dipping time (4, 7, 12, and 25 s) was short in the investigation of coating formation on top of the substrates shown in Table 2.6.

After dipping cold steel into the zinc bath, zinc will freeze in the contact surface of steel. Even a very short time contact between steel and zinc leads to the formation of Fe–Zn intermetallic compounds, which are in solid state. After 4 s of dipping in the molten zinc, a thin layer of intermetallic phases (ζ and δ) was observed with all tested silicon contents (Si < 0.01%, 0.06%, 0.11%, 0.17%, and 0.30%). Poor adhesion between the steel and the coating could be observed at a dipping time of 4 s.

After galvanizing for 4 s, the microstructure and thickness of the Zn–Fe layer were similar regardless of the content of silicon in the substrate. This is also confirmed by the experiments reported in (Liberski *et al.*, 2014). Figure 3.10 presents the microstructure of the zinc coating (Si 0.30 %) after a dipping time of 4 s. First, the ζ phase occurred, which was immediately followed by the δ and then, after incubation, by the Γ phase. The same test results were reported by Mandal *et al.* at the galvanizing temperature of 470 °C (Mandal *et al.*, 2009) and Lekbir *et al.* at the galvanizing temperature of 460 °C (Lekbir *et al.*, 2017). It is frequently reported that the first intermetallic compound that appears during HDG is the ζ phase (Foct *et al.*, 1993). However, Kopyciński postulated that the Γ phase nucleates first, followed by the δ and ζ phases in a Zn–Ni bath at 450 °C (Kopyciński, 2010). It is difficult to evaluate the Γ phase because of its small thickness.

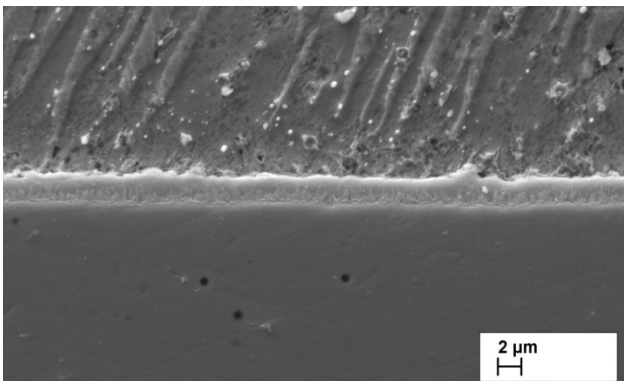


Figure 3.10 Microstructure of the zinc coating after the dipping time of 4 s (Si 0.30%)

Furthermore, with a dipping time of 4 s, a thick η layer (ca 800 μm) was present in the coating. It is hypothesized that as the specimen's inside temperature after the galvanizing time of 4 s is low (less than 300 $^{\circ}\text{C}$, Fig. 2.2) and probably the temperature in the contact surface of steel and zinc is below the melting temperature of zinc, the nucleation of intermetallic phases takes place in solid state and therefore a thick η layer is present in the coating with the dipping time of 4 s. However, other authors (Liberski *et al.*, 2014 and 2009) claim that nucleation of the phases takes place in the solid–liquid border. Therefore, further research is needed to find out if zinc is completely melted in the contact surface of the specimen when nucleation of the phases takes place.

With an increase in the dipping time, the thickness of the Fe–Zn intermetallic phase increased. Until 25 s, only minor differences occurred in the thicknesses of the intermetallic layer and in the microstructure of specimens with different silicon contents, although a small Sandelin curve appeared with the dipping time of 25 s (Fig. 3.11). The thickness of the η phase was not taken into consideration because the η phase appeared when a specimen was pulled out from the zinc bath and at the beginning of the reaction the zinc was in solid state. The reactions that took place in the galvanizing process during the dipping time of < 25 s were not influenced by silicon content. This is also confirmed by other authors (Liberski *et al.*, 2014 and 2009; Lu *et al.*, 2006).

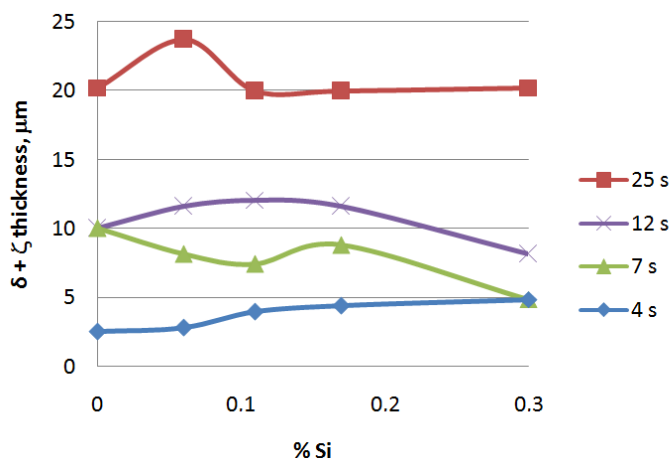


Figure 3.11 Sum of the thicknesses of the δ and ζ layers at different dipping times

During the first 25 s, the total thickness of the coating was related to the ζ phase and the δ phase was very narrow. Figure 3.12 shows the difference in the microstructure and the ζ phase thickness at the silicon content $< 0.01\%$ and 0.06% . During the first 25 s, the ζ phase dominated in the coating while the δ phase was growing very slowly. The influence of silicon was remarkable after longer dipping time (>25 s). (See *Paper V*).

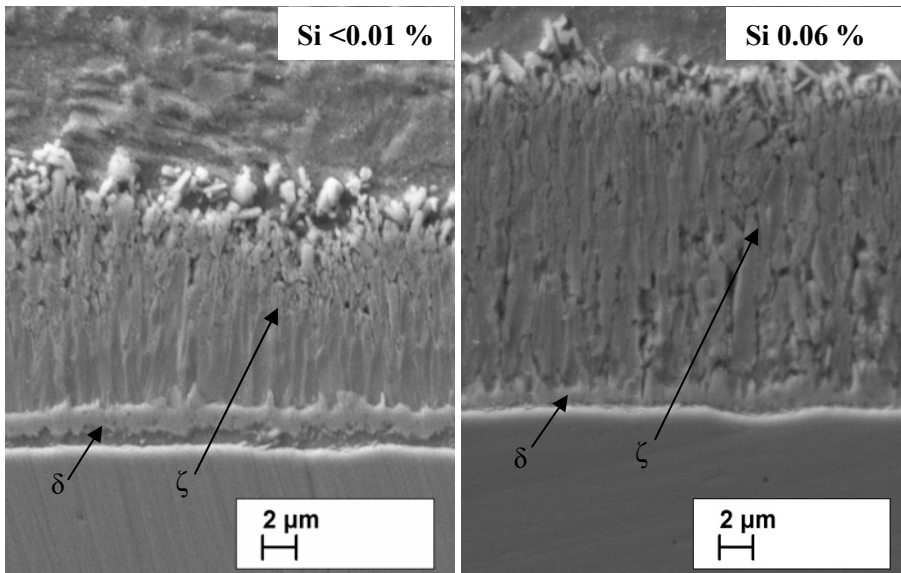


Figure 3.12 Microstructure of the zinc coating after the dipping time of 25 s

Coating growth with dipping times 195 and 1200 s

The dipping time of 195 s was chosen because it is the common galvanizing time. In addition, 1200 s was used to investigate the coating growth at a longer incubation time.

Coating growth with the dipping times 195 and 1200 s was strongly influenced by the silicon content of the steel. Figure 3.13 presents coating thicknesses with different substrate silicon content. Sandelin curve is based on the thickness results.

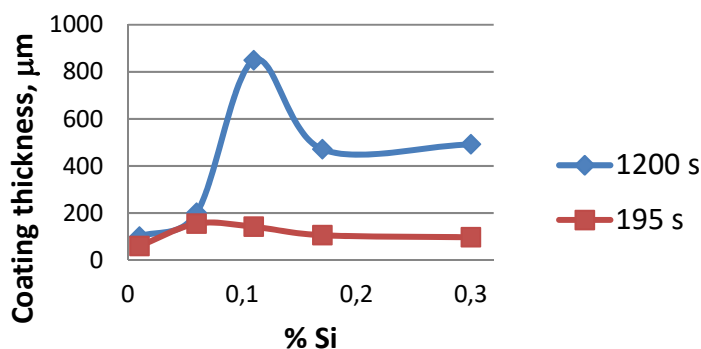


Figure 3.13 Coating thicknesses at different substrate silicon contents. Dipping time 195 and 1200 s

Table 3.6 Thicknesses of the δ and ζ layers with dipping times of 195 s and 1200 s

Si content, %	195 s		1200 s	
	Thickness of layers, μm			
	δ	ζ	δ	ζ
<0.01	3	20	44	40
0.06	3	143	33	168
0.11	3	151	1	849
0.17	10	83	26	396
0.30	30	58	41	467*

*contains also mixture of $\delta+\zeta$ phases

Each phase layer has its own growth kinetics, which depends on the silicon content and the dipping time. In *Paper V*, the coating microstructures after dipping time 195 and 1200 s are presented. Table 3.6 shows the δ and ζ layer thicknesses. The growth rate of the δ and ζ phase depends on the silicon content of the steel.

Stages of zinc coating formation

Based on the experimental results, five stages can be distinguished in zinc coating formation. A schematic model of the stages is shown in Fig. 3.14.

Stage 1 is the temperature growth of the specimen and the freezing of zinc after dipping the specimen in the molten zinc.

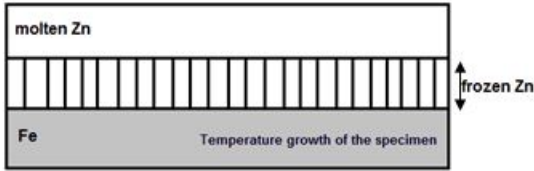
Stage 2 is the nucleation of the ζ phase, immediately followed by the δ phase. The formation of ζ and δ phases occurs most likely by solid-state diffusion during the dipping time 4 s.

Stage 3 (HDG time between 4 and 25 s) is the growth of the δ and ζ phases and the formation of the Γ phase. During this stage, the temperature of the substrate is higher than the melting temperature of zinc, and the frozen zinc is completely melted. However, the melting temperature of nucleated phases is higher. Stages 1–3 are not influenced by the silicon content of the steel.

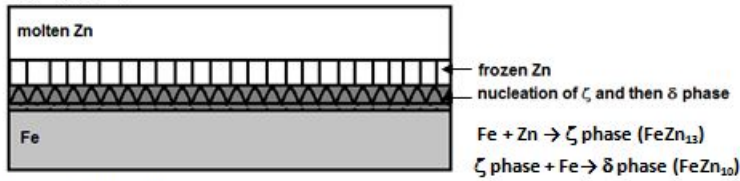
Stage 4 is influenced by the silicon content. The growth rate of the δ phase is higher than that of the ζ phase with low silicon steel (Si < 0.03%). In this stage, Sandelin steel is characterized by a high reaction rate of the ζ phase formation. The growth of the δ phase is restrained. The coating growth of Sebisty steel is related to the growth of the δ and ζ phases, although the ζ phase dominates in the coating. With the high silicon steel (Si 0.30%), a mixture of $\delta + \zeta$ phases appears in the coating.

The final stage 5 is the formation of the η layer while pulling the specimen out of the zinc bath. In the case of Sandelin steel, the Fe diffuses into the η layer during air cooling and as a result, the final layer is the ζ phase. In this experiment, the specimens were quenched in water after galvanizing to prevent further diffusion reaction.

Stage 1 (t_1)



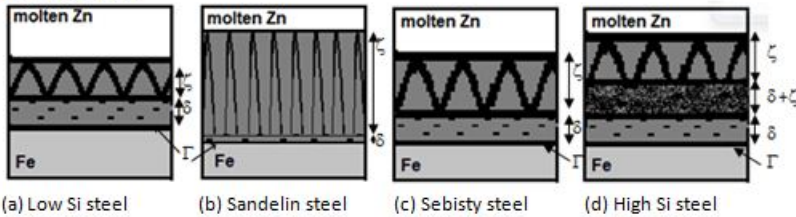
Stage 2 ($t_2 \leq 4$ s)



Stage 3 (4 s $> t_3 < 25$ s)



Stage 4 ($t_4 > 25$ s)



Stage 5 (t_5)

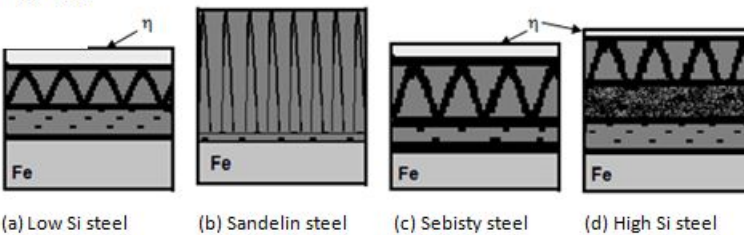


Figure 3.14 Schematic representation of the Fe–Zn layer formation

Appearance classification

Coating microstructure determines the coating appearance, which is visible with naked eyes. Arising from the absence of appearance specification of hot-dip galvanized coatings, the three appearance classification has been composed,

which is described in *Paper 1*. The classes described result from the galvanizing temperature 450 °C:

- Class 1. This class is characterized by a shiny or mirror-like coating with spangles. The spangle size might be different (regular spangle or minimized spangle), but grain should be visible to the naked eye. The steel reactivity is normal or low. The hot-dip galvanized coating consists of four separate layers: gamma (Γ) phase, delta (δ) phase, zeta (ζ) phase, and eta (η) phase. The surface roughness of the galvanized coating is low.
- Class 2. This class is characterized by a shiny coating with no spangles visible to the naked eye. The silicon or phosphorus content of the substrate steel is high and therefore the steel reactivity is high. Coating thickness increases with increasing silicon equivalent. ζ layer is not uniform and so the local outbursts might occur. This class will provide thick and rough coating.
- Class 3. This class is characterized by dull grey appearance with no spangles visible to the naked eye. Excessively thick coating may be formed due to high steel reactivity. This class will provide thick and rough coating with no external top η layer.

Low silicon steel and Sebisty steel will give Class 1 appearance. High silicon steel most probably belongs to Class 2 and Sandelin steel to Class 3.

4 CONCLUSIONS

The focus of this thesis research was on the effect of the properties of steel on the hot-dip galvanized coating and on the effect of the galvanizing process on the mechanical properties of steel. Conclusions of the thesis research with respect to the set objectives may be formulated as follows:

The effect of steel structure and composition

- 1) Ferrite grain size does not affect the thickness and morphology of zinc coatings with investigated materials and galvanizing conditions (galvanizing temperature 450 °C and 550 °C).
- 2) The total coating thickness is not influenced by ferrite grain shape with investigated materials and galvanizing conditions (galvanizing temperature 450 °C and 550 °C). However, at the galvanizing temperature 450 °C, zinc coating microstructure was different with elongated ferrite grains and with recrystallized grains with high Si substrate.
- 3) Smaller carbide grains caused thinner coating formation during HDG only at the galvanizing temperature 450 °C.
- 4) Differences in the shape of carbides have no influence on the coating formation at the galvanizing temperatures 450 °C and 550 °C.
- 5) Based on the experimental results, it is hypothesized that HDG between Fe and Zn takes place in solid state. The reactions that take place in the galvanizing process during the dipping time <25 s are not influenced by silicon concentrations. The influence of silicon is remarkable after longer dipping times (>25 s). Silicon most probably affects HDG reactions by influencing zinc diffusion into the steel and ferrum diffusion into the coating.

The effect of the galvanizing process on steel properties

- 1) Acid degreaser caused no hydrogen diffusion with the investigated materials and conditions. During pickling, hydrogen embrittlement occurred with substrate steels with Rockwell hardness ≥ 48.6 HRC (1550 MPa). During the fluxing process, hydrogen embrittlement occurred only at maximum hardness used in this study (55 HRC) and at maximum stress level.
- 2) During short time holding at the HDG temperature, aging takes place (strength properties are slightly increasing) and as a result, Lüder strain

might occur in the stress-strain curves. HDG temperature caused no ferrite grain growth or recrystallization. Hot-dip galvanized tensile test specimen's (with zinc coating) load at the tensile test is slightly higher due to the increase of the cross-section of the specimen.

- 3) During immersing the parts in the molten zinc, the quenched and tempered material hardness, which is over 40 HRC (1290 MPa), decreased (due to the tempering at the galvanizing temperature 450 °C).

Recommendations for steel selection

Customers may be given the following recommendations for steel selection in galvanizing:

- 1) Appearance, thickness and long term corrosion resistance of zinc coating is mostly influenced by the Si content of the steel. During steel selection, it is important to consider Si content to establish the desired results.
- 2) Quenched and tempered steel may suffer from hydrogen embrittlement and steel hardness may decrease as a result of zinc bath temperature. Experiments with C35 quenched and tempered steel parts suffered from hydrogen embrittlement if hardness was over 48.6 HRC (tensile strength over 1550 MPa). While considering galvanizing high strength steel, it is necessary to take into account that hydrogen embrittlement might occur with high strength steel constructions with local stresses. The higher the strength properties of the steel and the higher the applied load, the higher the risk of hydrogen damage.
- 3) Zinc bath temperature has a relatively minor effect on the mechanical properties of HSLA steel.

Future work

Results of the experiments in this thesis research enable us to establish fundamental understanding of how steel properties affect hot-dip galvanized coating and how the galvanizing process affects the properties of steel. However, various aspects need further investigation. In the future, it is planned to study LME and the effect of surface treatment (blasting effect, oxide layer effect) on the coating formation. Also, additional research should be conducted to find why carbide grain size influences the coating formation. The role of Si has been investigated; however, further studies are required to understand why the influence of Si emerges after the dipping time 25 s.

REFERENCES

A guide to good galvanizing (1972). – *Anti-Corrosion Methods and Materials*, 19 (8), 11 – 20.

[WWW] <http://www.emeraldinsight.com/doi/pdfplus/10.1108/eb006876>

Aden-Ali, S., Chamat, A., Gilgert, J., Petit, E.J., Dominiak, S., Schmitt, L., Gilles, M., Azari, Z. (2009). On the degradation the endurance of silicon-rich TRIP800 steel after hot-dip galvanization. – *Engineering Failure Analysis*, 16, 2009–2019.

Ahmadi, N.P., Rafiezadeh, E. (2009). Effect of aluminum on microstructure and thickness of galvanized layers on low carbon silicon-free steel. – *International Journal of ISSI*, 6 (1), 25–29.

Allegra, L., Hart, R.G., Townsend, H.E. (1983). Intergranular zinc embrittlement and its inhibition by phosphorus in 55 pct Al-Zn-coated sheet steel. – *Metallurgical Transactions A*, 14 (2), 401–411.

Allen, C., Mackowiak, J. (1962-63). The application of the inert-marker technique to solid/solid and solid/liquid iron/zinc couple. – *J. Inst. Met.*, 91, 369–372.

Bayraktar, E., Kaplan, D., Devillers, L., Chevalier, J.P. (2007). Grain growth mechanism during the welding of interstitial free (IF) steels. – *J. of Materials Processing Technology*, 189 (1-3), 114–125.

BNF Metals Technology Centre. (1975). *Galvanizing characteristics of structural steels and their weldments*, International Lead Zinc Research Organisation, New York.

Brahimi, S., (2014). *Fundamentals of Hydrogen Embrittlement in Steel Fasteners*. – *IBECA Technologies Corp.*

Carpio, J., Casado, J.A., Alvarez, J.A., Gutierrez-Solana, F. (2009). Environmental factors in failure during structural steel hot-dip galvanizing. – *Engineering Failure Analysis*, 16, 585–595.

Černý, L., Schindler, I., Pachlopník, R., Beran, K. (2006). Influence of hot-dip galvanizing technology on the properties of hot-dip galvanized steels. – *12th Hot Dip Galvanizing Conference*.

Chandrasekaran, D. (2003). *Grain Size and Solid Solution Strengthening in Metals*: Doctoral Dissertation, Stockholm, Royal Institute of Technology.

Chappell, E.L., Paul, C.Ely. (1930). The Pickling of Pipe Using Commercial Inhibitors. – *Industrial and Engineering Chemistry*, 22, 1201–1203.

Che, C., Lu, J., Kong, G. (2005). Interpretation of Seebast effect of hot dip galvanized steels. – *Trans. Nonferrous Met. Soc. China*, 15 (6), 1275–1279.

Che, C., Lu, J., Kong, G., Xu, Q. (2009). Role of silicon in steels on galvanized coatings. – *Acta Metall. Sin. (Engl. Lett.)*, 22 (2), 138–145.

Chen, Y., Zhu, Y., Peng, H., Ya, L., Su, X., Wang J. (2014). Influence of phosphorus on the growth of Fe–Zn intermetallic compound in Zn/Fe diffusion couples. – *Surface & Coatings Technology*, 240, 63–69.

Dimatteo, A., Lovicu, G., DeSanctis, M., Valentini R., D'Aiuto, F., Salvati. M. (2011). Influence of Galvanizing Process on Fatigue Resistance of Microalloyed Steels. – *Convegno Nazionale IGF XXI, Cassino (FR)*, 283–291.

EGGA Engineering Summary. (2009). Effect of Galvanizing on High Performance Steels and their Weldments. – Summary of the IZA ZC-21 Project.

Eliaz, N., Shachar, A., Tal, B., Eliezer, D. (2002) Characteristics of hydrogen embrittlement, stress corrosion cracking and tempered martensite embrittlement in high-strength steels. – *Engineering Failure Analysis*, 9, 167–184.

Foet, J., Reumont, G., Dupont, G., Perrot, P. (1993). How does silicon lead the kinetics of the galvanizing reaction to lose its solid-solid character? – *J. Phys. IV*, 3, 961–966.

Fratesi, R., Ruffini, N., Malavolta, M., Bellezze, T. (2002). Contemporary use of Ni and Bi in hot-dip galvanizing. – *Surface & Coatings Technology*, 157, 34–39.

Gabe, D.R. (1997). The role of hydrogen in metal electrodeposition processes. – *J. of Applied Electrochemistry*, 27, 908–915.

Galvanizing - 2014. (2016). [WWW]
<http://www.galvinfo.com/Documents/Galvanizing%202014.pdf>

Giorgi, M.L., Durighello, P., Nicolle R., Guillot, J.B. (2004). Dissolution kinetics of iron in liquid zinc. – *J. of Materials Science*, 39, 5803–5808.

Gladman, T., Holmes, B., Pickering, F.B. (1973). Some effects of steel composition on the formation and adherence of galvanized coatings. – *Iron Steel Inst*, 211 (11), 765–777.

Grabke, H.J., Riecke, E. (2000). Absorption and diffusion of hydrogen in steels. – *Mater. Tehnol*, 34, 331–342.

Guertsman, V.Y., Essadiqi, E., Dionne, S., Dremailova, O., Bouchard, R., Voyzelle, B. (2008). AISI/DOE Technology Roadmap Program. TRP 9946 – Properties of Galvanized and Galvannealed Advanced High Strength Hot Rolled Steels.

Guttman, M. (1994). Diffusive Phase Transformations in Hot Dip Galvanizing. – *Materials Science Forum*, 527–548.

Heat Treating, ASM Handbook, Volume 04, ASM International Handbook Committee, 1991, ASM International.

Hemmilä, M., Laitinen, R., Liimatainen, T., Porter, D. Mechanical and technological properties of ultra high strength Optim steels. [WWW] http://www.oxycoupage.com/FichiersPDF/Ruukki_Pdf/English/Ruukki-Technical-article-Mechanical-and-technological-properties-of-ultra-high-strength-Optim-steels.pdf (27.01.2016).

Hisamatsu, Y. (1989). Science and technology of zinc and zinc alloy coated steel sheet. – *Proc. of the International Conference on Zinc and Zinc Alloy Coated Steel Sheet* (Galvatech), Tokyo, 3–12.

Hornsby, M.J. (1995). *Hot-dip Galvanizing: A Guide to Process Selection and Galvanizing Practice*. London: Intermediate Technology Publications.

Horstmann, D. (1975). Reactions between liquid zinc and silicon-free and silicon-containing steels. – *Proc. Seminar on Galvanizing of Silicon-Containing Steels. ILZRO*, 86–96.

Hortsmann, D., Peters, F.K. (1970). The reaction between iron and zinc. – *Proc. 9th International Conference on Hot Dip Galvanizing*, Düsseldorf, 75–106.

Industrial Galvanizers Specifiers Manual. 2016. [WWW] <http://manual.ingal.com.au/18.php> (20.01.2016).

Inspection course. (2016). [WWW] <http://www.galvanizeit.org/inspection-course/galvanizing-process> (19.01.2016).

Jordan, C.E., Marded, A.R. (1997 a). Effect of substrate grain size on iron-zinc reaction kinetics during hot dip galvanizing. – *Metall. Mater. Trans. A.*, 28A, 2683–2694.

Jordan, C.E., Marder. (1997 b). Fe-Zn phase formation in interstitial-free steels hot-dip galvanized at 450°C: Part I 0.00 wt% Al-Zn baths. – *J. of Materials Science*, 32 (21), 5593–5602.

Khondker, R., Mertens, A., McDermid, J.R. (2007). Effect of annealing atmosphere on the galvanizing behaviour of a dual-phase steel. – *Materials Science and Engineering*, A 463, 157–165.

Kopyciński, D. (2010). The shaping of zinc coating on surface steels and ductile iron casting. – *Archives of Foundry Engineering*, 10, 463–468.

Kuklik, V. (2011). Hot dip zinc coatings on burnt areas. – *Proc. 17th Hot Dip Galvanizing Conference*, Ostrava, 26–38.

Langill, T.J. (2009). Mechanical Properties of Hot-Dip Galvanized Steel. – *Proc. Structures Congress 2009*, 243–248.

Lekbir, C., Dahoun, N., Guetitech, A. (2017). Effect of Immersion Time and Cooling Mode on the Electrochemical Behavior of Hot-Dip Galvanized Steel in Sulfuric Acid Medium. – *J. of Materi Eng and Perform*, 26 (6), 2502–2511.

Liberski, P., Tatarek, A., Kania, H., Podolski, P. (2009). Coating growth on silicon-containing iron alloys in hot dip galvanizing process. – *Proc. 22nd International Galvanizing Conference INTERGALVA*, Madrid, 181–187.

Liberski, P., Tatarek, A., Mendala, J. (2014). Investigation of the Initial Stage of Hot Dip Zinc Coatings on Iron Alloys with Various Silicon Contents. – *Solid State Phenomena*, 212, 121–126.

Liu, Y., Zhou, B., Lv, W., Wu, C., Su, X., Wang, J. (2016). Experimental investigation and thermodynamic assessment of the Zn–Si–P system. – *Surface & Coatings Technology*, 306, 370–377.

- Lu, J., Che, C., Kong, G., Xu, Q., Chen, J. (2006). Influence of silicon on the α -Fe/ Γ interface of hot-dip galvanized steels. – *Surface & Coatings Technology*, 200, 5277–5281.
- Luthle, A., Pohl, M. (2015). On the influence of cold deformation on liquid metal embrittlement of a steel in a liquid zinc bath. – *Materials and Corrosion*, 66 (12), 1491–1497.
- Mabhoa, N., Bergersb, K., Flockb, J., Telghedera, U. (2010). Determination of diffusible and total hydrogen concentration in coated and uncoated steel using melt and solid extraction techniques: Part I. – *Talanta*, 82, 1298–1305.
- Mackowiak, J., Short, N.R. (1979). Metallurgy of galvanized coatings. – *Inter. Met. Rev.*, 1, 1–19.
- Mandal, K.K., Mandal, D., Das, S.K., Balasubramaniam, R., Mehrotra, S.P. (2009). Microstructural study of galvanized coatings formed in pure as well as commercial grade zinc baths. – *Transactions of the Indian Institute of Metals*, 62 (1), 35–40.
- Mao, X., Huo, X., Sun, X., Chai, Y. (2010). Strengthening mechanisms of a new 700 MPa hot rolled Ti-microalloyed steel produced by compact strip production. – *J. of Materials Processing Technology*, 210 (12), 1660–1666.
- Marder, A.R. (2000). The metallurgy of zinc-coated steel. – *Progress in Materials Science*, 45, 191–271.
- Meier, M.L., Broumas, A. Lüders band formation in steel –video. [WWW] <http://www.kstreetstudio.com/science/natedwkshp/files/Meier-NEW-2001-2.pdf> (12.12.2015).
- Mraz, L., Lesay, J. (2009). Problems with reliability and safety of hot dip galvanized steel structures. – *Soldagem Insp. São Paulo*, 14 (2), 184–190.
- Nicholas, M.G., Old, C.F. (1979). Liquid metal embrittlement. – *J. of Materials Science*, 14 (1), 1–18.
- Notowidjojo, B.D. (1990). *A Study of Zinc-nickel Galvanized Coating of Silicon Steels*: PhD Thesis, University of Wollongong, Australia

- Okafor, I.C., O'Malley, R.J., Prayakarao, K.R., Aglan, H.A. (2013). Effect of zinc galvanization on the microstructure and fracture behavior of low and medium carbon structural steels. – *Engineering*, 5, 656–666.
- Oktay, E., Cevat, S.K. (2016). Influence of Mechanical Surface Treatments on Sandelin Phenomenon in Silicon Containing Steels. – *Hittite J. of Science and Engineering*, 3 (2), 81-85.
- Paramonov, A.V., Adamov, A.S., Chernetsov, V. Yu. (2011). Production problems of hot dip galvanized metal structures. – *Metallurgist*, 54 (11–12), 793–796.
- Pelerin, J., Hoffman, J., Leroy, V. (1981). Influence of silicon and phosphorus on the commercial galvanization of mild steels. – *Metall*, 35, (9), 870–873.
- Peng, F., Yin, F., Su, X., Zhi, L., Zhao, M. (2005). 560 °C isothermal section of Zn–Fe–Ni system at the Zn-rich corner. – *J. Alloys and Compd.*, 402, 124–129.
- Petit, E.J., Grosbety, Y., Aden-Ali, S., Schmitt, L., Gilgert, J., Azari, Z. (2012). Fatigue toughness of galvanized high strength steels for structural applications for automotive industry. – *Proc. 20nd International Galvanizing Conference INTERGALVA*, Paris.
- Pokorny, P., Kolisko, J., Balik, L., Novak, P. (2016 a). Effect of chemical composition of steel on the structure of hot-dip galvanized coating. – *Metallurgija*, 55 (1), 115–118.
- Pokorny, P., Kolisko, J., Balik, L., Novak, P. (2016 b). Reaction kinetics of the formation of intermetallic Fe-Zn during hot-dip galvanizing of steel. – *METABK*, 55(1), 111–114.
- Porter, F. (1991). *Zinc Handbook: Properties, Processing, and Use in Design*. New York: CRC Press.
- Pressouyre, G.M. (1983). Hydrogen traps, repellers, and obstacles in steel; Consequences on hydrogen diffusion, solubility, and embrittlement. – *Metallurgical and Materials Transactions A*, 14, 2189–2193.
- Proskurin, E.V., Popovich, V.A., Morozov, A.T. (1988). *Galvanizing: Handbook*. Metallurgiya, Moscow, [in Russian].

Rädecker, W. (1973). Der interkristalline Angriff von Metallschmelzen auf Stahl. – *Materials and Corrosion*, 24, 851–859.

Rashid, M.S. (1976). Strain aging kinetics of Vanadium or Titanium strengthened high strength low-alloy steels. – *Metallurgical Transactions A*, 7A, 497–503.

Ritakallio, P.O. (2012). Cold-formed high-strength tubes for structural applications. – *Steel Construction Design and Research*, 3(5), 158–167.

Rostoker, W., McCaughey, J.M., Markus, H. (1960). *Embrittlement by Liquid Metals*. – Reinhold Publishing Corporation, New York.

Rowland, D.H. (1947). *Transactions*, American Society for Metals, 40, 982.

Sandelin, R.W. (1940 a). Galvanizing characteristics of different types of steel. – *Wire Prod*, 15(11), 655–676.

Sandelin, R.W. (1940 b). Galvanizing characteristics of different types of steel. – *Wire Prod*, 15(12), 721–749.

Schulz, W.D., Schubert, P., Thiele, M. (2003). An alternative approach to explaining the effect of silicon on the galvanizing reaction. – *Proc. 20th International Galvanizing Conference INTERGALVA*, Amsterdam, 61–64.

Sebisty, J.J., Palmer, R.H. (1967). Hot-dip Galvanizing with Less Common Bath Additions. – *Proc. 7th Int. Conf. on Hot Dip Galvanizing*, London, 209, 235 – 265.

Sepper, S., Peetsalu, P., Mikli, V., Saarna, M. (2012). The effect of substrate microstructure on formation of hot dip galvanized coatings – *Proc. 23rd International Galvanizing Conference INTERGALVA*, Paris.

Shirband, Z., Shishesaz, M.R., Ashrafi, A. (2011). Hydrogen degradation of steels and its related parameters, a review. – *Phase Transit.*, 84, 924–943.

Standard Specification for Zinc Coating, Hot-Dip, Requirements for Application to Carbon and Alloy Steel Bolts, Screws, Washers, Nuts, and Special Threaded Fasteners. (2011) ASTM F2329.

Steels suitable for galvanizing. (2016). [WWW]
<http://www.nordicgalvanizers.com/narvar/Steelssuitableforgalvanizing.htm>
(23.01.2016).

Surface engineering, ASM Handbook. Volume 05, ASM International Handbook Committee, 1994, ASM International.

Tang, N.Y. (2008). Control of Silicon Reactivity in General Galvanizing. – *J. of Phase Equilibria and Diffusion*, 29 (4), 337–344.

Thiele, M., Schulz, W.D. (2006). Coating formation during hot dip galvanizing between 435 °C and 620 °C in conventional zinc melts – a general description. – *Proc. 21st International Galvanizing Conference INTERGALVA*, Naples, 1–10.

Timmins, P.F. (1996). Predictive Corrosion Failure and Control in Process Operations. – *ASM International*, Materials Park.

Uchiyama, Y., Koga, H., Inokuchi, H. (1983). Reaction between Fe-Si alloys and liquid zinc. – *Transactions of the Japan Institute of Metals*, 24 (5), 272–280.

Wegrzynkiewicz, S., Jedrzejczyk, D., Szlapa, I., Hajduga, M. (2014 a). The influence of additional processing after Oxy-acetylene cutting on the structure and corrosion resistance of the zinc coating. – *Proc. Metal*.

Wegrzynkiewicz, S., Jedrzejczyk, D., Szlapa, I., Hajduga, M., Boczek, S. (2014 b). Influence of a substrate surface on the (Zn)-coating formation. – *Archives of Metallurgy and Materials*, 59 (4), 1373–1378.

Xu, J., Bright, M.A., Liu, X., Barbero, E. (2007). Liquid metal corrosion of 316L stainless steel, 410 stainless steel, and 1015 carbon steel in a molten zinc bath. – *Metallurgical and Materials Transactions A*, 38 (11), 2727–2736.

Zeinab, A. H., Sayed, A. E. R., Moustafa, I. (2017). Effectiveness of Si contents in the steel composition on the corrosion performance of galvanized steel. – *Anti-Corrosion Methods and Materials*, 64 (5), 479-485.

Zinc coatings -- Guidelines and recommendations for the protection against corrosion of iron and steel in structures -- Part 2: Hot dip galvanizing: ISO 14713-2:2009, Switzerland.

ACKNOWLEDGEMENTS

I am grateful for the unique opportunity provided to carry out my research with industrial applications supported by The DoRa programme activity 3, “Research cooperation between universities and businesses”.

I would like to thank my supervisors Priidu Peetsalu and Priit Kulu from Tallinn University of Technology and Jussi Ustal from AS Paldiski Tsingipada. I am thankful to all my colleagues from the AS Paldiski Tsingipada for their willingness to help me during my experimentation.

Special thanks go to PhD Valdek Mikli for helping me with the SEM studies and to PhD Mart Saarna for helping me with tensile testing.

Finally, I would like to thank my family and friends for their continuous support and encouragement throughout my doctoral studies and thesis writing.

ABSTRACT

Steel Selection Considerations for Hot-Dip Galvanizing

This thesis research was based on cooperation of three parties – the author, Tallinn University of Technology and AS Paldiski Tsingipada (Zincpot). The author is employed as a technologist at the company.

Hot-dip galvanizing is used to protect substrate metal surfaces from corrosion. The three main steps in the hot-dip galvanizing process are surface preparation, galvanizing, and post-treatment. One key factor in providing high quality zinc coating is proper steel selection. The chemistry of the steel (especially silicon and phosphorus content) influences the appearance, thickness, smoothness and adhesion of the coating. Besides the chemical composition of the steel, the microstructure and the mechanical properties of the steel are important properties of structural steel. New steel grades are a challenge to the galvanizers to produce quality coating. Galvanizers and the customers must be aware of how steel selection might affect the final result: how the chemical composition and the microstructure of the steel affect the coating formation and how zinc bath temperature might affect the mechanical properties of the steel.

Advanced knowledge of how the properties of high strength steel can affect the quality of hot-dip galvanized coatings is essential to establish the quality that satisfies the costumers' demands in relation to the following:

- 1) zinc coating appearance and corrosion resistance (coating thickness)
- 2) reliability (mechanical properties of steel) of hot-dip galvanized steel structures.

From the main objectives of the study, the following findings resulted:

1. Influence of the substrate microstructure (ferrite grain size, ferrite grain shape, carbide grain size, carbide grain shape) on the hot-dip galvanizing

It was found that ferrite grain size does not affect the thickness and morphology of zinc coatings at 450 °C and 550 °C. Ferrite grain shape influenced the zinc

coating microstructure (but not the coating thickness). Smaller carbide grains caused thinner coating formation during HDG only at the galvanizing temperature 450 °C. Differences in the shape of carbides do not influence the coating formation at the galvanizing temperature 450 °C and 550 °C.

2. Possibility of hydrogen embrittlement of high strength steel during the pre-treatment process

It was found that acid degreaser causes no hydrogen diffusion. During pickling, hydrogen embrittlement occurs with substrate steels with Rockwell hardness ≥ 48.6 HRC (1550 MPa) and during the fluxing process, with steels with Rockwell hardness ≥ 55 HRC.

3. Effect of zinc bath temperature on the mechanical properties of galvanized steel

It was found that during holding for a short time (5 min) at the HDG temperature, aging takes place (strength properties are slightly increasing). Quenched and tempered steel hardness, which is over 40 HRC, decreases during HDG (due to the tempering at the galvanizing temperature 450 °C).

4. The effect of the chemical composition of steel (silicon content) on the zinc coating formation lays the basis of the appearance and corrosion resistance of the coating.

The reactions that take place in the galvanizing process during the dipping time < 25 s are not influenced by silicon concentrations. The influence of silicon is remarkable after longer dipping times (> 25 s). Based on the experimental results, it is hypothesized that HDG between Fe and Zn takes place in solid state.

KOKKUVÕTE

Terase valiku mõjurid kuumtsinkimiseks

Käesoleva doktoritöö osapoolteks on Tallinna Tehnikaülikool ja AS Paldiski Tsingipada. Uurimustöö raames töötasin AS Paldiski Tsingipajas tehnoloogina.

Kuumtsinkimise eesmärgiks on kaitsta terast korrosiooni eest. Tsinkimisprotsess koosneb detailide keemilisest puhastamisest (õli ja rooste eemaldamine, räbuse kastmine), eelkuumutamist ning kastmisest vedelasse tsinki. Kvaliteetse tsinkpinde saavutamiseks on vajalik teadlik terase valik. Nimelt terase keemiline koostis (eriti räni ja fosfori sisaldus) mõjutab tsinkpinde paksust, välisilmet ning nakkuvust. Lisaks on olulised omadused terase mehhaanilised omadused ja mikrostruktuur. Kõrgtugevate teraste kasutuselevõtt on väljakutseks kuumtsinkijatele, sest tuleb olla teadlik, kuidas uute kõrgtugevate terasmärkide tsinkimine mõjutab terase mehhaanilisi omadusi ning kuidas terase keemiline koostis ja mikrostruktuur mõjutab pinde moodustumise protsessi.

Paremad teadmised, kuidas kõrgtugevate teraste omadused mõjutavad tsinkimise kvaliteeti on olulised, et rahuldada klientide nõudmisi tulenevalt:

- 1) tsinkpinde välisilmest ja korrosioonikaitsest (pinde paksus)
- 2) terase mehhaanilistest omadustest pärast kuumtsinkimist ja neist valmistatud konstruktsioonide ohutusest

Doktoritöö käigus uuriti ja selgitati välja:

- 1) Terasse mikrostruktuuri mõju (ferriidi tera suuruse ja kuju, karbiidi tera suuruse ja kuju) pinde tekkele

Leiti, et ferriidi tera suurus ei mõjuta tsinkpinde paksust ja struktuuri temperatuuridel 450 ja 550 °C. Ferriidi tera kuju mõjutas tsinkpinde struktuuri (kuid mitte pinde paksust) tsinkimise temperatuuril 450 °C. Väiksema karbiidi tera korral oli tsinkpinde paksus väiksem tsinkimise temperatuuril 450 °C. Tsinkimise temperatuuril 550 °C karbiidi tera suurus tsinkpinde paksust ei mõjutanud. Karbiidi tera kuju tsinkpinde moodustumist ei mõjutanud nii temperatuuril 450 kui ka 550 °C.

- 2) Vesinikhapruse tekkimise võimalikkusest kõrgtugevatel terastel eelpuhastus kemikaalides

Leiti, et happeline rasvaeemaldus vesinikhaprust ei põhjusta. Vesinikhaprus tekib soolhappes töötlemisel teraste korral, mille kõvadus on >48.6 HRC (1550 MPa) ja räbus teraste korral, mille kõvadus on 55 HRC ja enam.

3) Tsingivanni temperatuuri mõju terase mehhaanilistele omadusele

Leiti, et 5-minutiline sukeldamine tsingivanni põhjustab vananemisprotsessi, mille tagajärjel tugevusnäitajad veidi tõusevad. Tsinkpinne suurendab terase tõmbetugevust. Karastatud ja noolutatud teraste korral kõvadus kuumtsinkimise käigus väheneb, kui algne kõvadus on >40 HRC.

4) Räni mõju tsinkpinde tekkimisele, pinde välisilmele ja korrosioonikindlusele

Leiti, et räni ei mõjuta paksu pinde teket, kui sukeldamisaeg tsinki oli < 25 s. Pikema tsinkimisprotsessi kestusel oli räni mõju pinde paksusele ja struktuurile märkimisväärne. Selgitati välja, et kuumtsinkimise reaktsioon raua ja tsingi vahel toimub juba tardolekus.

Doktoritöö uudsus seisneb eelkõige eksperimentides, milles uuriti:

- a) Kuidas ferriiditera ja karbiiditera suurus mõjutab tsinkpinde teket uute terasmarkide seisukohalt vaadates.
- b) Tsingivanni temperatuuri mõju hindamisel terase mehhaanilistele omadustele tehti katsetusi lisaks sulatsingis ka sulasoola sukeldamisel, elimineerides tsingi ja terase omavahelise keemilise reaktsiooni mõju ning tsinkpinde mõju.
- c) Selgitati välja, et erinevalt senistest arusaamadest, tsinkpinne moodustub mitte vedelas vaid tardolekus.

APPENDICES

Curriculum vitae

1. Personal data

Name: Sirli Sepper
Date and place of birth: 09.01.1986, Tallinn
Citizenship: Estonian
E-mail address: sirli.sepper@gmail.com

2. Education

2010 – 2017 Tallinn University of Technology, Materials Engineering, Doctoral study
2008 – 2010 Tallinn University of Technology, Master of Science in Engineering
2005 – 2008 Tallinn University of Technology, Bachelor of Science in Engineering
1993 – 2005 Saku Gymnasium, High school education

3. Language competence/skills

Estonian	mother tongue
English	fluent
Russian, German	basic skills

4. Research activity

2016 – 2017 The physical characteristics of aging overhead line conductors - Phase II
2009 – 2012 Investigation of fatigue mechanics of engineering materials and hard PVD coatings, project no. ETF7889
2008 – 2013 Hard coatings and surface engineering, project no. SF0140091s08
2006 – 2009 A study on the applicability of modified Fenton oxidation in combined schemes for elimination of organics in wastewater treatment, project no. ETF6564

5. Professional employment

2010 – ... Zincpot, technologist

6. Academic degrees

M. Sc. Thesis: A study on the textile industry wastewater pre-treatment processes. Tallinn University of Technology, 2010. Supervisors: Marina Trapido and Niina Dulova

7. Research activity

4. Natural Sciences and Engineering; 4.12. Process Technology and Materials Science; CERCS SPECIALTY: T155 Coatings and surface treatment

Elulookirjeldus

1. Isikuandmed

Ees- ja perekonnanimi: Sirli Sepper

Sünniaeg ja -koht: 09.01.1986, Tallinn

Kodakondsus: eesti

E-posti aadress: sirli.sepper@gmail.com

2. Hariduskäik

2010 – 2017 Tallinna Tehnikaülikool, Mehaanikateaduskond, Mehhanotehnika, PhD

2008 – 2010 Tallinna Tehnikaülikool, Keemia- ja materjalitehnoloogia teaduskond, Keemia- ja keskkonnakaitse tehnoloogia, magister

2005 – 2008 Tallinna Tehnikaülikool, Keemia- ja materjalitehnoloogia teaduskond, Keemia- ja keskkonnakaitse tehnoloogia, bakalaureus

1993 – 2005 Saku Gümnaasium, keskkool

3. Keelteoskus

eesti emakeel

inglise kõrgtase

vene, saksa algtase

4. Teadusprojektid

2016 – 2017 Vananevate juhtmete füüsikalised omadused – II etapp

2009 – 2012 Tehnomaterjalide ja aurustussadestatud kõvapinnete väsimusmehaanika uurimine, projekt ETF7889

2008 – 2013 Kõvapinded ja pinnatehnika, projekt SF0140091s08

2006 – 2009 Modifitseeritud Fenton-protsessi kasutamise uurimine orgaaniliste saasteainete kõrvaldamiseks kombineeritud heitvee töötlusskeemides, projekt ETF6564

5. Teenistuskäik

2010 – ... Paldiski Tsingipada, tehnoloog

6. Kaitstud lõputööd

Tehnikateaduste magistrikraad: Tekstiilitööstuse reovee eelpuhastusprotsesside uurimine. Tallinna Tehnikaülikool, 2010. Juhendajad: Marina Trapido; Niina Dulova

7. Teadustegevus

4. Loodusteadused ja tehnika; 4.12. Protsessitehnoloogia ja materjaliteadus; CERCS ERIALA: T155 Pinded ja pinnatehnoloogia

PUBLICATIONS

Paper I

Sepper, S., Peetsalu, P., Saarna, M. Methods to evaluate the appearance of hot dip galvanized coatings. *Agronomy Research*, 9(S1), 2011, 229 - 236.

Methods for evaluating the appearance of hot dip galvanized coatings

S. Sepper¹, P. Peetsalu^{1,2} and M. Saarna¹

¹Department of Materials Engineering, Tallinn University of Technology

²Tartu College, Tallinn University of Technology; e-mail: sirli.sepper@emu.ee

Abstract. Although the science and technology of hot dip galvanizing have improved significantly over the years, it is still a challenge to produce high-quality coatings for decorative and constructional applications. Different applications require specific appearance of galvanized coatings (e.g. dull appearance in roof construction). The appearance of the coatings depends on processing properties, steel content, and substrate surface conditions. The purpose of this study is to work out a technique how to evaluate the appearance of hot dip galvanized coatings. Under observation are substrate steel parameters (chemical composition, surface conditions e.g. roughness), which affect the appearance of hot dip galvanized coatings. Based on this research appearance classifications have been established.

Key words: Hot dip galvanizing, iron–zinc phases, coating appearance, spangle size.

INTRODUCTION

Hot dip galvanizing is used as a very effective steel corrosion protection method, providing a long service-life. The corrosion protection is dependent on the coating thickness and environmental conditions (ASM Handbook, 1994). Zinc coated components are also used to give a good appearance to the constructions. In recent years the interest in hot dip galvanizing for decorative and constructional applications has increased. The difference in the field of use determines the requirements to the coating appearance. Duller coating finish is desired in buildings, because shiny coatings with high reflectivity may cause problems with passing traffic. At the same time most customers prize the bright spangled look for decorative applications. As a result of customer demands the requirements to the coatings and especially to the appearance have increased. Coating appearance is affected by processing properties, steel chemistry, and substrate surface condition.

Coating appearance and zinc consumption mainly depend on the zinc–steel reactivity and on the drainage of zinc from workpieces during their withdrawal (Fratesi et al., 2002). The zinc–steel reactivity is mostly influenced by the silicon and phosphorus content in the steel, but also carbon in excess of about 0.2% and manganese in excess of about 1.3% increase Zn-Fe layer formation (Hornsby, 1995). The zinc drainage is influenced by bath fluidity. The addition of low amounts of certain elements, such as Al, Pb, Ge, V, Ti, Ni, Bi, Cu, Cd, Sn inhibit zinc-steel reactivity and/or increase the bath fluidity (Jalel Ben nasr et al., 2008; Xuping et al., 2010; Pistofidis et al, 2007).

The surface of the galvanized coatings is commonly characterized by spangles (snowflake-like pattern). Zinc coatings with spangles are decorative coatings, and its appearance is closely related to the orientation of zinc crystals and the distribution of alloy elements in the coating. Spangle formation is favoured when Sb, Bi, and especially Pb are added to the zinc bath because all these metals lower the surface tension ahead of the growing dendrites, resulting in larger grains. Grain size is also influenced by the cooling rate and the smoothness of the substrate (Marder, 2000; Pavlidou et al., 2005; Lu Jin-tang et al., 2007; ShuPeng et al., 2010).

The roughness of the steel surface influences the thickness and structure of the coatings. A rough steel surface as obtained by grit blasting and coarse grinding have a higher surface area and thus generate thicker galvanized coatings. The effect of surface unevenness of the substrate metal generally remains visible after galvanizing. Galvanized coatings are not effective at hiding defects of the steel and indicate steel surface quality problems (defects associated with casting, rolling, and manufacturing processes) (ISO/FDIS 14713-2:2009).

Unfortunately there are no quantitative specifications how to evaluate the appearance of galvanized sheet. International standard ISO 14713-2:2009 divides coating characteristics into two groups relating to steel chemical composition:

1) Coating has a shiny appearance with a finer texture. Coating structure includes outer zinc layer.

2) Coating has a darker appearance with a coarser texture. Iron/Zinc alloys dominate coating structure and often extend to the coating surface, with reduced resistance to handling damage.

The main objective of this study is to work out a technique how to evaluate the appearance of hot dip galvanized coating. Under observation are steel chemical composition and substrate surface condition, not defects arising from the hot dip galvanizing process. The appearance evaluation applies only for fresh zinc coatings, without protective layer zinc corrosion usually causes the appearance of the coated steel to turn a dull grey.

EXPERIMENTAL

Five materials were used in the experiment (with different silicon equivalent). The chemical compositions of the steels are shown in Table 1.

Table 1. Chemical composition of the substrate steels, wt %.

Steel	C	Si	P	S	Mn	Al	Cr	Mo	Silicon equivalent
a	0.09	<0.01	0.012	0.006	0.33	0.034	0.02	0.03	<0.04
b	<0.01	<0.01	0.051	0.008	0.21	0.037	0.03	0.03	<0.14
c	0.35	0.23	0.009	0.001	0.64	0.030	0.18	0.03	0.25
d	0.79	0.27	0.014	0.005	0.68	0.026	0.09	0.05	0.31
e	0.58	0.05	0.007	<0.001	0.69	0.012	0.24	0.05	0.07

The steel sheets were degreased for 15min in acid degreasing agent and then pickled for 45min with a 13% HCl containing inhibitor for the protection of metal surfaces. Next the sheets were rinsed in water and then dipped in a flux bath consisting of 242g l⁻¹ ZnCl₂ and 186g l⁻¹ NH₄Cl which was kept at 40°C.

The fluxed sheets were dried for 15 min at 120°C in drying oven. Then the sheets were dipped in the zinc bath for 6 min at the temperature 460°C. The zinc bath consists of zinc (99.3 wt. % Zn) containing also Al, Bi, Fe, Ni, Sn, Pb.

For the examination of the microstructure, hot dip galvanized specimens were cross sectioned, hot mounted and polished. A nital etchant (nitric acid: 3 wt. %) was used to reveal the microstructures of the specimens and observations were made with optical microscopy.

The thickness of coatings was determined by electromagnetic thickness gauge (Dualscope MP0). The surface roughness of galvanized steels was measured with surface texture measuring system “Perthometer Concept” produced by company MAHR.

RESULTS AND DISCUSSION

Steel chemical composition

The selection of the materials used in this experiment was based on differences in chemical composition of the steels to evaluate the influence of substrate chemical composition to the appearance of hot dip galvanized coatings.

The characteristic photographs of the above mentioned galvanized steels ‘*a-d*’ are presented in Fig. 1. Steel ‘*a*’ (silicon equivalent <0.04) and ‘*c*’ (silicon equivalent 0.25) have shiny spangled appearance. Steel ‘*b*’ has dull appearance as a result of the phosphorus present (0.05wt. %) in the substrate steel. Steel ‘*d*’ has shiny appearance with no visible spangle. This difference in appearance is a result of the rapid zinc-iron intermetallic growth that consumes all of the bright, pure zinc. The surface roughness of galvanized steels is presented in Table 2. Coatings with spangles have lower surface roughness.

Table 2. Surface roughness of galvanized steels.

Steel	R _a , μm	R _z , μm
a	1.4	8.8
b	8.1	55.5
c	3.0	17.8
d	9.5	46.3

The optical micrographs (magnification 200x) of the cross-sections of the coatings are shown in Fig. 2. Microscopic level differences occur due to the amount of silicon and phosphorus in the steel being hot dip galvanized. Steel ‘*a*’ has a typical microstructure of the hot dip coating, which is typical for steels with low silicon equivalent. Four layers could be distinguished based on their relief: gamma (Γ) phase, delta (δ) phase, zeta (ζ) phase and eta (η) phase.

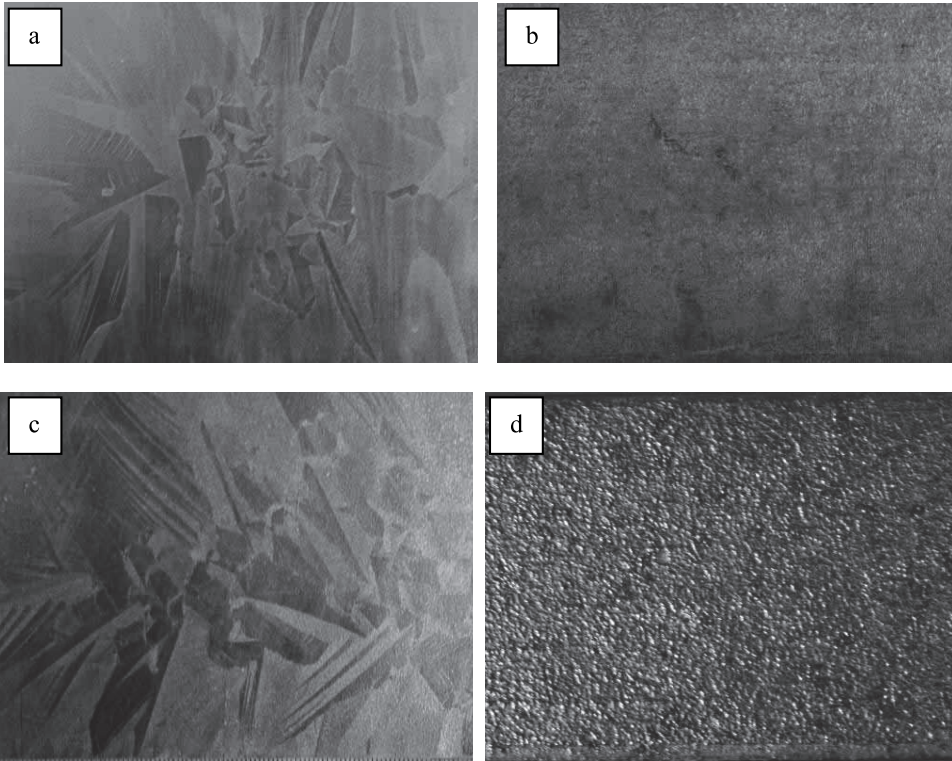


Figure 1. Visual appearance of hot dip galvanized steel sheets a–d. Sheet ‘a’ and ‘c’ with shiny spangled appearance. Sheet ‘b’ with dull appearance and ‘d’ with shiny appearance with no visible spangle.

From the coating microstructure of steel ‘b’ and ‘d’ we can see the excessive growth of the ζ phase, however, ζ layer is not uniform and so the local bursts of the ζ phase layer have occurred. As a result of this the surface roughness is high. Steel ‘c’ has also increased ζ layer and compose most of the galvanized coating thickness.

Fig. 2 can be used to describe the coating thickness differences due to substrate chemical composition. The amount of silicon and phosphorus (silicon equivalent) in the substrate steel strongly influences the thickness and appearance of the galvanized coating.

Steel chemical composition has a major effect on the appearance of hot dip galvanized coatings. Silicon and phosphorus content influence the reaction rate between zinc and iron and thus control the alloy layer growth and formation during hot dip galvanizing. The visual appearance of the coating depends on Fe/Zn alloys. Local outbursts of the ζ phase influence the coating surface roughness and coating appearance.

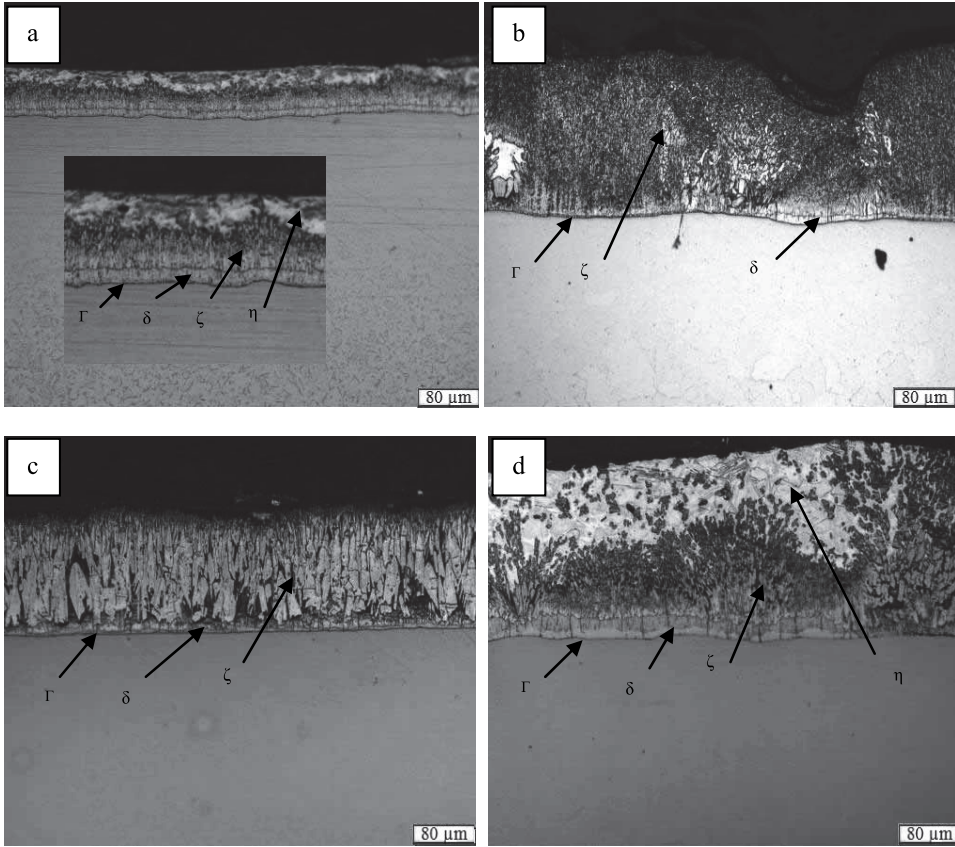


Figure 2. The micrographs of the cross-sections of the coatings with following silicon equivalents: sheet 'a' 0.04, 'b' 0.14, 'c' 0.25 and 'd' 0.31.

Effect of article surface condition

The substrate steel roughness and surface defects also affect the appearance of the coating. The roughness of the steel surface has an influence on the thickness, structure, and appearance of the coating. Fig. 3 shows visual appearance differences of steel 'e' due to substrate surface roughness. The steel was ground with 80 grit (Fig. 3.1) and 240 grit sand paper (Fig. 3.2). Ground steel with 80 grit sand paper had zinc coating with peaks and valleys while 240 grit gave smooth, shiny and spangled appearance.

The micrographs of steel with different surface roughness after galvanizing are presented in Fig. 4. The steel 'e' is reactive steel and zeta layer is overgrown and compose most of the galvanized coating thickness (Fig. 3.2). Roughening the reactive steel creates peaks and valleys which interfere with the growth of the zeta intermetallic layer (Fig. 3.1).

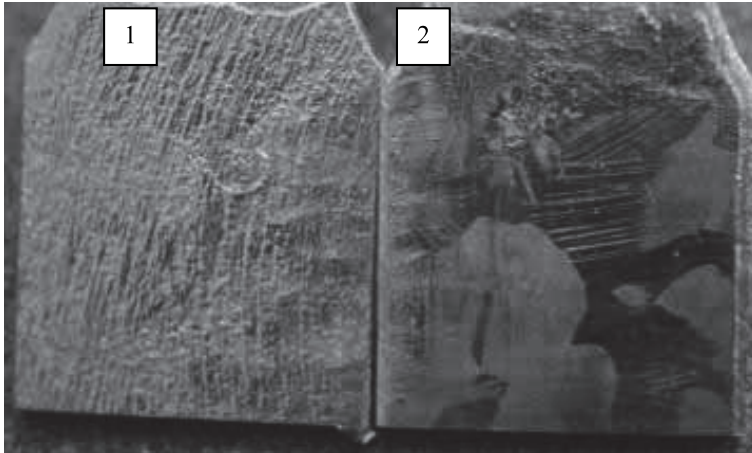


Figure 3. Differences in visual appearance due to surface roughness:
 (1) – 80 grit, (2) – 240 grit.

A rough steel surface gave a thicker coating. The average coating thickness of roughened steel (80 grit) was 105 μm and 240 grit gave coating thickness 165 μm .

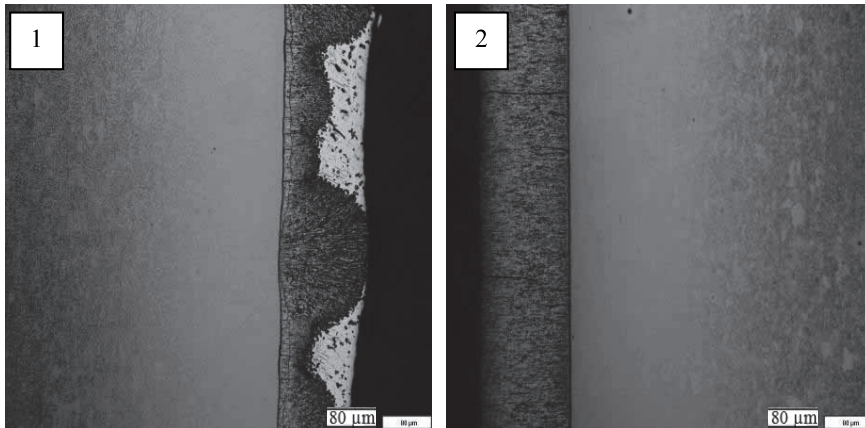


Figure 4. Substrate surface roughness effect on the galvanized coating:
 (1) – 80 grit, (2) – 240 grit.

The surface unevenness and defects of the substrate metal generally remain visible after hot dip galvanizing. Steel 'c' had a surface defect presented in Fig. 5.1. The reason of the defect was probably contact with a chemical, which caused intergranular corrosion of the steel surface (defect depth 6 μm).

Zinc coating has two different microstructures (Fig. 5.2) which were divided by 'wavy line'. Differences were also in coating thicknesses: 98 μm and 133 μm . Surface with intergranular corrosion had thinner zinc coating.

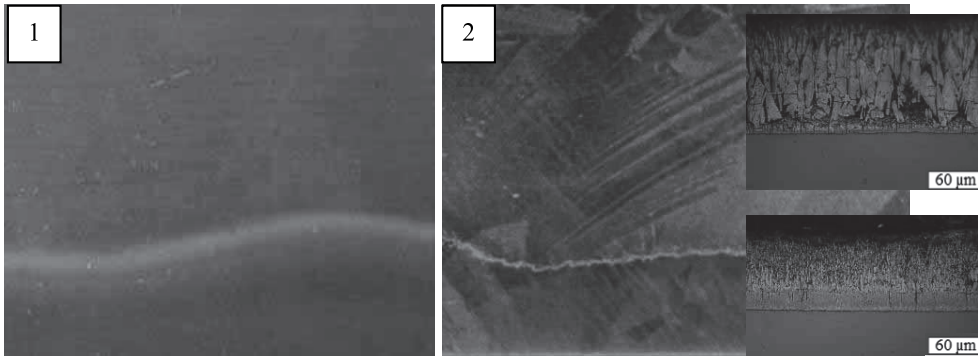


Figure 5. Surface defect before (1) and after (2) hot dip galvanizing.

The chemical composition of steel combined with its surface condition will affect the appearance and the thickness of the galvanized coating. The surface roughening is used to obtain thicker coating but in case of reactive steel the result might be reverse. Rough substrate surface can also affect the spangle formation and coating surface roughness. Surface defects associated with casting, rolling, and manufacturing processes generally remain visible after galvanizing.

Appearance classification

Arising from absence of appearance specification of hot dip galvanized coatings, the three appearance classifications could be composed based on this research.

Class 1. This class is characterized by shiny or mirror-like coating with spangles. The spangle size might be different (regular spangle or minimized spangle), but grain should be visible to the naked eye. Steel reactivity is normal or low. The hot dip galvanized coating consists of four separate layers: gamma (Γ) phase, delta (δ) phase, zeta (ζ) phase, and eta (η) phase. In some cases the pure zinc layer (η) might be absent. The surface roughness of galvanized coating is low.

Class 2. This class is characterized by shiny coating with no spangles visible to the naked eye. The silicon or phosphorus content of the substrate steel is high and therefore the steel reactivity is high. Coating thickness increases with increasing silicon equivalent. ζ layer is not uniform and so local outbursts might occur. This class will provide thick and rough coating.

Class 3. This class is characterized by dull grey appearance with no spangles visible to the naked eye. Excessively thick coating may be formed due to high steel reactivity. This class will provide thick and rough coating with no external top η layer.

Established appearance classification describes only common coating appearances. There might be occasions when classification is not so easy (e.g. half of the coating is dull and the other part is shiny). In that case it is possible to divide steel coatings into classifications by percentage (70% class 1 and 30% class 2).

Galvanized steels, which were used in this study, may be divided as follows (Figs. 1 and 3):

- 1) Class 1 – steel ‘a’, ‘c’ and ‘e’ ground with 240 grit sand paper;
- 2) Class 2 – steel ‘d’ and ‘e’ ground with 80 grit sand paper;
- 3) Class 3 – steel ‘b’.

CONCLUSIONS

In the present paper, the influencing factors which affect the hot dip galvanized coatings have been studied. Three appearance classifications have been composed based on visual appearance (spangle size), coating roughness and Fe/Zn alloy layer growth and formation. The following conclusions can be drawn from the present study:

1. Hot dip galvanized coating appearance may be divided into 3 classes.
2. The substrate steel chemical composition has major effect on coating appearance.
3. The substrate roughness and surface defects also have an impact on coating appearance.

ACKNOWLEDGEMENTS: This research was supported by European Social Fund's Doctoral Studies, Internationalisation Programme DoRa, and Estonian Science Foundation targeted financing project SF0140091s08. Cooperation was carried out with AS Paldiski Tsingipada.

REFERENCES

- ASM Handbook. Surface engineering, vol 5, ASM International, 1994.
- Fratesi, R., Ruffini, N., Malavolta, M., Bellezze, T. Contemporary use of Ni and Bi in hot-dip galvanizing. – *Surface and Coatings Technology*, 2002, 157, 34–39.
- Hornsby, M. J. Hot dip galvanizing: A guide to process selection and galvanizing practice. London: Intermediate Technology Publications, 1995.
- Jalel Ben nasr, Ali Snoussi, Chedly Bradai, Foued Halouani. Effect of the withdrawal speed on the thickness of the zinc layer in hot dip pure zinc coatings. – *Materials Letters*, 2008, 62, 2150–2152.
- Xuping Su, Changjun Wu, Daniel Liu, Fucheng Yin, Zhongxi Zhu, Sui Yang. Effect of vanadium on galvanizing Si-containing steels. – *Surface & Coatings Technology*, 2010, 205, 213–218.
- Pistofidis, N., Vourlias, G., Konidaris, S., Pavlidou, E., Stergiou, A., Stergioudis, G. The effect of bismuth on the structure of zinc hot-dip galvanized coatings. – *Materials Letters*, 2007, 61, 994–997.
- Marder, A. R. The metallurgy of zinc-coated steel. – *Progress in Materials Science*, 2000, 45, 191–271.
- Pavlidou, E., Pistofidis, N., Vourlias, G., Stergioudis, G. Modification of the growth-direction of the zinc coatings associated with element additions to the galvanizing bath. – *Materials Letters*, 2005, 59, 1619–1622.
- Lu Jin-tang, Wang Xin-hua, Che Chun-shan, KONG Gang, Chen Jin-hong, Xu Qiao-yu. Crystallographic research of spangle on hot dip galvanized steel sheets. – *Trans. Nonferrous Met. SOC. China*, 2007, 17, 351–356.
- Shu Peng, Jintang Lu, Chunshan Che, Gang Kong, Qiaoyu Xu. Morphology and antimony segregation of spangles on batch hot-dip galvanized coatings. – *Applied Surface Science*, 2010, 256, 5015–5020.
- Zinc coatings- Guidelines and recommendations for the protection against corrosion of iron and steel in structures. Part 2, Hot dip galvanizing: ISO/FDIS 14713-2:2009.

Paper II

Sepper, S., Peetsalu, P., Mikli, V., Saarna, M. The effect of substrate microstructure on morphology of zinc coatings. *Proceedings of the 8th International Conference of DAAAM Baltic Industrial Engineering, 2012, 717 -722.*

THE EFFECT OF SUBSTRATE MICROSTRUCTURE ON MORPHOLOGY OF ZINC COATINGS

Sepper, S.; Peetsalu, P.; Mikli, V.; Saarna, M.

Abstract: *in this paper the influence of substrate microstructure on iron-zinc alloy layer formation was studied. To achieve different microstructures laboratory heat treatment was used. Heat treatment parameters were chosen to imitate the heat affected zone in welding and thermal cutting processes. Steel grades S355JR, S700MC, C45E and C60E with different microstructures were immersed in a zinc bath at the temperature 450 °C. Results show that the ferrite grain size does not affect the coating formation. The coating structure and thickness are influenced by carbide grain size.*

Key words: hot dip galvanizing, iron-zinc phases, substrate microstructure, heat affected zone

1. INTRODUCTION

Hot dip galvanization has gained importance in recent years, especially in the construction manufacturing, as a very effective corrosion protection method. Increase in the sizes and capacities of galvanizing kettles makes galvanizing large constructions possible [1]. Hot-dip galvanized constructions might consist of different steel grades: carbon steels and high-strength microalloyed steels, which are welded together in fabrication. Construction production might also include thermal cutting processes, which change the steel microstructure in the heat affected zone (Figure 1). The metal in the heat affected zone (HAZ) undergoes a thermal cycle, which leads to significant micro-

structural modifications during welding or thermal cutting process [2].

Although the hot-dip galvanizing has existed for more than 250 years, the precise mechanism of coating formation has still not found a completely satisfactory explanation [3, 4, 5, 6]. There are many investigations describing the influence of steel chemical composition on the hot dip galvanizing, but little research has been done on the effect of substrate microstructure on morphology of zinc coatings.

Hisamatsu [7] postulated that finer grain size of interstitial-free steel is more reactive. More grain boundary area is available for reaction and more rapid Fe-Zn phase growth results. Recent investigations have shown that the substrate grain size has no significant effect on the kinetics of phase growth in a galvanizing bath containing less than 0.001 wt% Al [8]. Galvanizing bath containing 0.20 wt% Al led to outburst formation with finer substrate grain size [8]. Thiele [9]



Fig. 1. Heat affected zone of plasma cutting

postulated that annealing Si-containing steels before galvanizing reduces the coating thickness because potential hydrogen traps are to be expected.

The objective of the present study is to investigate the effects of substrate microstructure on Fe-Zn reaction kinetics and phase formation during hot dip galvanizing process.

2. EXPERIMENTAL

2.1 Substrate preparation

Four steel grades (hot rolled S355JR and S700MC with thermo-mechanical treatment, cold rolled softly annealed C45E and C60E) with different silicon equivalents were used in the experiment. The chemical compositions of the steels are presented in Table 1. The substrate materials were 3 mm thick.

To achieve different microstructures with same chemical composition laboratory heat treatment was used:

- 1) Changing the ferrite grain size – substrate specimens were austenitized at the temperature 900 °C, 1000 °C and 1200 °C for 2 hours followed by water quench and tempering at the temperature of 600 °C for 1 hour.
- 2) Changing the size of carbide grains – C45E and C60E were austenitized at the temperature 900 °C for 30 minutes, quenched in water and tempered at the temperature 200 °C, 300 °C, 400 °C, 500 °C, 600 °C, 700 °C for 1 hour.

To guarantee the same chemical composition and surface roughness of the specimens the decarburized layer was removed by mechanical grinding before hot dip galvanizing process.

2.2 Hot dip galvanizing process

Steel sheets were degreased for 15 minutes in acid degreasing agent (KeboClean VZS) and then pickled for 45 minutes with a 10% HCl containing inhibitor for the

protection of metal surfaces. Next the sheets were rinsed in water and then dipped in a flux bath consisting of 233 g/l ZnCl₂ and 189 g/l NH₄Cl which was kept at 40 °C. The fluxed sheets were dried for 15 minutes at 120 °C in drying oven. Then the sheets were dipped in the zinc bath for 4 minutes at the temperature 450 °C. The zinc bath consists of zinc (99.3 wt. % Zn) containing also Al (0.0025 wt. %), rest Bi, Fe, Ni, Sn, Pb.

2.3 Microstructure studies

For the examination of the microstructure, hot dip galvanized specimens were cross sectioned, hot mounted, grinded and polished. Final polishing was done using a 0.05 μm Masterpolish suspension (Buehler). A nital etchant (nitric acid: 3 wt.%) was used to reveal the microstructures of the specimens and observations were made with optical microscopy Axiovert 25 and scanning electron microscopy EVO MA-15 (Carl Zeiss).

2.4 Coating thickness, Vickers hardness and ferrite grain size measurements

The thickness of coatings was determined by electromagnetic thickness gauge (Dualscope MP0). The Vickers hardness was measured with Micromet 2001 microhardness tester. Vickers hardness at the load of 1 kg was measured at the polished cross-section of a specimen after galvanizing process. Ferrite grain size (G) was determined with reference images of the standard DIN 50601.

Steel	C	Si	P	Mn	Cr	Si _{eq}
S355JR	0.10	0.01	0.015	0.42	0.02	0.05
S700MC	0.05	0.45	0.016	1.85	0.35	0.49
C45E	0.44	0.21	0.007	0.66	0.21	0.23
C60E	0.58	0.05	0.001	0.69	0.24	0.05

Table 1. Chemical composition of the substrate steels, wt %

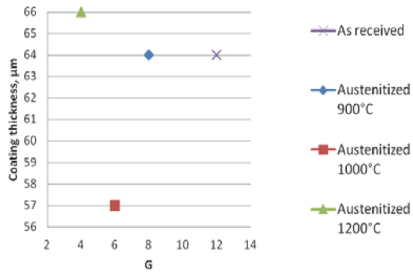


Fig. 2. Effect of S355JR ferrite grain size on coating thickness

3. RESULTS AND DISCUSSION

3.1 Effect of ferrite grain size

Ferrite grain growth in the HAZ is the dominant microstructural feature of the material's welding and cutting processes. Also different strengthening mechanisms are used in steel production process, which change the ferrite grain size and during hot dip galvanizing might affect the formation and the appearance of the coating.

Heat treat.	S355JR		S700MC		C45E	
	G	Coating thickness, μm	G	Coating thickness, μm	G	Coating thickness, μm
1	12	64	14	135	12	124
2	8	64	10	147	8	105
3	6	57	8	149	6	100
4	4	66	4	140	3	106

Table 2. Effect of ferrite grain size. Heat treatments: (1) – as received; austenitized (2) – 900 °C, (3) – 1000 °C, (4) – 1200 °C followed quenching in water and tempering 600 °C

To achieve different ferrite grain size above mentioned laboratory heat treatments were used. To determine the overall rate of reaction, the total Fe-Zn alloy layer thickness was measured. The effect of ferrite grain size on formation of hot dip galvanized coating is presented in Figure 2 and Table 2. The total Fe-Zn layer growth for each steel grade showed the

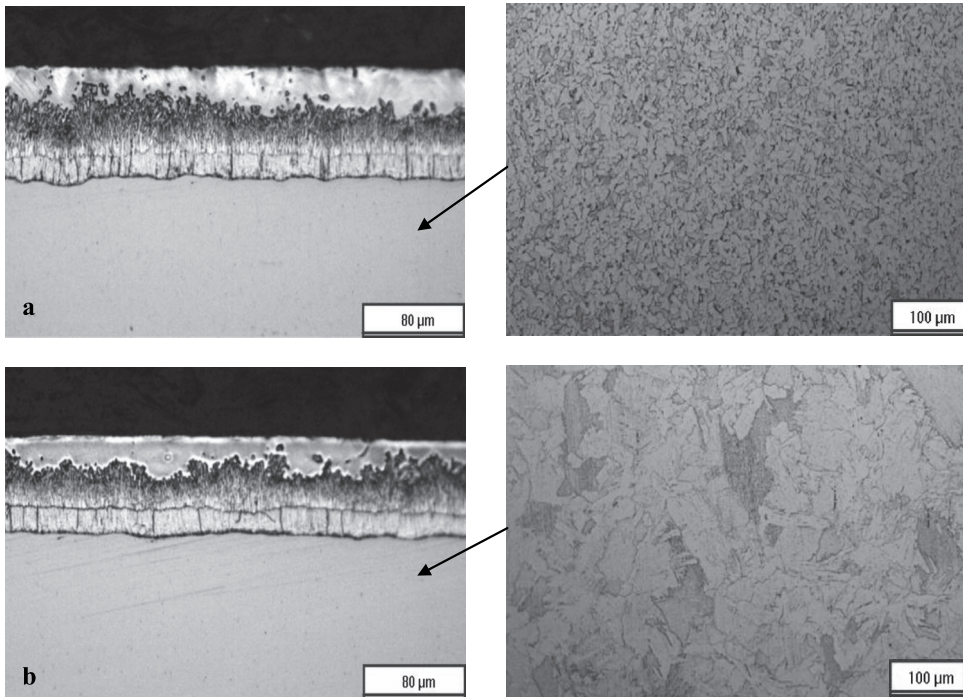


Fig. 3. The micrographs of the cross-sections of the coatings – (a) S355JR with ferrite grain size G12, (b) S355JR with ferrite grain size G4

same behaviour despite the ferrite grain size. In Figure 3 is shown the coating microstructure of steel S355JR with ferrite grain size G12 and G4. The results show that coating structure and thickness is not connected with substrate ferrite grain size.

3.2 Effect of the size of carbide grain

As a result of heat treatment in HAZ, the carbide grain size might also change. To achieve different carbide grain sizes above

mentioned laboratory heat treatments were used. In the present study the consideration that the substrate hardness increases with decreasing of carbide size was taken into account.

Differences in the size of carbides influence the coating formation. The higher the hardness of substrate, the smaller the carbide grain size and during hot dip galvanizing thinner coating is formed (Figure 4, Figure 5). The effect of carbide

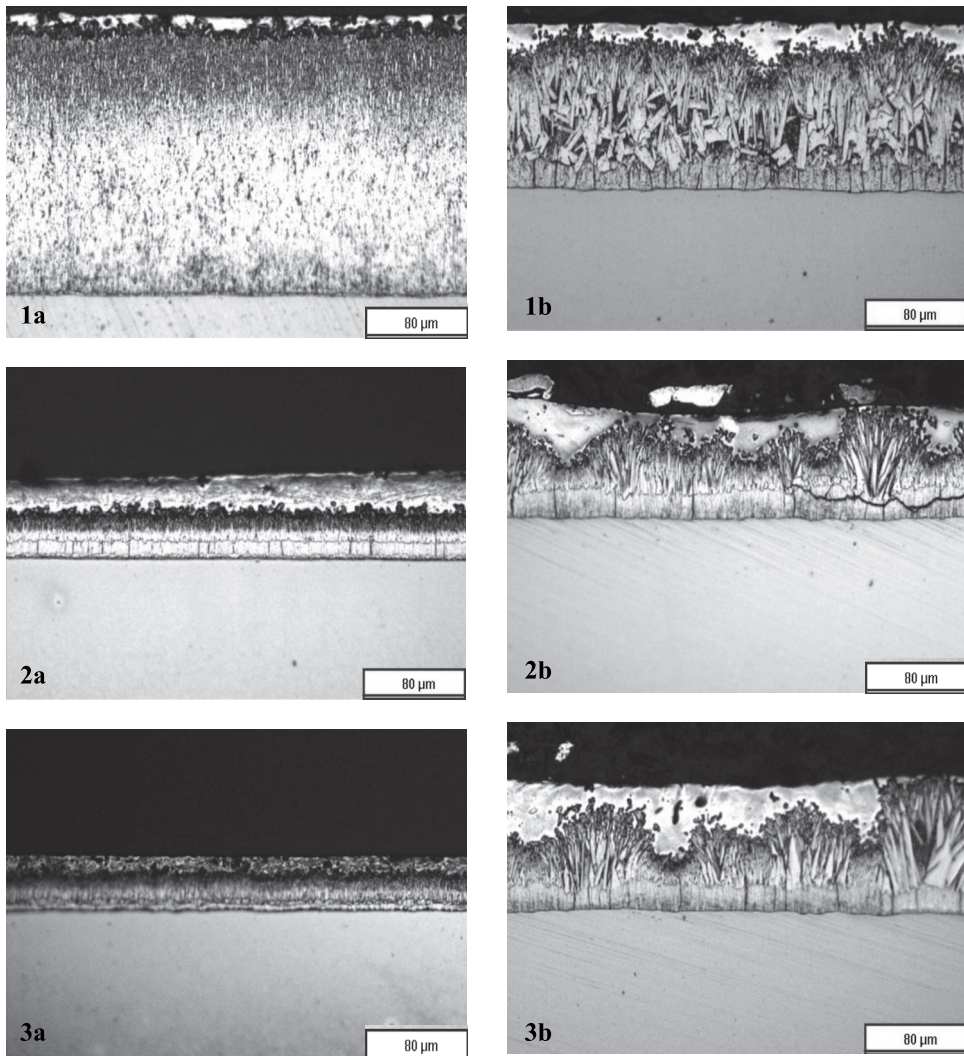


Fig. 4. Effect of „a“ C60E and „b“ C45E carbide grain on formation of hot dip galvanized coatings. Heat treatments: (1) as received (softly annealed); (2) austenitized 900°C, tempered 300°C; (3) quenched in water

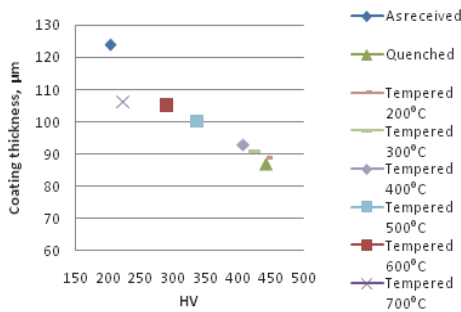


Fig. 5. The relationship between the coating thickness and substrate (C45E) hardness

grain on formation of hot dip galvanized coatings is presented in Figure 4. The reduction in coating thickness was remarkable with steel C60E (Figure 4-a). The silicon content of substrate belongs to the Sandelin range and during galvanizing process a rapid growth of the alloy layers occurred, producing a coating with excessive thickness. As a result of hardening, carbide size decreased and continuous, compact zinc coating formed. Heat treatment reduced the layer thickness from 207µm (as received condition- softly annealed) to 40 µm (quenched in water). Heat treatment of C45 (silicon equivalent 0.23) changed the carbide size and reduced the layer thickness from 124 µm (as received condition- softly annealed) to 87 µm (quenched in water). The different microstructures of heat treated C60E is shown in Figure 6. In

softly annealed microstructure are spheroidal carbides (the size of carbides 0.5 – 4µm). Austenitized and tempered 300 °C microstructure has small carbides in nanometric scale.

Results obtained that the austenization and tempering of the substrate influence the coating thickness and the coating microstructure. Hardening reduces iron-zinc reactivity and thinner coating is formed (reduction is remarkable with steel from Sandelin range). Larger carbides accelerate the zinc coating formation. The thinnest coatings were formed on quenched substrates, were originally after heat treatment no carbides are in the steel microstructure. Carbides are formed in quenched specimens during hot dip galvanizing process where steel is heated to 450 °C (zinc bath temperature). The effect of carbide grain size on coating thickness is influenced by silicon equivalent.

Drawing parallels with enamelling process where fish-scale formation is characterized by the hydrogen permeability (T_H) and the microstructure of the substrate might assume that hydrogen permeability plays also an important role in galvanizing process [9]. The hydrogen does not distribute homogeneously in steel, but various trapping sites exist for hydrogen atoms [10]. Fabian et al. [11] have proposed that the carbide shape and the

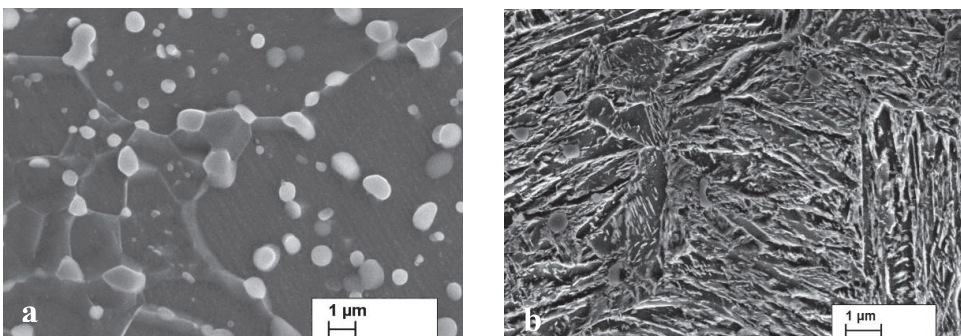


Fig. 6. The microstructure of C60 with different carbide grain sizes. Heat treatments: (a) as received (softly annealed); (b) austenitized 900 °C, tempered 300 °C

carbide size play an important role in the T_H time, but ferrite grain size has no significant effect on T_H value. However, more experiments are needed to draw parallels between the hot dip galvanizing process and enamelling process.

4. CONCLUSIONS

In the present paper the laboratory heat treatment was used to imitate the formation of heat affected zone in welding and cutting process to understand how the substrate microstructure affect the hot dip galvanized coatings. The following conclusions can be drawn from the present study:

1. The thickness of the coating and iron-zinc reactivity is related with the microstructure of the substrate.
2. Ferrite grain size does not affect the morphology of zinc coatings.
3. Differences in the size of carbides influence the coating formation. The higher the hardness of substrate, the smaller the carbide grain size and during hot dip galvanizing thinner coating is formed.
4. Silicon equivalent affects coating reduction with different sizes of carbides.

Further research is needed to support the hypotheses of hydrogen role in hot dip galvanized coating formation.

5. ACKNOWLEDGEMENTS

This research was supported by European Social Fund Fund's Doctoral Studies and Internationalisation Programme DoRa. Cooperation was made with AS Paldiski Tsingipada.

6. REFERENCES

1. Hot-dip galvanizing for corrosion protection [WWW]
www.pdengineer.com/courses/ma/MA-3002.pdf (01.03.2012)

2. Bayraktar, E., Kaplan, D., Devillers, L., Chevalier, J.P. Grain growth mechanism during the welding of interstitial free (IF) steels. *J. Mater. Process. Tech.*, 2007, **189**, 114-125.
3. Chunshan, C., Jintang, L., Gang, K., Qiaoyu, X. Role of silicon in steels on galvanized coatings. *Acta Metall. Sin (Engl. Lett.)*, 2009, **22**, 138-145.
4. Uchiyama, Y., Koga, H., Inokuchi, H. Reaction between Fe-Si alloys and liquid zinc. *T. Jpn. I. Met.*, 1983, **24**, 272-280.
5. Jintang, L., Chunshan, C., Gang, K., Qiaoyu, X., Jinhong, C. Influence of silicon on the α -Fe/ Γ interface of hot dip galvanized steels. *Surf. Coat. Tech.*, 2006, **200**, 5277-5281.
6. Gellings, P.J. Mechanism of the reaction between liquid zinc and steel. *Corros. Sci.*, 1974, **14**, 507-509.
7. Hisamatsu, Y. Science and technology of zinc and zinc alloy coated steel sheet. In *Proceedings of the International Conference on Zinc and Zinc Alloy Coated Steel Sheet* (Galvatech). ISIJ, Tokyo, 1989, 3-12.
8. Jordan, C.E., Marded, A.R. Effect of substrate grain size on iron-zinc reaction kinetics during hot dip galvanizing. *Metall. Mater. Trans. A.*, 1997, **28A**, 2683-2694.
9. Thiele, M., Schulz, W.D. Layer formation by hot dip galvanizing between 435 °C and 620 °C in conventional zinc melts – a general presentation. *Mater. Corros.*, 2006, **57**, 852- 867.
10. Volkov, A.K., Ryabov, R.A. Effect of the heat treatment on the hydrogen permeability of steel 40Kh. *Met. Sci. Heat Treat.*, 1997, **39**, 31-33.
11. Fábíán, E.R., Veró, B. Effect of the microstructure of Al-killed low carbon enamel-grade steel sheets on fish-scale formation. In *XXI International enamellers congress*, Shanghai, 2008, 293-304.

Paper III

Sepper, S., Peetsalu, P., Saarna, M., Kirs, V., Mikli, V. High strength steel behaviour during hot dip galvanizing. Proceedings 20th International Federation for Heat Treatment and Surface Engineering (IFHTSE) Congress, 2012, 525 - 529.

High strength steel behaviour during hot dip galvanizing

S. Sepper^a, P. Peetsalu^a, M. Saarna^a, V. Kirs^b, V. Mikli^c, a*

^aDepartment of Materials Engineering, Tallinn University of Technology, Ehitajate Tee 5, Tallinn 19086, Estonia

^bKirs engineering OÜ, Kirsioja talu, Jõesse küla, Marina vald, Läänemaa 90622, Estonia

^cMaterials Research Centre, Tallinn University of Technology, Ehitajate Tee 5, Tallinn 19086, Estonia

Abstract

Present study focuses on investigating the hydrogen diffusion during the hot dip galvanizing. This leads to understanding the cause of hydrogen embrittlement of high strength steels during the galvanizing process. In addition the mechanical properties of high strength steels before and after hot dip galvanizing were observed.

A batch type hot dip galvanizing process was used and zinc bath temperature was 450 °C. The bath consisted of 99.3 wt. % Zn and Al, Bi, Fe, Ni, Sn, Pb in balance. Substrate materials were chosen with similar thickness but from different grades of steels (S700 MC, Ruuki Optim 650 MC, C60 E and C35). In case of C60 E and C35 laboratory heat treatment was used (quenching and tempering). Result of the study show the behaviour of high strength steel during hot dip galvanizing process.

Keywords: Hot dip galvanizing; high strength steels; hydrogen embrittlement; mechanical properties

1. Introduction

High strength steels have attracted much interest in recent years because they make it possible to lighten the structures while maintaining load carrying capabilities. However, in order to use thinner gauges and meet customer's durability expectations, corrosion protection, and hence hot dip galvanizing, becomes crucial [1,2].

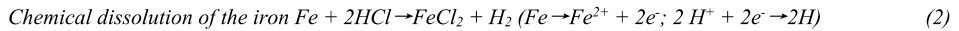
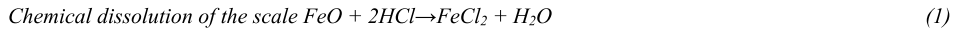
The first issue that involves high strength steel behaviour during hot dip galvanizing process is a phenomenon called hydrogen embrittlement, which can lead to the premature failure of the structure. ASTM F2329 warns of the risk of internal hydrogen embrittlement when parts with a specified hardness of 33 HRC and higher are acid pickled prior to galvanizing [3]. In general, the higher the strength levels of the steel the greater the risk of hydrogen embrittlement [4]. Also failures of welded structures fabricated from structural steel grade S355 have been reported. Local stresses, high hardness (in the heat affected zone) and diffusible hydrogen are the main factors responsible for failures of zinc coated products in general [5].

Hydrogen diffuses into the steel only in atomic form [6]. The atomic hydrogen absorbed in steel is located in two positions in the microstructure: interstitial lattice positions (diffusible hydrogen) or crystalline defects (trapped hydrogen) [7]. Atomic hydrogen can combine within the steel to form molecular hydrogen, which is trapped in the region of dislocations. An internal gas pressure can become so high which might promote plastic deformation of the microstructure and cracking mechanism [8, 9].

Atomic hydrogen can be absorbed by the steel during the surface preparations steps such as pickling and fluxing process [10]. During pickling two major reactions can occur:

* Corresponding author. Tel.: +372 620 3470

E-mail address: sirli.sepper@ttu.ee



The removal of scale (more commonly Fe_3O_4) is the desired result in pickling process. The chemical dissolution of the iron is usually unwanted and inhibitors are used to eliminate or decrease it [11].

Carpio et al. [10] measured the hydrogen content after each operation in galvanizing process. They stated that during fluxing the hydrogen content increases; this phenomenon does not occur during pickling due to the inhibitor presence, which does not allow reactions between acids and steel.

Another issue of concern in galvanizing high strength steels is the zinc bath temperature, which might affect the mechanical properties of high strength steels. At the galvanizing temperature – usually around 450°C – the steel being processed will lose approximately 50% of its room temperature yield strength, regaining it on cooling after galvanizing [9].

The objective of the study is to investigate the high strength steel behaviour during hot dip galvanizing.

2. Experimental

2.1. Substrate preparation

Four steel grades (hot rolled S700MC, Ruuki optim 650 MC with thermo-mechanical treatment, cold rolled soft annealed C35 and C60E) were used in the experiment. The chemical compositions of the steels are presented in Table 1. The substrate materials were 3 mm thick.

Table 1. Chemical composition of the substrate steels, wt %

Steel grade	C	Si	P	Mn	Cr
C35	0.40	0.19	0.009	0.62	0.33
S700 MC	0.07	0.13	0.001	2.21	0.09
Ruuki optim 650 MC	0.05	0.17	0.001	1.94	0.04
C60E	0.58	0.05	0.001	0.69	0.24

To evaluate the hydrogen embrittlement during hot dip galvanizing surface preparation steps specimens (substrate steel C35) which were under stress were used (Figure 1). Hydrogen embrittlement was studied with different strain levels and with different substrate heat treatments. As a result of hydrogen embrittlement, crack occurred where the maximum stress was applied (Figure 1 a). Strain level was adjusted with screw, the change in dimensions (Δ) was measured. The higher the value of Δ , the higher the stress level. Two different strains were used: dimension reduction $\Delta 3$ mm and $\Delta 2$ mm.

Different mechanical properties of the substrates were achieved with laboratory heat treatments. C35 was austenitized at the temperature 860°C for 20 minutes, quenched in water and tempered at the temperature 200°C , 300°C for 1 hour. The Rockwell hardness after heat treatment is shown in Table 2.

C60E was austenitized at the temperature 900°C for 30 minutes, quenched in water and tempered at the temperature 200°C , 300°C , 450°C , 650°C for 45 minutes to evaluate how the zinc bath temperature affects the mechanical properties of steel.

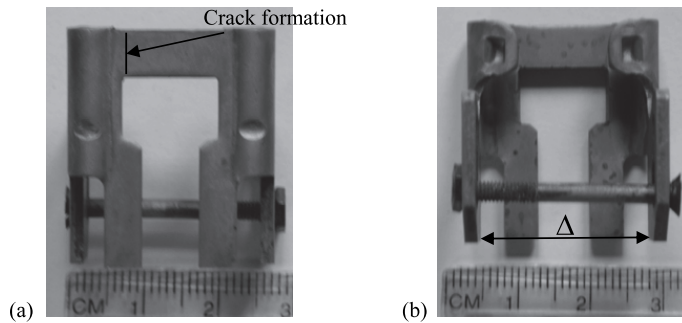


Fig. 1. Specimen to evaluate hydrogen embrittlement. (a) crack formation as a result of hydrogen embrittlement; (b) applied stress Δ measurement

Table 2. The Rockwell hardness of C35 after heat treatment

Heat treatment	HRC
Quenched	55.0
Quenched + tempered 200° C	48.6
Quenched + tempered 300° C	46.3

2.2. Hot dip galvanizing process to evaluate the change in mechanical properties

Hot dip galvanizing experiments were done in hot dip galvanizing factory called Zincpot (AS Paldiski Tsingipada). Steel sheets were degreased for 15 minutes in acid degreasing agent and then pickled for 120 minutes with 9.3 % HCl, containing an inhibitor for the protection of metal surfaces. Next the sheets were rinsed in water and then dipped in a flux bath for 30 seconds consisting of 243 g/l $ZnCl_2$ and 208 g/l NH_4Cl which was kept at 40 °C. The fluxed sheets were dried for 15 minutes at 120 °C in drying oven. Then the sheets were dipped in the zinc bath for 4 minutes at the temperature 450 °C. The zinc bath consists of zinc (99.3 wt. % Zn) containing also Al, Bi, Fe, Ni, Sn, Pb.

2.3. Steel analysis

Substrate material chemical composition was measured using Spectrolab M. The Rockwell hardness was measured with Zwick Roell hardness testing machine. Tensile strength was measured with using Instron 8800 servo-hydraulic testing machine.

3. Results and discussion

3.1. Evaluating the hydrogen embrittlement

During the hot dip galvanizing surface preparation (degreasing, pickling and fluxing) is used which can induce hydrogen into the substrate material and enhance the hydrogen embrittlement. To study the hydrogen effect during hot dip galvanizing it is necessary to have specimens with different high

mechanical properties at the different tensions. Specimens have to indicate the high hydrogen diffusion rate and sensibility to failure during hot dip galvanizing process. Therefore C35 steel was used with different heat treatments and tensions (Figure 1). Mechanical properties of the studied specimens are describing the quenched and tempered part properties or heat affected zone (HAZ) properties in welding.

Specimens were immersed in surface preparation chemicals which are used during hot dip galvanizing process. Δ was taken as indicator of applied stresses. The specimens were dipped in the pre-treatment chemicals until hydrogen embrittlement occurred. The risk of hydrogen embrittlement is the highest with maximum hardness values and with maximum applied load.

The first step in hot dip galvanizing is the degreasing process to remove grease and oil from the surface of the steel. Acid degreasing solutions are new cost saving development as no water rinsing is required before the acid pickle and no heating is required. Acid degreaser contains acids which might cause hydrogen embrittlement. The usual degreasing time in galvanizing process is 30 minutes.

Quenched specimens (HRC 55) with applied stress $\Delta 3$ mm were dipped in the acid degreasing solution (contains inhibitors). Hydrogen embrittlement did not occur with dipping time 3 hours. There was not observed hydrogen embrittlement during degreasing process with investigated conditions.

The next pre-treatment step is pickling to remove rust and scale from the steel surface. The relationship between the Rockwell hardness, applied stresses and hydrogen embrittlement is shown in Figure 2. The hydrogen embrittlement did not occur with substrate Rockwell hardness 46.3 with investigated strain levels. The higher is the substrate hardness and applied strain, the more rapidly hydrogen embrittlement occurred.

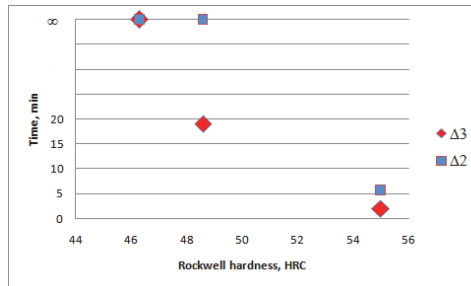


Fig. 2. Hydrogen embrittlement formation with different substrate hardness in pickling solution

The final pre-treatment chemical is flux (zinc ammonium chloride) to assist the molten zinc to react with the steel surface to form the galvanized coating. The regular dipping time is 0.5 – 1 minute. The crack formation occurred with quenched specimens with strain level $\Delta 3$ mm in 27 minutes. Quenched specimens with strain level $\Delta 2$ mm did not suffer from hydrogen embrittlement after dipping for 24 hours.

In this study the hydrogen-entry occurred in the pickling and fluxing solutions (hydrogen embrittlement in the degreasing solution was not observed). But the main process which caused hydrogen embrittlement was pickling process, although pickling solution contained inhibitor. Hydrogen embrittlement occurred when the substrate hardness was higher than 48.6 HRC (tensile strength $R_m \geq 1550$ MPa). Usually steels with so high tensile strength are not hot dip galvanized. The risk of hydrogen embrittlement is higher with higher applied stress values.

Quenched and tempered parts which are hot dip galvanized should have hardness less than 48 HRC to avoid the hydrogen induced failure. The HAZ in welding should have hardness less than 480 HV which is

not allowed according to the quality requirements of welding. Failures occurring with lower hardness are related to the complex failure mode where hydrogen is not the only reason of the failure.

3.2. The effect of zinc bath temperature on mechanical properties of steels

Zinc bath temperature is at the range 430-550 °C and dipping time depends on the size of construction, ranging 5-12 minutes. The effect of zinc bath temperature can be studied with two cases: the aging of the thermo-mechanically rolled low carbon steel or tempering the quenched and tempered steel. Both cases have to be taken into account in engineering that construction properties are affected by short time heating during dipping in the molten zinc. Aging is the mechanism which increases the strength properties while elongation is decreased [12]. Aging can vary with the same steel grade as it can be produced using different chemistry and thermo mechanical rolling or even cold rolling. Aging can be explained by C and N atoms diffusion to the dislocations and locking them. At this study two steels were used to see the heat effect to the steel mechanical properties with normal immersion times. Material mechanical properties are shown in the Table 3 and tensile test diagrams are shown in Figure 3.

Table 3. Mechanical properties of steels before and after hot dip galvanizing

Steel grade	Rp 0.2 %	Rm MPa	Ag %	A %
Optim 650 MC	805.5 ± 9.6	827 ± 15.4	8.8 ± 0.2	16.5 ± 1.5
Optim 650 MC after hot dip galvanizing	826.3 ± 14.0	836,3 ± 10	8.8 ± 0.3	15.0 ± 0.8
S700 MC	756.2 ± 15.9	836 ± 18	6.5 ± 1.6	8.7 ± 0.7
S700 MC after hot dip galvanizing	833 ± 0.5	853,5 ± 6.2	7.2 ± 0.3	9.1 ± 2.5

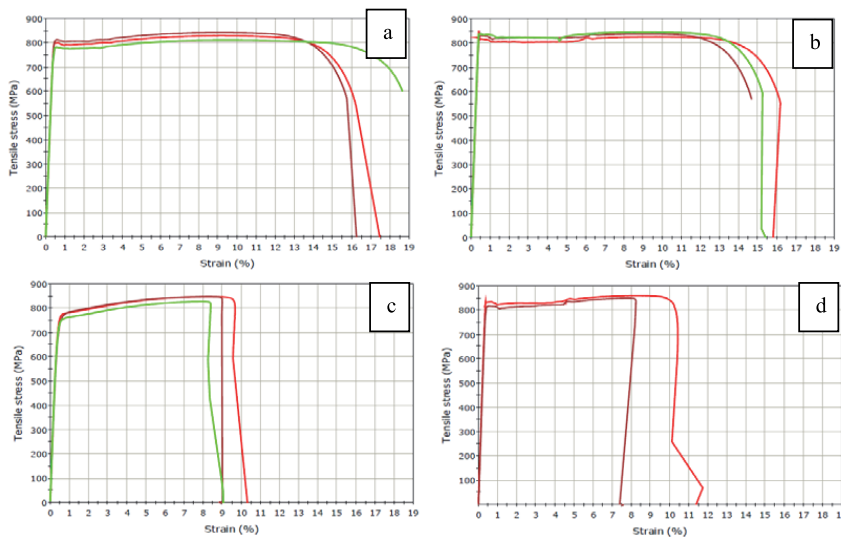


Fig. 3. Stress-strain curves. „a“ - Optim 650 MC; „b“ - Optim 650MC after hot dip galvanizing; „c“ - S700 MC; „d“ - S700 MC after hot dip galvanizing

The mechanical properties after hot dip galvanizing are changed where yield and tensile strength is increasing and elongation slightly decreasing. In the case of steel grade S700 MC the Lyders strain (yield extension) is appearing after hot dip galvanizing.

HSLA steels are suspected to the aging process during immersion to the zinc bath even with relatively short heating time. Test made with carbon steel C35 showed that hydrogen diffuses from pickling process to the steel even in the case of acid with inhibitor. Hydrogen leads parts to the failure when hardness is over 48 HRC which responses to the tensile strength 1550 MPa. HSLA steels tensile strength and hardness is under 48 HRC and therefore hydrogen induced failure cannot be reason of the failure during hot dip galvanizing even after aging. The hydrogen can make material more brittle and stresses in construction with welding defects can lead to the failure during hot dip galvanizing.

Hot dip galvanizing heat effect to the quenched and tempered parts is shown at the Figure 4. Specimens were made from C60E and laboratory heat treatment was used before hot dip galvanizing. Hardness will decrease less in tempering at shorter time than in longer time [13]. The results show that during short dipping hardness decreases to the 42-43 HRC while 45 min tempering causes hardness 40 HRC at the same temperature (Figure 4). Heating during dipping will decrease hardness of quenched and tempered parts which have higher tempering temperature than 450 °C. Higher temperature tempered parts has no loss in hardness, but it has to taken into the consideration that the second tempering is made to the 450 °C and may cause tempering embrittlement. HAZ at welding has same behaviour at the point of view heat treatment. Hardness in the HAZ may decrease and also tempering embrittlement may occur as a result of heating during hot dip galvanizing.

Heating during dipping in to the molten zinc reduces the hydrogen content of the steel (baking process). Hydrogen induced cracking during hot dip galvanizing can happen when construction material or HAZ have high hardness (over 48 HRC) and stresses with stress concentrators. Failures will happen before or during dipping in the molten zinc as the heating in the zinc bath releases the hydrogen.

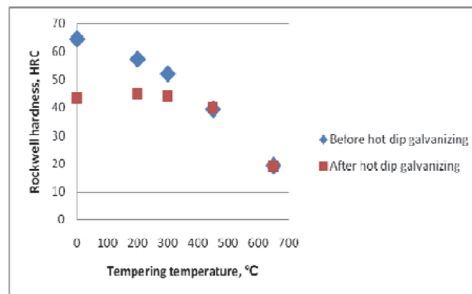


Fig. 4. Hot dip galvanizing heat effect to the quenched and tempered parts

4. Conclusions

In the present paper the high strength steel behaviour — suffering from hydrogen embrittlement during pre-treatment process and the effect of zinc bath temperature on mechanical properties of steel — was studied. The following conclusions can be drawn:

- (1) Acid degreaser did not cause hydrogen diffusion with investigated materials and with investigated conditions.
- (2) During pickling hydrogen embrittlement occurred with substrate steels with Rockwell hardness ≥ 48.6

HRC. Pickling process is the most hydrogen induced process even with inhibitor present.

(3) During fluxing process hydrogen embrittlement occurred only with maximum hardness used in this study and with maximum stress level. The dipping time in flux was 27 minutes, during pickling hydrogen embrittlement occurred with the same specimen in 2 minutes.

(4) Quenched and tempered parts can fail during pickling or fluxing process if hardness is over 48 HRC (tensile strength over 1550 MPa) or HAZ in welding is over 480 HV. During immersing the parts in the molten zinc the quenched and tempered material hardness may decrease (short time tempering at the galvanizing temperature) and possible tempering embrittlement can be introduced.

(5) Short time heating in zinc bath causes aging process with HSLA steels were strength properties are increasing. Even with increased strength properties tensile strength of the HSLA steel is not over 1550 MPa and therefore only hydrogen embrittlement can not be the cause of failure during hot dip galvanizing.

Acknowledgements

This research was supported by European Social Fund Fund's Doctoral Studies and Internationalisation Programme DoRa. Cooperation was made with AS Paldiski Tsingipada (Zincpot).

References

- [1] Petit E.J, Grosbety Y, Aden-Ali S, Schmitt L, Gilgert J, Azari Z. Fatigue toughness of galvanized high strength steels for structural applications for automotive industry. *Intergalva* 2012.
- [2] Khondker R, Mertens A, McDermid J.R. Effect of annealing atmosphere on the galvanizing behaviour of a dual-phase steel. *Materials Science and Engineering A* 463, 2007, p. 157–165
- [3] ASTM F2329 - 11 Standard Specification for Zinc Coating, Hot-Dip, Requirements for Application to Carbon and Alloy Steel Bolts, Screws, Washers, Nuts, and Special Threaded Fasteners
- [4] Eliaz N, Shachar A, Tal B, Eliezer D. Characteristics of hydrogen embrittlement, stress corrosion cracking and tempered martensite embrittlement in high-strength steels. *Engineering Failure Analysis* 9, 2002, p. 167-184.
- [5] Mraz L, Lesay J. Problems with reliability and safety of hot dip galvanized steel structures. *Soldagem Insp. São Paulo*, Vol. 14, No. 2, p.184-190
- [6] Gabe D.R. The role of hydrogen in metal electrodeposition processes. *Journal of applied electrochemistry*, 1997, 27, p. 908-915
- [7] Shirband Z, Shishesaz M.R, Ashrafi, A. Hydrogen degradation of steels and its related parameters, a review. *Phase Transit.*, 2011, 84, p. 924–943.
- [8] Timmins P.F. Predictive corrosion failure and control in process operations. ASM International, Materials Park, 1996.
- [9] Galvanizers Association. Guidance Note: The design, specification and fabrication of structural steelwork that is to be galvanized.
- [10] Carpio J, Casado J.A, Alvarez J.A, Gutierrez-Solana F. Environmental factors in failure during structural steel hot-dip galvanizing. *Eng. Fail. Anal.*, 2009, 16, p. 585–595.
- [11] Chappell E. L, Paul C. Ely. The Pickling of Pipe Using Commercial Inhibitors. *Industrial and engineering chemistry*, 22, p. 1201-1203
- [12] Rashid, M.S. Strain aging kinetics of Vanadium or Titanium strengthened high strength low-alloy steels. *Metallurgical transactions A*, 7A, 1976, p. 497-503.
- [13] ASM Handbook, Volume 04 - Heat Treating, ASM International Handbook Committee, 1991, ASM International

Paper IV

Sepper, S., Peetsalu, P., Saarna, M., Mikli, V., Kulu, P. Effect of hot dip galvanizing on the mechanical properties of high strength steels. *Key Engineering Materials*, 2014, 12 - 15.

Effect of hot dip galvanizing on the mechanical properties of high strength steels

Sirli Sepper^{1, a *}, Priidu Peetsalu^{1, b}, Mart Saarna^{1, c}, Valdek Mikli^{2, d} and Priit Kulu^{1, e}

¹Department of Materials Engineering, Tallinn University of Technology, Estonia

²Materials Research Centre, Tallinn University of Technology, Estonia

^asirli.sepper@ttu.ee, ^bpriidu.peetsalu@ttu.ee, ^cmart.saarna@ttu.ee, ^dvaldek.mikli@ttu.ee, ^epriit.kulu@ttu.ee

Keywords: Hot dip galvanizing; high strength steels; mechanical properties; tensile test

Abstract. Present study focuses on investigating the hot dip galvanizing effect on the mechanical properties of high strength steel. The effect of chemical pre-treatment (hydrogen diffusion) and the effect of hot dip galvanizing temperature on mechanical properties was studied with high strength steel S650MC. Additional tests were made with widely used structural steel S355J2. A batch type hot dip galvanizing process was used and zinc bath temperature was 450 °C and 550 °C. Results of the study show the behaviour of high strength steel during hot dip galvanizing process.

Introduction

High strength steels have attracted much interest in recent years because they make it possible to lighten the structures while maintaining load carrying capabilities. However, in order to use thinner gauges and meet customer's durability expectations corrosion protection becomes crucial [1].

The first issue that involves high strength steel behaviour during hot dip galvanizing process is a phenomenon called hydrogen embrittlement. In general, the higher the strength levels of the steel the greater the risk of hydrogen embrittlement [2].

Another issue of concern in galvanizing high strength steels is the zinc bath temperature, which might affect the mechanical properties of high strength steels. At the galvanizing temperature – usually around 450 °C – the steel being processed will lose approximately 50% of its room temperature yield strength. Nevertheless, these mechanical properties are recovered after galvanizing [3]. Langill et al. [4] investigated mechanical properties of different steels after hot dip galvanizing and concluded that hot dip galvanizing has a relatively minor effect on the mechanical properties of investigated steels.

As new steel grades with higher yield and tensile strengths have come to the market it is necessary to learn how they are affected by galvanizing process. The objective of the study is to investigate the effect of hot dip galvanizing on the mechanical properties of high strength steels.

Materials and methods

Substrate preparation. Hot rolled structural steel S355J2 and high strength low alloy steel S650MC with thermo-mechanical treatment were used in the experiment as substrate materials. The chemical compositions of the steels are presented in Table 1. Hot dip galvanizing experiments were done in hot dip galvanizing factory Zincpot (AS Paldiski Tsingipada).

Table 1. Chemical composition of the substrate steels, wt %

Steel grade	C	Si	P	Mn	Cr
S650 MC	0.05	0.16	0.008	1.71	0.03
S355J2	0.06	0.02	0.006	0.74	0.05

Steel analysis. Tensile strength was measured with Instron 8800 servo-hydraulic testing machine. For the examination of the microstructure, hot dip galvanized specimens were cross sectioned, hot mounted, ground and polished. A nital etchant was used to reveal the microstructures of the specimens and observations were made with optical microscope Zeiss Axiovert 25. Ferrite grain size (G) was determined according to reference images of the standard DIN 50601.

Results and discussion

Hot dip galvanizing effect on the tensile strength results was investigated in three cases: pickling effect to the tensile strength results, galvanizing temperature heat effect to the tensile strength results, zinc coating effect to the tensile strength results.

1) During the hot dip galvanizing surface preparation steps (degreasing, pickling and fluxing) are used which can induce hydrogen into the substrate material and enhance the hydrogen embrittlement. According to our previous study [5] the main process which caused hydrogen embrittlement was pickling, although pickling solution contained inhibitor. This is why the tensile test specimens were pickled for two hours in 10 % HCl acid containing inhibitor to investigate if pickling process can affect the mechanical properties of the steel. The tensile test was made immediately after pickling. The results of the study showed that pickling process did not affect the mechanical properties of construction steel S355J2 and high strength steel S650MC (Table 2, 3).

2) To study the galvanizing temperature effect to the mechanical properties of high strength steels two temperatures were investigated – 450 °C (normal galvanizing temperature) and 550 °C (high temperature galvanizing temperature). To eliminate the effect of chemical reaction between the iron and zinc, tests were made with dipping the tensile test specimens into the molten salt (450 °C and 550 °C). Material mechanical properties are shown in the Table 2 and Table 3 and tensile test diagrams are shown in Fig. 1.

Table 2. S650MC tensile test results

Steel grade	$R_{p0.05}$ [MPa]	$R_{p0.2}$ [MPa]	R_m [MPa]	A_g [%]	A_{80} [%]	Load at R_m [kN]
S650MC	727 ± 17.9	782 ± 2 1.4	826 ± 9.0	8.9 ± 0.5	14.9 ± 0.1	48.7 ± 0.8
S650MC after pickling	721 ± 13.6	774 ± 4.6	827 ± 0.4	8.6 ± 0.7	14.8 ± 1.1	48.8 ± 0.3
S650MC after dipping in the salt 450 °C	794 ± 16.9	772 ± 8.5	819 ± 8.2	9.0 ± 0.7	15.6 ± 0.2	48.4 ± 1.7
S650MC after dipping in the salt 550 °C	806 ± 23	784 ± 2.1	825 ± 3.5	8.6 ± 0.6	14.4 ± 1.1	48.6 ± 0.8

Table 3. S355J2 tensile test results

Steel grade	$R_{p0.2}$ [MPa]	R_m [MPa]	A_g [%]	A_{80} [%]	Load at R_m [kN]
S355 J2	424 ± 3.5	489 ± 3.2	15.7 ± 0.2	26.9 ± 0.5	29.9 ± 0.6
S355J2 after pickling	428 ± 2.0	493 ± 1.3	15.2 ± 0.1	26.2 ± 0.3	30.0 ± 0.2
S355J2 after dipping in the salt 450 °C	481 ± 13.5	495 ± 4.0	14.9 ± 0.2	25.9 ± 0.7	30.3 ± 0.4
S355J2 after dipping in the salt 550 °C	470 ± 7.6	496 ± 2.0	15.2 ± 0.4	25.4 ± 0.5	29.9 ± 0.2

After heating S650MC and S355J2 in the molten salt there is an increase in $R_{p0.05}$ and $R_{p0.2}$ results, but A_{80} , R_m and A_g virtually do not change (minor changes). The biggest change is visible in stress-strain curves (S650MC and S355J2), where Lüders strain (yield extension) is appearing after heating. This behavior is characterized by an initially high yield stress followed immediately by a sudden fall in stress. With continued straining the stress stays approximately unchangeable for several strain percent's before normal strain hardening behavior begins [6]. This effect is also the reason of the increase in $R_{p0.05}$ (and $R_{p0.2}$) results.

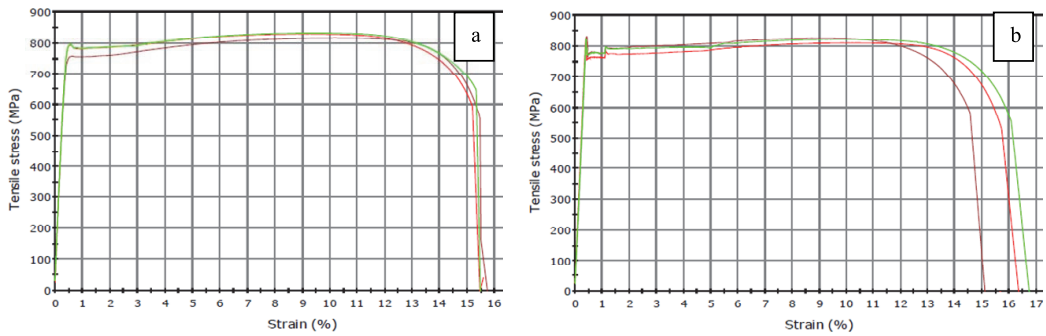


Fig. 1. Stress-strain curves. “a” – S650MC as received; “b” – S650MC after dipping in salt 450 °C.

Short heating of low carbon steel in the hot dip galvanizing temperature (usual dipping time in molten zinc is 4 – 8 minutes) does not cause ferrite grain growth (Fig.2). In the Fig. 2 is shown the microstructure of S650MC after heating in a laboratory furnace at 550 °C for 30 minutes. The ferrite grain size of S650MC in as received condition is 14 according to DIN 50601. After heating in different temperatures (450 °C, 550 °C, and 650 °C) the grain size did not change.

Locking of dislocations (during hot dip galvanizing process) is probably caused by C and N atoms diffusion to the dislocations (aging process). Additional stress over that normally required for the movement of the dislocations is needed in order to tear some of the dislocations away from their restraining impurity atoms. This results in the increase in stress, which sets some dislocations in motion, and corresponds to the upper yield point stress. When the dislocation line is pulled free from the influence of the solute atoms, it can slip at a lower yield point stress (Cottrell's theory).

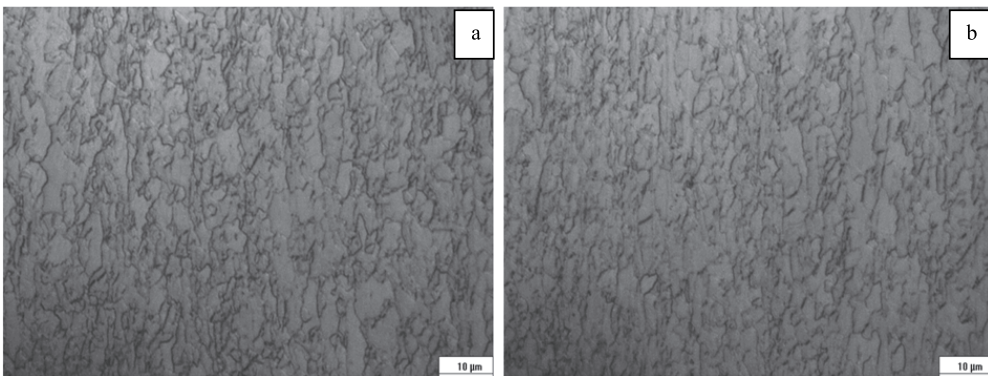


Fig. 2. The microstructure of S650MC: “a” – as received; “b” – heat treatment 550 °C.

3) The tensile test results of hot dip galvanized S355J2 and S650MC are presented in Table 4, and Table 5. Tensile test results in hot dip galvanized specimens with zinc coating include zinc coating thickness in the calculations and that is why these results are not comparable with “as received” results. When discounting the coating thickness and calculate yield and tensile strength using only the base steel thickness an extra load resistance during tensile test is expected. Load at R_m in both investigated steels is higher with zinc coating because zinc coating increases the strength of the specimen.

After zinc coating removal in 10 % HCl, there is the same tendency increase in $R_{p0.05}$ value (and in case of S355J2 increase in $R_{p0.2}$ value) compared with as received specimens. Lüders strain is appearing in stress-strain curves after hot dip galvanizing (in both steels investigated – S650MC and S355J2) as a result of heating and aging effect.

Table 4. Tensile test results (S650MC) after hot dip galvanizing

Specimen	$R_{p0.05}$ [MPa]	$R_{p0.2}$ [MPa]	R_m [MPa]	A_g [%]	A_{80} [%]	Load at R_m [kN]	Thickness [mm]
Hot dip galvanized (450 °C) with zinc coating	766 ±11.7	738±8.1	775±8.7	9.2±0.2	15±1.8	50.2±0.7	3.16
Hot dip galvanized (450 °C) without zinc	822 ±17.7	785 ± 3.7	826 ± 1.5	9.3 ± 0.2	16.1 ± 0.5	48.4±1.7	2.98
Hot dip galvanized (550 °C) with zinc coating	779 ±10.8	752±5.5	790±4.8	9.3±0.4	15.9±0.7	50.3±0.2	3.10
Hot dip galvanized (550 °C) without zinc	798 ±5.2	784 ± 1.6	823 ± 2.4	9.7 ± 0.1	16.4 ± 0.4	49.6 ± 0.4	2.98

Table 5. Tensile test results (S355J2) after hot dip galvanizing

Steel grade	$R_{p0.2}$ [MPa]	R_m [MPa]	A_g [%]	A_{80} [%]	Load at R_m [kN]	Thickness [mm]
Hot dip galvanized (450 °C) with zinc coating	465±5.8	477±2.7	13.8±0.1	24.9±0.7	30.8±0.3	3.14
Hot dip galvanized (450 °C) without zinc	488 ±2.9	496 ±1.3	14.3 ±0.2	23.9 ±1.2	29.7 ±0.4	3.00
Hot dip galvanized (550 °C) with zinc coating	470±11.7	476±5.9	14.2±0.1	23.6±0.5	30.2±0.8	3.12
Hot dip galvanized (550 °C) without zinc	475 ±8.3	489 ±3.6	15.5 ±0.5	25.9 ±1.0	29.4 ±0.8	2.98

Summary

In the present paper the high strength steel behaviour was studied. The following conclusions can be drawn:

- (1) Pickling specimens in 10 % HCL acid did not change tensile test results with investigated steels at room temperature.
- (2) During short time heating in the hot dip galvanizing temperature aging takes place and as a result Lüder strain occurs in stress-strain curves. Lüders strain occurred not only with high strength steel S650MC but also with construction steel S355J2.
- (3) Hot dip galvanizing temperature did not cause ferrite grain growth or recrystallization.
- (4) Hot dip galvanized tensile test specimen's (with zinc coating) load at tensile test is slightly higher because zinc coating increases the strength of the specimen.

Acknowledgements

This research was supported by European Social Fund Fund's Doctoral Studies, Internationalisation Programme DoRa and AS Paldiski Tsingipada.

References

- [1] R. Khondker, A. Mertens, J.R.McDermid, Effect of annealing atmosphere on the galvanizing behaviour of a dual-phase steel, *Mat. Sci. Eng.* 463 (2007) 157–165.
- [2] N. Eliaz, A. Shachar, B. Tal, D. Eliezer, Characteristics of hydrogen embrittlement, stress corrosion cracking and tempered martensite embrittlement in high-strength steels. *Eng. Fail. Anal.* 9 (2002) 167-184.
- [3] J. Carpio, J.A. Casado, J.A. Alvarez, F. Gutierrez-Solana, Environmental factors in failure during structural steel hot-dip galvanizing, *Eng. Fail. Anal.* 16 (2009) 585–595.
- [4] T. Langill, Mechanical Properties of Hot-Dip Galvanized Steel, *Structures Congress 2009*. 1-6.
- [5] S. Sepper, P. Peetsalu, M. Saarna, V. Kirs, V. Mikli, High strength steel behaviour during hot dip galvanizing, *Proceedings 20th IFHTSE*. 2012, 525 - 529.
- [6] Information on <http://www.kstreetstudio.com/science/natedwkshp/files/Meier-NEW-2001-2.pdf>

Paper V

Sepper, S., Peetsalu, P., Kulu, P., Saarna, M., Mikli, V. The role of silicon in the hot dip galvanizing process. *Proceedings of the Estonian Academy of Sciences*, 2016, 65, 2, 159–165.



The role of silicon in the hot dip galvanizing process

Sirli Sepper*, Priidu Peetsalu, Priit Kulu, Mart Saarna, and Valdek Mikli

Department of Materials Engineering, Tallinn University of Technology, Ehitajate tee 5, 19086 Tallinn, Estonia

Received 19 October 2015, revised 12 January 2016, accepted 14 January 2016, available online 14 March 2016

Abstract. The study focuses on the role of silicon in the hot dip galvanizing process. Coating formation and growth were analysed. Centrifugal casting was used to prepare steel substrates with different silicon concentrations (<0.01%, 0.06%, 0.11%, 0.17%, and 0.30%). Hot dip galvanizing was performed at 450 °C in the industrial galvanizing plant Zincpot (Estonia). The galvanizing time for coating formation was 4–25 s and for coating growth 195 and 1200 s after a longer incubation time. The thickness of the coating was measured and the microstructure of the Zn–Fe coating was examined. Even a very short time contact (4 s) between steel and zinc led to the formation of Fe–Zn intermetallics. The first phase was the ζ phase, immediately followed by the δ and then, after incubation the Γ phase. The reactions that took place in the galvanizing process during the shorter dipping times (<25 s) were not influenced by silicon concentrations, but the influence of silicon was remarkable after longer dipping times (>25 s). A schematic model of zinc coating formation is presented. Silicon affects hot dip galvanizing reactions by influencing Zn diffusion into steel and Fe diffusion into the coating.

Key words: hot dip galvanizing, Sandelin effect, role of silicon, coating microstructure, iron–zinc phases.

1. INTRODUCTION

Structural steels contain a small amount of silicon because it is used as a de-oxidant in the steel making process. Silicon is also a low-cost and very effective strengthening alloying element for steels [1]. Silicon concentration in steel plays a major role in the hot dip galvanizing process. It influences the growth and microstructure of coatings. Steels containing small amounts of silicon (<0.03%) have a compact and continuous zinc coating (galvanizing temperature 450 °C), which is composed of Γ , δ , ζ , and η layers. The presence of Si at certain levels, i.e. 0.03–0.14% (Sandelin area) and above 0.3%, produces a coating with excessive thickness, grey appearance, and poor adherence. Steels containing 0.15–0.25% Si also produce a compact and coherent coating (Sebisty effect) [2,3].

The growth of the alloy layer may be controlled by both the chemical composition of the molten zinc and

the physical operating parameters: immersion time and the speed of withdrawal. The addition of small amounts of certain elements, such as Al, Pb, Ge, Ti, Bi, Cu, Cd, or Sn, can contribute to the problem resolution by inhibiting the zinc–steel reactivity and/or increasing the bath fluidity [4]. Nickel addition is also considered favourable, because it changes the kinetics, morphology, and thermodynamic equilibrium between the Fe–Zn phases. As a result, Ni at a low concentration (0.06%) inhibits the Sandelin effect [5,6]. However, at a high silicon concentration, the layer thickness might increase if Ni was present in the zinc bath [6].

Most of the studies that describe the effect of silicon during galvanizing use samples that contain many elements. So silicon is not the only variable in their experiments. For example, Kopyciński [7] studied four different steel grades (Si > 0.20%) and two ductile irons. Galvanizing was performed in a Zn–Ni bath at 450 °C at the dipping time up to 10 min. The growth rates for the δ and ζ phases indicated a leading role of the ζ phase and a slow growth rate of the δ phase [7].

* Corresponding author, sirli.sepper@ttu.ee

Mandal et al. [8] investigated interstitial free steel behaviour, morphology, and the kinetics of the growth of the coatings during galvanizing in pure as well as commercial grade zinc baths at 470 °C. They found no delay in the formation of the ζ or δ phases in the studied zinc baths [8].

Uchiyama et al. [9] melted electrolytic iron and a given amount of silicon to analyse silicon reactivity in galvanizing. Galvanizing was performed in the temperature range from 440 °C to 600 °C for 600 s in a pure zinc bath. They presented an existence area map of different coating layers depending on the silicon concentration and the immersion temperature [9].

This paper describes the coating formation with different substrate silicon concentrations at 450 °C, which is the common galvanizing temperature. The aim of the study is to describe the role of Si in coating formation and to deploy the know-how to industry.

2. MATERIALS AND METHODS

To investigate how silicon affects the reaction between steel and liquid zinc, centrifugal casting was used to prepare specimens with different silicon concentrations. Steel powder (ATOMET 1001) and a calculated amount of Fe–Si powder (Si 46.10%) were melted in a vacuum induction furnace and cast into a copper mould.

The diameter of the cast samples was 35 mm at the thickness of 3 mm. The chemical composition of each specimen was measured using Spectrolab M. The results are presented in Table 1. Sample 1 in Table 1 is steel powder ATOMET 1001 without Fe–Si powder addition. The specimens were annealed at 730 °C for one hour and then air cooled. The oxidation layer was removed by mechanical grinding (80 grit). A small hole was drilled near the edge of each sample to help hang the specimens during the galvanizing process.

A batch-type hot dip galvanizing process was used. The zinc bath temperature was 450 °C. Galvanizing was performed in the industrial galvanizing plant AS Paldiski Tsingipada (Zincpot). According to common practice of the hot dip galvanizing process, which includes degreasing, pickling in HCl, rinsing, and fluxing, the samples were subjected to pre-treatment. The zinc bath consisted of 99.3% Zn, 0.055% Ni, and Al, Bi, Fe, and Sn in balance. The dipping times in the liquid zinc were from 4 s up to 1200 s.

Table 1. Chemical composition of the specimens, %

Sample	C	Si	Mn	P	Fe
1	<0.01	<0.01	0.04	0.005	99.72
2	<0.01	0.06	0.04	0.007	99.66
3	<0.01	0.11	0.05	0.006	99.60
4	<0.01	0.17	0.05	0.006	99.54
5	<0.01	0.30	0.05	0.007	99.40

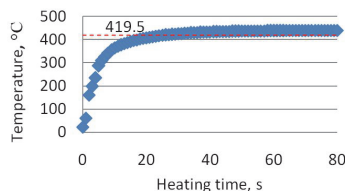


Fig. 1. Temperature change inside the specimens.

After galvanizing, the specimens were quenched in water to prevent further diffusion reaction during air cooling. For the examination of the microstructure, hot dip galvanized specimens were cross-sectioned, hot mounted, ground, and polished. A nital etchant was used to reveal the microstructures of the specimens and observations were made with optical microscope Zeiss Axiovert 25 and scanning electron microscopy EVO MA-15 (Carl Zeiss).

To study temperature changes in the wall of a specimen during dipping in the molten zinc, a Vernier Software thermocouple was used. Figure 1 shows the heating curve of the specimens during dipping in the molten zinc at 450 °C. It took approximately 20 s to establish the melting temperature of zinc (419.5 °C) with the investigated specimens.

3. RESULTS AND DISCUSSION

3.1. Coating growth with dipping time up to 25 s

Dipping time (4, 7, 12, 25 s) was short in the investigation of coating formation on top of the substrates shown in Table 1. After dipping cold steel into the zinc bath, zinc will freeze in the contact surface of steel. Even a very short time contact between steel and zinc leads to the formation of Fe–Zn intermetallics, which are in solid state. After 4 s of dipping in the molten zinc, a thin layer of intermetallic phases (ζ and δ) was observed with all tested silicon concentrations (Si <0.01%, 0.06%, 0.11%, 0.17%, 0.30%). Poor adhesion between the steel and the coating could be observed at a dipping time of 4 s.

After galvanizing for 4 s, the microstructure and thickness of the Zn–Fe layer were similar regardless of the content of silicon in the substrate. This is also confirmed by experiments reported in [10]. Figure 2 presents the microstructure of the zinc coating (Si 0.30%) after a dipping time of 4 s. First, the ζ phase occurred, which was immediately followed by the δ and then, after incubation, by the Γ phase. The same test results were reported by Mandal et al. at the galvanizing temperature of 470 °C [8]. It is frequently admitted that the first intermetallic compound that appears during hot dip galvanizing is the ζ phase [11]. However, Kopyciński postulated that the Γ phase nucleates first, followed by the

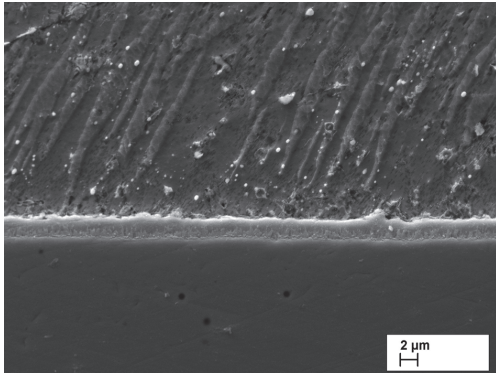


Fig. 2. Microstructure of the zinc coating after the dipping time 4 s (Si 0.30%).

δ and ζ phases in a Zn–Ni bath at 450°C [7]. It is difficult to evaluate the Γ phase because of its small thickness.

Furthermore, with a dipping time of 4 s, a thick η layer was present in the coating (ca 800 μm). It is hypothesized that as the specimen's inside temperature after the galvanizing time of 4 s is low (less than 300°C, Fig. 1) and probably the temperature in the contact surface of steel and zinc is below the melting temperature of zinc, the nucleation of intermetallic phases takes place in solid state and therefore a thick η layer is present in the coating with the dipping time of 4 s. However, other authors [10,12] claim that nucleation of the phases takes place in the solid–liquid border. Therefore, further research is needed to understand if zinc is completely melted in the contact surface of the specimen when nucleation of the phases takes place.

With an increase in the dipping time, the thickness of the Fe–Zn intermetallic phase increased. Until 25 s, only minor differences occurred in the thicknesses of the intermetallic coating and in the microstructure of specimens with different silicon contents, although a small Sandelin curve appeared with the dipping time of 25 s (Fig. 3). The thickness of the η phase was not taken into consideration because the η phase appeared when a specimen was pulled out from the zinc pot and at the beginning of the reaction the zinc was in solid state. The reactions that took place in the galvanizing process during the dipping time of <25 s were not influenced by silicon concentrations. This is also confirmed by other authors [10,12,13]. The reason might lie in the substrate steel temperature, which in this experiment was below the melting temperature of zinc until 20 s (Fig. 1).

During the first 25 s, the total thickness of the coating was related to the ζ phase and the δ phase was very narrow. Figure 4 shows the difference in the microstructure and the ζ phase thickness at silicon content <0.01% and 0.06%. During the first 25 s, the ζ phase

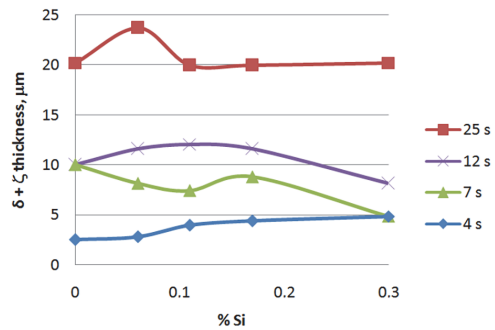


Fig. 3. Sum of the thicknesses of the δ and ζ layers at different dipping times.

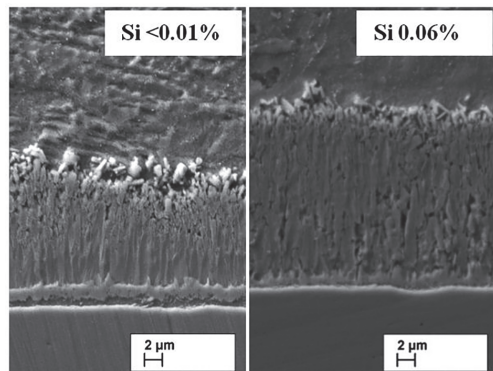


Fig. 4. Microstructure of the zinc coating after the dipping time of 25 s.

dominated in the coating while the δ phase was growing very slowly. The influence of silicon was remarkable after longer dipping times (>25 s).

3.2. Coating growth with dipping times 195 and 1200 s

The dipping time of 195 s was chosen because it is the common galvanizing time. In addition, 1200 s was used to investigate the coating growth at a longer incubation time.

Coating growth with the dipping times 195 and 1200 s was strongly influenced by the silicon content of the steel (Fig. 5). The Sandelin curve at about Si content of 0.08–0.15% reflects the thickness of the coating.

Each phase layer has its own growth kinetics, which depends on the silicon content and the dipping time. On the sample with silicon content <0.01%, a compact and continuous zinc coating is visible with the Γ , δ , ζ , and η layers (Fig. 6a). There was a large difference in the

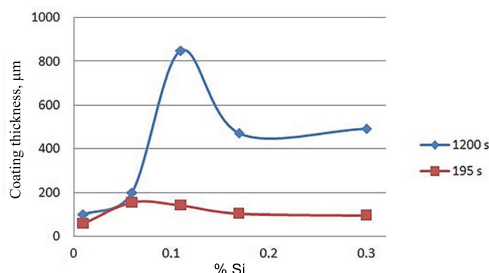
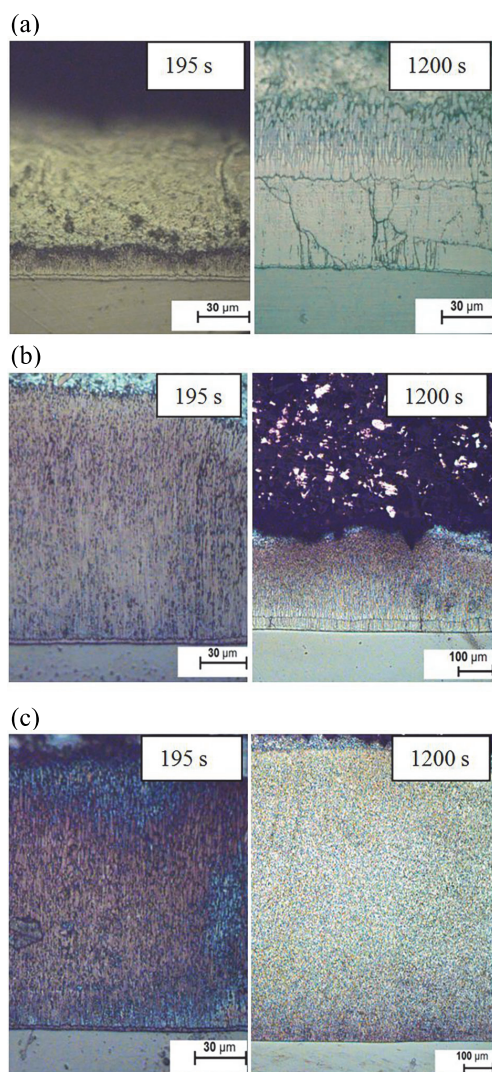


Fig. 5. Coating thicknesses at different substrate silicon contents. Dipping time 195 and 1200 s.



microstructure of the zinc coating and the thickness of the δ layer between the dipping times of 195 and 1200 s (Table 2). After 195 s, the growth of the ζ phase was impeded while the growth of the δ phase dominated. The δ layer of the coating with an immersing time of 1200 s has a greater thickness than the ζ layer. The silicon content in the Sandelin range ($Si 0.06\%$ and 0.11%) resulted in a thick coating at the dipping times of 195 and 1200 s (Figs 6b and 6c). The coating consists of a thin δ layer and a thick ζ layer (Table 2).

The substrate with the silicon content of 0.17% (Sebisty range) has larger ζ grain size than the low silicon steel ($Si < 0.01\%$). The growth in the δ layer is

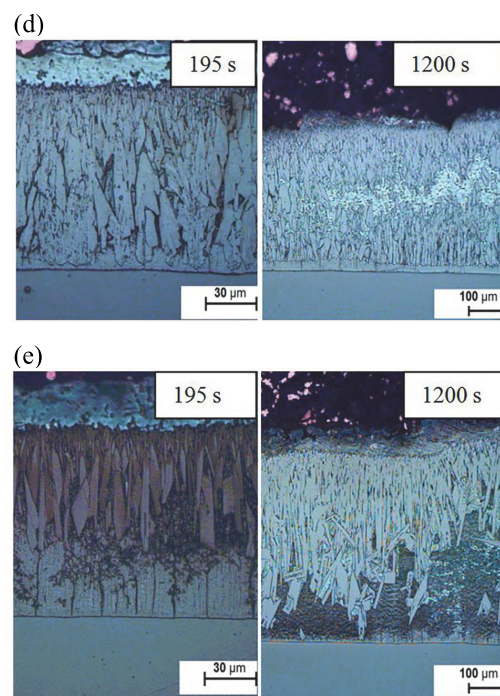


Fig. 6. Microstructure of the zinc coating after different dipping times (195 and 1200 s): (a) $Si < 0.01\%$, (b) $Si 0.06\%$, (c) $Si 0.11\%$, (d) $Si 0.17\%$, (e) $Si 0.30\%$.

Table 2. Thicknesses of the δ and ζ layers with dipping times 195 s and 1200 s

Si content, %	195 s		1200 s	
	Thickness of layers, μm			
	δ	ζ	δ	ζ
<0.01	3	20	44	40
0.06	3	143	33	168
0.11	3	151	1	849
0.17	10	83	26	192
0.30	30	58	41	467*

* Contains also a $\delta + \zeta$ mixture phase.

visible at a longer dipping time, but the ζ layer still dominates in the coating thickness (Fig. 6d, Table 2).

The coating of the sample with the silicon content of 0.30% is characterized by a thin δ layer and a thick $\delta + \zeta$ layer with a floating ζ (Fig. 6e, Table 2).

3.3. Stages of zinc coating formation

When the substrate steel is immersed in a liquid zinc bath, a number of reactions occur depending upon the bath composition, bath temperature, and the impurities of the steel. According to the Fe–Zn phase diagram (Fig. 7), during hot dip galvanizing at 450 °C, an intermetallic layer is formed. It is composed of Γ -Fe₃Zn₂₁, δ -FeZn₁₀, ζ -FeZn₁₃, and η -layers. The enthalpies of the formation of all intermetallic compounds are very close to one another and this is why an unstable behaviour of the system might occur with small additions in steel [14].

Based on the experimental results, five stages can be distinguished in zinc coating formation. A schematic model of the stages is shown in Fig. 8.

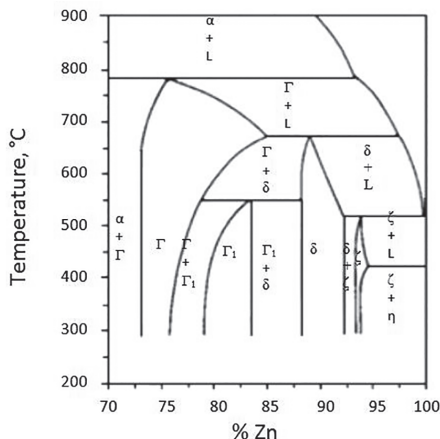


Fig. 7. Binary Fe–Zn phase diagram (Zn-rich corner) [14].

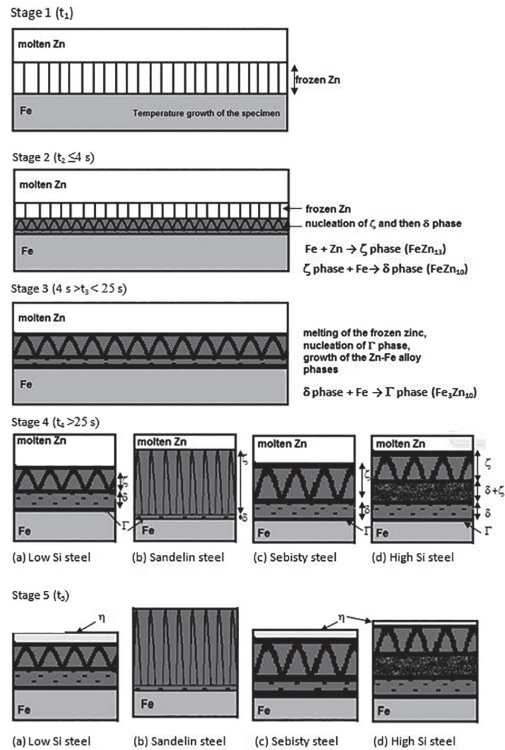


Fig. 8. A schematic representation of the Fe–Zn layer formation.

Stage 1 is temperature growth of the specimen and the freezing of zinc after dipping the specimen in the molten zinc.

Stage 2 is the nucleation of the ζ phase, immediately followed by the δ phase. The formation of ζ and δ phases occurs probably by solid-state diffusion during the dipping time 4 s.

Stage 3 (hot dip galvanizing time between 4 and 25 s) is the growth of the δ and ζ phases and the formation of the Γ phase. During this stage, the temperature of the substrate is higher than the melting temperature of zinc, and the frozen zinc is completely melted. Stages 1–3 are not influenced by the silicon content of the steel.

Stage 4 is influenced by the silicon content. The growth rate of the δ phase is higher than that of the ζ phase with the low silicon steel (Si < 0.03%). In this stage, Sandelin steel is characterized by a high reaction rate of the ζ phase formation. The growth of the δ phase is restrained. The coating growth of Sebisty steel is related to the growth of the δ and ζ phases, although the ζ phase dominates in the coating. With the high silicon steel (Si 0.30%), a $\delta + \zeta$ mixture phase appears in the coating.

The final, fifth stage is the formation of the η layer while pulling the specimen out of the zinc bath. In the case of Sandelin steel, the Fe diffuses into the η layer during air cooling and as a result, the final layer is the ζ phase. In this experiment, the specimens were quenched in water after galvanizing to prevent further diffusion reaction; as a result, the η layer can be seen in Figs 6b and 6c.

Hot dip galvanized coating formation can be described as a diffusion process. Zinc diffuses into the steel and iron diffuses into the zinc. As the diffusion coefficient of zinc is higher than that of steel ($D_{Zn} > D_{Fe}$), it is believed that zinc readily diffuses into the steel and forms intermetallic compounds [15]. On the other hand, it is known that when solid iron is immersed into liquid zinc, loss of iron weight takes place. The total iron loss consists of iron dissolved into the zinc bath and iron that has remained in the alloy layers. The iron loss of the substrate depends on the silicon concentration of the steel up to 520 °C [9]. According to data from Uchiyama et al. [9], it can be concluded that the zinc coating thickness, which depends on the silicon concentration at 450 °C, is related to the total iron loss of the substrate. It is possible to draw the Sandelin curve with the x -axis of Si concentration (%) and the y -axis of the total iron loss of the steel. Thus, it is possible that silicon affects hot dip galvanizing reactions by influencing zinc diffusion into the steel and iron diffusion into the coating.

Many studies have described the influence of silicon on the coating formation, but a fundamental understanding of the phenomenon is still lacking. Most researchers agree that the low solubility of silicon in the ζ layer is important. It leads silicon segregation to the grain boundaries and formation of areas of liquid Zn between the ζ crystals. However, some theories state that ferrosilicon particles in the coating can act as nucleation sites for the nucleation of the ζ phase [16]. This theory seems questionable because many researchers have not found Si particles in the coating (including experiments made in Tallinn University of Technology). In recent investigations it is claimed that the Si content in steel has no direct influence on the galvanizing process but affects it indirectly by influencing the effusion of hydrogen [17]. More research is needed to develop a holistic theory of layer formation.

4. CONCLUSIONS

The focus of the study was on the role of silicon in the hot dip galvanizing process. The following conclusions can be drawn:

- Based on experimental results it is hypothesized that hot dip galvanizing reactions between Fe and Zn take place in solid state. During galvanizing, zinc solidifies in the steel surface and as a result, the

coating will grow in the contact surface of steel and solid zinc. There is no contact between Fe and liquid Zn. Further research is needed to confirm the hypothesis.

- Even a very short contact time (4 s) between steel and zinc leads to the formation of Fe–Zn intermetallics. First, the ζ phase occurs, immediately followed by the δ , and then, after incubation, by the Γ phase.
- The reactions that take place in the galvanizing process during the dipping time <25 s are not influenced by silicon concentrations. The influence of silicon is remarkable after longer dipping times (>25 s).
- Silicon most probably affects hot dip galvanizing reactions by influencing zinc diffusion into the steel and Fe diffusion into the coating. The higher the Fe diffusion, the thicker the Zn coating is.

ACKNOWLEDGEMENTS

This research was supported by the European Social Fund of Doctoral Studies and the Internationalization Programme DoRa. The authors would like to express their gratitude to the Paldiski Tsingipada AS (Zincpot) for support and cooperation.

REFERENCES

1. Nai-Yong Tang. Control of silicon reactivity in general galvanizing. *Journal of Phase Equilibria and Diffusion*, 2008, **29**(4), 337–344.
2. Che, C., Lu, J., Kong, G., and Xu, Q. Role of silicon in steels on galvanized coatings. *Acta Metall. Sin. (Engl. Lett.)*, 2009, **22**(2), 138–145.
3. Che, C., Lu, J., and Kong, G. Interpretation of Sebsty effect of hot dip galvanized steels. *Trans. Nonferrous Met. Soc. China*, 2005, **15**(6), 1275–1279.
4. Jalel Ben nasr, Snoussi, A., Bradai, C., and Halouani, F. Optimization of hot-dip galvanizing process of reactive steels: minimizing zinc consumption without alloy additions. *Mater. Lett.*, 2008, **62**, 3328–3330.
5. Pistofidis, N., Vourlias, G., Konidaris, S., Pavlidou, El., and Stergioudis, G. The combined effect of nickel and bismuth on the structure of hot-dip zinc coatings. *Mater. Lett.*, 2007, **61**, 2007–2010.
6. Maass, P. and Peissker, P. (eds). *Handbook of Hot-Dip Galvanization*. Wiley-VCH Verlag, Weinheim, 2011.
7. Kopyciński, D. The shaping of zinc coating on surface steels and ductile iron casting. *Arch. Foundry Eng.*, 2010, **10**, 463–468.
8. Mandal, K. K., Mandal, D., Das, S. K., Balasubramaniam, R., and Mehrotra, S. P. Microstructural study of galvanized coatings formed in pure as well as commercial grade zinc baths. *T. Indian I. Metals*, 2009, **62**(1), 35–40.
9. Uchiyama, Y., Koga, H., and Inokuchi, H. Reaction between Fe–Si alloys and liquid zinc. *T. Jpn. I. Met.*, 1983, **24**(5), 272–280.

10. Liberski, P., Tatarek, A., and Mendala, J. Investigation of the initial stage of hot dip zinc coatings on iron alloys with various silicon contents. *Solid State Phenom.*, 2013, **212**, 121–126.
11. Foct, J., Reumont, G., Dupont, G., and Perrot, P. How does silicon lead the kinetics of the galvanizing reaction to lose its solid–solid character. *J. Phys. IV*, 1993, **3**, 961–966.
12. Liberski, P., Tatarek, A., Kania, H., and Podolski, P. Coating growth on silicon-containing iron alloys in hot dip galvanizing process. In *Proceedings 22nd International Galvanizing Conference INTERGALVA*. Madrid, 2009, 181–187.
13. Lu, J., Che, C., Kong, G., Xu, Q., and Chen, J. Influence of silicon on the α -Fe/ Γ interface of hot-dip galvanized steels. *Surf. Coat. Tech.*, 2006, **200**, 5277–5281.
14. Guttman, M. Diffusive phase transformations in hot dip galvanizing. *Mater. Sci. Forum*, 1994, **155–156**, 527–548.
15. Xu, J., Bright, M. A., Liu, X., and Barbero, E. Liquid metal corrosion of 316L stainless steel, 410 stainless steel, and 1015 carbon steel in a molten zinc bath. *Metall. Mater. Trans. A*, 2007, **38**(11), 2727–2736.
16. Porter, F. C. *Zinc Handbook: Properties, Processing, and Use in Design*. CRC Press, 1991.
17. Schulz, W.-D., Schubert, P., and Thiele, M. An alternative approach to explaining the effect of silicon on the galvanizing reaction. In *Edited Proceedings – Twentieth International Galvanizing Conference*. Amsterdam, 2003, 61–64.

Räni mõju kuumtsinkimisprotsessis

Sirli Sepper, Priidu Peetsalu, Priit Kulu, Mart Saarna ja Valdek Mikli

On käsitletud terases sisalduva räni mõju kuumtsinkimisprotsessile. Et katsekehades oleks ainsaks muutujaks ränisisaldus, kasutati katsekehade valmistamiseks tsentrifugaalvalu, kus sulatati omavahel Fe-pulber ja arvutatud kogus Fe-Si-pulbrit. Ränisisalduseks valiti Si <0,01, 0,06, 0,11, 0,17 ja 0,30%. Tsinkimine viidi läbi kuumtsinkimistehases AS Paldiski Tsingipada (Zincpot), kus tsingivanni temperatuur oli 450°C. Kasutati nii lühikest kui ka pikka kastmisaega. Lühike kastmisaeg tsingivanni oli 4–25 sekundit, et uurida kattes erinevate faaside teket. Pika tsingivannis hoidmise aja (195 ja 1200 sekundit) eesmärgiks oli uurida erinevate faaside kasvu ajas.

Kastmisaja 4 sekundi jooksul tekkisid juba esimesed Fe-Zn-faasid terase ja tsingi kokkupuutepinnal. Esimene tekkinud faas oli ζ kiht, koheselt järgnes δ kiht ja peale inkubatsiooniaega Γ kiht. Kuumtsinkimisreaktsioonid kastmisajaga <25 sekundit ei sõltunud alusmaterjali ränisisaldusest. Räni mõju on suur pikema kastmisajaga (>25 sekundit). Katsetulemuste põhjal loodi skemaatiline mudel, kus kirjeldati katte tekkimist erinevate ränisisalduste korral. Järeldati, et räni mõjutab tsingi difusiooni terasesse ja raua difusiooni kattesse.

**DISSERTATIONS DEFENDED AT
TALLINN UNIVERSITY OF TECHNOLOGY ON
*MECHANICAL ENGINEERING***

1. **Jakob Kübarsepp**. Steel-Bonded Hardmetals. 1992.
2. **Jakub Kõo**. Determination of Residual Stresses in Coatings & Coated Parts. 1994.
3. **Mart Tamre**. Tribocharacteristics of Journal Bearings Unlocated Axis. 1995.
4. **Paul Kallas**. Abrasive Erosion of Powder Materials. 1996.
5. **Jüri Pirso**. Titanium and Chromium Carbide Based Cermets. 1996.
6. **Heinrich Reshetnyak**. Hard Metals Serviceability in Sheet Metal Forming Operations. 1996.
7. **Arvi Kruusing**. Magnetic Microdevices and Their Fabrication methods. 1997.
8. **Roberto Carmona Davila**. Some Contributions to the Quality Control in Motor Car Industry. 1999.
9. **Harri Annuka**. Characterization and Application of TiC-Based Iron Alloys Bonded Cermets. 1999.
10. **Irina Hussainova**. Investigation of Particle-Wall Collision and Erosion Prediction. 1999.
11. **Edi Kulderknup**. Reliability and Uncertainty of Quality Measurement. 2000.
12. **Vitali Podgurski**. Laser Ablation and Thermal Evaporation of Thin Films and Structures. 2001.
13. **Igor Penkov**. Strength Investigation of Threaded Joints Under Static and Dynamic Loading. 2001.
14. **Martin Eerme**. Structural Modelling of Engineering Products and Realisation of Computer-Based Environment for Product Development. 2001.
15. **Toivo Tähemaa**. Assurance of Synergy and Competitive Dependability at Non-Safety-Critical Mechatronics Systems design. 2002.
16. **Jüri Resev**. Virtual Differential as Torque Distribution Control Unit in Automotive Propulsion Systems. 2002.
17. **Toomas Pihl**. Powder Coatings for Abrasive Wear. 2002.
18. **Sergei Letunovitš**. Tribology of Fine-Grained Cermets. 2003.
19. **Tatyana Karaulova**. Development of the Modelling Tool for the Analysis of the Production Process and its Entities for the SME. 2004.
20. **Grigori Nekrassov**. Development of an Intelligent Integrated Environment for Computer. 2004.
21. **Sergei Zimakov**. Novel Wear Resistant WC-Based Thermal Sprayed Coatings. 2004.

22. **Irina Preis.** Fatigue Performance and Mechanical Reliability of Cemented Carbides. 2004.
23. **Medhat Hussainov.** Effect of Solid Particles on Turbulence of Gas in Two-Phase Flows. 2005.
24. **Frid Kaljas.** Synergy-Based Approach to Design of the Interdisciplinary Systems. 2005.
25. **Dmitri Neshumayev.** Experimental and Numerical Investigation of Combined Heat Transfer Enhancement Technique in Gas-Heated Channels. 2005.
26. **Renno Veinthal.** Characterization and Modelling of Erosion Wear of Powder Composite Materials and Coatings. 2005.
27. **Sergei Tisler.** Deposition of Solid Particles from Aerosol Flow in Laminar Flat-Plate Boundary Layer. 2006.
28. **Tauno Otto.** Models for Monitoring of Technological Processes and Production Systems. 2006.
29. **Maksim Antonov.** Assessment of Cermets Performance in Aggressive Media. 2006.
30. **Tatjana Barashkova.** Research of the Effect of Correlation at the Measurement of Alternating Voltage. 2006.
31. **Jaan Kers.** Recycling of Composite Plastics. 2006.
32. **Raivo Sell.** Model Based Mechatronic Systems Modeling Methodology in Conceptual Design Stage. 2007.
33. **Hans Rämmal.** Experimental Methods for Sound Propagation Studies in Automotive Duct Systems. 2007.
34. **Meelis Pohlak.** Rapid Prototyping of Sheet Metal Components with Incremental Sheet Forming Technology. 2007.
35. **Priidu Peetsalu.** Microstructural Aspects of Thermal Sprayed WC-Co Coatings and Ni-Cr Coated Steels. 2007.
36. **Lauri Kollo.** Sinter/HIP Technology of TiC-Based Cermets. 2007.
37. **Andrei Dedov.** Assessment of Metal Condition and Remaining Life of In-service Power Plant Components Operating at High Temperature. 2007.
38. **Fjodor Sergejev.** Investigation of the Fatigue Mechanics Aspects of PM Hardmetals and Cermets. 2007.
39. **Eduard Ševtšenko.** Intelligent Decision Support System for the Network of Collaborative SME-s. 2007.
40. **Rünno Lumiste.** Networks and Innovation in Machinery and Electronics Industry and Enterprises (Estonian Case Studies). 2008.
41. **Kristo Karjust.** Integrated Product Development and Production Technology of Large Composite Plastic Products. 2008.

42. **Mart Saarna**. Fatigue Characteristics of PM Steels. 2008.
43. **Eduard Kimmari**. Exothermically Synthesized B₄C-Al Composites for Dry Sliding. 2008.
44. **Indrek Abiline**. Calibration Methods of Coating Thickness Gauges. 2008.
45. **Tiit Hindreus**. Synergy-Based Approach to Quality Assurance. 2009.
46. **Karl Raba**. Uncertainty Focused Product Improvement Models. 2009.
47. **Riho Tarbe**. Abrasive Impact Wear: Tester, Wear and Grindability Studies. 2009.
48. **Kristjan Juhani**. Reactive Sintered Chromium and Titanium Carbide-Based Cermets. 2009.
49. **Nadežda Dementjeva**. Energy Planning Model Analysis and Their Adaptability for Estonian Energy Sector. 2009.
50. **Igor Krupenski**. Numerical Simulation of Two-Phase Turbulent Flows in Ash Circulating Fluidized Bed. 2010.
51. **Aleksandr Hlebnikov**. The Analysis of Efficiency and Optimization of District Heating Networks in Estonia. 2010.
52. **Andres Petritšenko**. Vibration of Ladder Frames. 2010.
53. **Renee Joost**. Novel Methods for Hardmetal Production and Recycling. 2010.
54. **Andre Gregor**. Hard PVD Coatings for Tooling. 2010.
55. **Tõnu Roosaar**. Wear Performance of WC- and TiC-Based Ceramic-Metallic Composites. 2010.
56. **Alina Sivitski**. Sliding Wear of PVD Hard Coatings: Fatigue and Measurement Aspects. 2010.
57. **Sergei Kramanenko**. Fractal Approach for Multiple Project Management in Manufacturing Enterprises. 2010.
58. **Eduard Latõsov**. Model for the Analysis of Combined Heat and Power Production. 2011.
59. **Jürgen Riim**. Calibration Methods of Coating Thickness Standards. 2011.
60. **Andrei Surzhenkov**. Duplex Treatment of Steel Surface. 2011.
61. **Steffen Dahms**. Diffusion Welding of Different Materials. 2011.
62. **Birthe Matsi**. Research of Innovation Capacity Monitoring Methodology for Engineering Industry. 2011.
63. **Peeter Ross**. Data Sharing and Shared Workflow in Medical Imaging. 2011.
64. **Siim Link**. Reactivity of Woody and Herbaceous Biomass Chars. 2011.
65. **Kristjan Plamus**. The Impact of Oil Shale Calorific Value on CFB Boiler Thermal Efficiency and Environment. 2012.
66. **Aleksei Tšinjan**. Performance of Tool Materials in Blanking. 2012.

67. **Martinš Sarkans.** Synergy Deployment at Early Evaluation of Modularity of the Multi-Agent Production Systems. 2012.
68. **Sven Seiler.** Laboratory as a Service – A Holistic Framework for Remote and Virtual Labs. 2012.
69. **Tarmo Velsker.** Design Optimization of Steel and Glass Structures. 2012.
70. **Madis Tiik.** Access Rights and Organizational Management in Implementation of Estonian Electronic Health Record System. 2012.
71. **Marina Kostina.** Reliability Management of Manufacturing Processes in Machinery Enterprises. 2012.
72. **Robert Hudjakov.** Long-Range Navigation for Unmanned Off-Road Ground Vehicle. 2012.
73. **Arkadi Zikin.** Advanced Multiphase Tribo-Functional PTA Hardfacings. 2013.
74. **Alar Konist.** Environmental Aspects of Oil Shale Power Production. 2013.
75. **Inge Roos.** Methodology for Calculating CO₂ Emissions from Estonian Shale Oil Industry. 2013.
76. **Dmitri Shvarts.** Global 3D Map Merging Methods for Robot Navigation. 2013.
77. **Kaia Lõun.** Company's Strategy Based Formation of e-Workplace Performance in the Engineering Industry. 2013.
78. **Maido Hiimaa.** Motion Planner for Skid-Steer Unmanned Ground Vehicle. 2013.
79. **Dmitri Goljandin.** Disintegrator Milling System Development and Milling Technologies of Different Materials. 2013.
80. **Dmitri Aleksandrov.** Light-Weight Multicopter Structural Design for Energy Saving. 2013.
81. **Henrik Herranen.** Design Optimization of Smart Composite Structures with Embedded Devices. 2014.
82. **Heiki Tiikoja.** Experimental Acoustic Characterization of Automotive Inlet and Exhaust System. 2014.
83. **Jelena Priss.** High Temperature Corrosion and Abrasive Wear of Boiler Steels. 2014.
84. **Aare Aruniit.** Thermoreactive Polymer Composite with High Particulate Filler Content. 2014.
85. **Dmitri Gornostajev.** Development of the Calculation Method for Barge Hull. 2014.
86. **Liina Lind.** Wear of PVD Coatings on Fineblanking Punches. 2014.

87. **Nikolai Voltšihhin.** Design and Technology of Oxides-Containing Ceramic-Based Composites. 2014.
88. **Aleksander Šablinski.** RANS Numerical Modelling of Turbulent Polydispersed Flows in CFB Freeboard. 2015.
89. **Tanel Aruväli.** Wireless Real-time Monitoring of Machining Processes. 2015.
90. **Andrei Bogatov.** Morphological Changes on Diamond and DLC Films During Sliding Wear. 2015.
91. **Raimo Kabral.** Aero-Acoustic Studies and Innovative Noise Control with Application to Modern Automotive Gas Exchange System. 2015.
92. **Jevgeni Sahno.** Dynamic Management Framework for Continuous Improvement of Production Processes. 2015.
93. **Ott Pabut.** Optimal Design of Slotless Permanent Magnet Generators. 2015.
94. **Merili Kukuškin.** Value Centric Business Development for Estonian Manufacturing Small and Medium Sized Enterprises. 2015.
95. **Kaimo Sonk.** Development of Additive Manufacturing Based on Functional Requirements. 2015.
96. **Marina Aghayan.** Functionalization of Alumina Nanofibers with Metal Oxides. 2016.
97. **Marek Jõelett.** Titanium Carbide Cermet as Ballistic Protection Material. 2016.
98. **Heikki Sarjas.** Novel Synthesized and Milled Carbide-based Composite Powders for HVOF Spray. 2016.
99. **Klodian Dhoska.** Measurement Methods with 3D Coordinate Measuring Machine and Improved Characterization Setup for Detector Performance. 2016.
100. **Aleksei Snatkin.** Development and Optimisation of Production Monitoring System. 2016.
101. **Igor Poljantšikov.** Partners Selection Tool for Virtual Enterprise in SMEs Network. 2016.
102. **Sergei Žigailov.** Experimental and Analytical Modelling of Pelvic Motion. 2016.
103. **Rommi Källo.** Synergy-Based Chaos Control in the Multi-Agent Hierarchical Systems. 2016.
104. **Der-Liang Yung.** ZrC-based and ZrC-doped Composites for High-Temperature and Wear Applications. 2016.
105. **Viive Pille.** Development of a Model for the Prevention of Work-Related Musculoskeletal Disorders in the Upper Extremities. 2016.
106. **Agus Pramono.** Investigation of Severe Plastic Deformation Processes for Aluminum Based Composites. 2016.

107. **Zorjana Mural.** Technology and Properties of Fine-grained Nd-Fe-B Magnets. 2017.
108. **Eero Väljaots.** Energy Efficiency Evaluation Method for Mobile Robot Platform Design. 2017.
109. **Viktoria Baškite.** Decision-Making Tool Development for Used Industrial Equipment Life Cycle Evaluation and Improvement. 2017.
110. **Kaspar Kallip.** High Strength Ductile Aluminium Matrix Composite. 2017.
111. **Maria Drozdova.** Electroconductive Oxide Ceramics with Hybrid Graphenated Nanofibers. 2017.
112. **Roman Ivanov.** Chemical Vapour Deposition of Graphene Coating onto Ceramic Nanofibers Substrates and Applications Thereof. 2017.